IN VIVO DETECTION OF LIGHT STRESS INDUCED REACTIVE OXYGEN SPECIES IN PLANTS

Ph.D. Thesis

Csengele Barta

Supervisor: Dr. Éva Hideg

Biological Research Centre of the Hungarian Academy of Sciences
Institute of Plant Biology
Laboratory of Molecular Stress-and Photobiology

Szeged
2004

CONTENTS

ABBREVIATIONS

A – absorption

APX – ascorbate-peroxidase

Cab – chlorophyll *a*/*b* binding protein

CAT – catalase

Chl – chlorophyll

DAB – 3,3' diamino-benzidine

DanePy – 5-Dimethylamino-naphthalene-1-sulfonic acid (2-diethylamino-ethyl)-(2,2,5,5-tetramethyl-2,5-dihydro-1*H*-pyrrol-3-ylmethyl)-amide

DHA – dehydroascorbate

DHAR – dehydroascorbate reductase

EPR– electron-paramagnetic resonance

GSH – glutathione

GSSG – glutathione disulfide

H_2O_2 – hydrogen peroxide

HO-1889NH – 5-Dimethylamino-naphthalene-1-sulfonic acid (2,2,5,5-tetramethyl-2,5-dihydro-1*H*-pyrrol-3-ylmethyl)-amide

HO-2941 – 3-N-(2,2,5,5-tetramethyl-2,5-dihydro-1 H-pyrrol-3-carboxoamidopropyl) sulforhodamine **LHCII** – light harvesting complex II

L-2204 – 2-Methyl-1-oxy-3,4-dihydro-2*H*-pyrrole-2-carboxylic-acid [2-(5-dimethylamino-naphthalene-1-sulfonylamino)-ethyl]-amide

MDA – monodehydro ascorbate

MDAR – monodehydro ascorbate reductase

NADP(H) – nicotine adenine dinucleotide phosphate (reduced form)

$^1O_2$ – singlet oxygen

$O_2^{-\bullet}$ – superoxide anion radical

$^\bullet$OH – hydroxyl radical

PAR – photosynthetically active radiation (400-700 nm)

P_{680} – photosystem II reaction center chlorophyll

P_{700} – photosystem I reaction center chlorophyll

PSII – photosystem II

PSI – photosystem I

Pheo – pheophytin

Q_A – first quinone acceptor in PSII

Q_B – second quinone acceptor in PSI

ROS – reactive oxygen species

$ROO^{\cdot}$ – peroxyl radical

SOD – superoxide dismutase

UV – ultraviolet radiation

1. INTRODUCTION

During their life cycle plants are daily exposed to naturally occurring adverse environmental impacts, such as high intensities of photosynthetically active radiation (PAR), increased fluxes of ultraviolet radiation, extreme temperatures, water deprivation or pathogen attack, or to the combination of these. All the above conditions may cause morphological changes and physiological alterations leading to decreased viability. When plants are exposed to various stress conditions, a number of metabolic functions are affected through the generation of reactive oxygen species (ROS). If the balance between the production and the removal of the deleterious active oxygen derivatives is disturbed, the excess ROS may initiate oxidative reactions, which may damage lipids, proteins, pigments and DNA. One of the most frequent stress conditions occurring in the field is the stress induced by excess PAR. Plants may often be exposed to high irradiances of both visible (400-700 nm) and ultraviolet radiation (280-390 nm). The study of the excess irradiation-induced damages is an important field of plant stress research.

Our studies were focused on the investigation of light stress at the level of *in vivo* ROS production. Due to the abundance of oxygen in the chloroplasts, the photosynthetic electron transport is extremely vulnerable to oxidative damage provoked by excess PAR or by UV radiation. We were interested to study which types of ROS are involved in the mechanism of *in vivo* photoinhibition and stress by both UV-A and UV-B irradiation. We aimed to adapt a direct ROS detection method for *in vivo* plant applications, and to use this technique as well to study the impact of light stress on plants at the level of active oxygen production.

1.1. Solar radiation. General considerations.

Besides being the driving force of photosynthesis, light may as well be damaging for photosynthetic organisms. High doses of photosynthetically active radiation result in photoinhibition, on the other hand, increasing doses of ultraviolet radiation cause physiological alterations.

The incoming solar radiation is greatly modified by atmospheric and surface processes, before reaching the Earth. The industrial development triggered the common use and emission into the atmosphere of chlorofluorocarbons and of other pollutants, which contributed to partial destruction of the protecting ozone shield. The ozone layer selectively absorbs a part of the high energy, damaging UV-B radiation (Frederick and Lubin, 1988, McFarland and Kaye, 1992). The solar radiation reaching the Earth's surface is divided into ultraviolet B (UV-B: 280-320 nm), ultraviolet A (UV-A: 320-400 nm) and visible (PAR: 400-700 nm) radiation, the latter one being used for photosynthesis by the vegetation. The lower wavelength UV-C (< 280 nm) radiation is totally absorbed by the atmosphere, the UV-B only partially, while the UV-A is not absorbed (Fig. 1.1).

The amount and the spectral composition of the solar radiation reaching the Earth's surface is influenced by ozone depletion, which serves as a natural shield for the surface (Kerr and McElroy, 1993, Madronich et al., 1998). Ozone is formed by combining molecular oxygen with atomic oxygen formed in a process activated by short wavelength UV-C (240 nm) radiation. The apparition of the ozone hole was first reported in the Antarctic region, but later in the agriculturally important regions of the Northern hemisphere as well. Therefore the study of the effect of increased ultraviolet radiation on biological systems had a central role in a multitude of studies in the last decades (Tevini, 1988, Tevini and Teramura, 1989, Stapleton, 1992, Teramura and Sullivan, 1994, Strid et al., 1994, Vass, 1996, Rozema et al., 1997, Jansen et al., 1998, Caldwell et al., 1998, Caldwell et al., 2003).

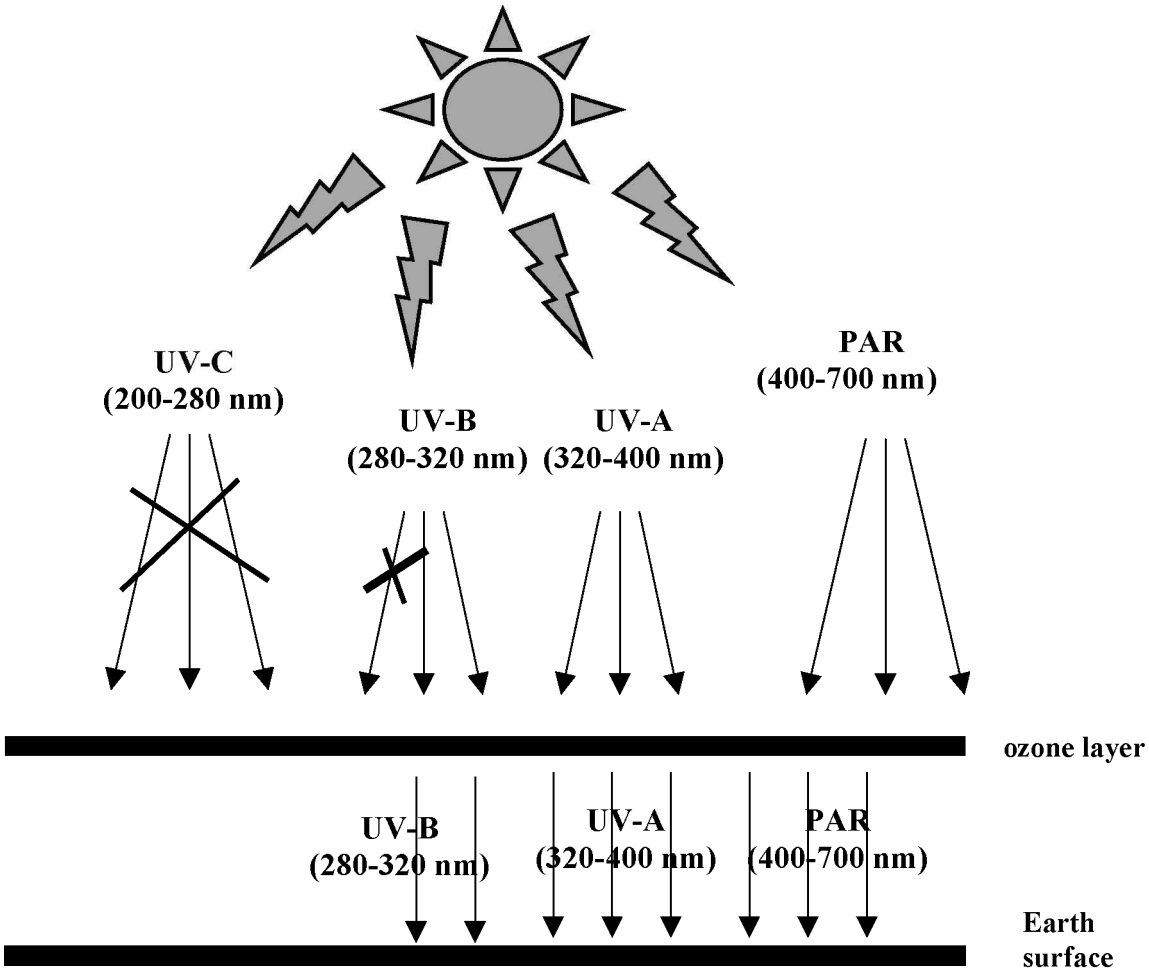

Fig. 1.1.: Incoming solar radiation is partially absorbed by the ozone layer, before reaching the Earth's surface: UV-C radiation (200-280 nm) is totally absorbed, UV-B (280-320 nm) only partially, UV-A (320-400 nm) and visible irradiation (PAR: 400-700 nm) reach the ground surface.

The solar flux received by plants at a particular location can be different, depending on the natural fluctuations throughout the annual cycle and on the artificial changes brought about by the introduction of air pollutants. The distribution of the radiation and its interaction with the vegetation is influenced by multiple factors, such as weather conditions, altitude, or micro-climatic components (Madronich et al., 1998).

The 400-700 nm range of the solar radiation is indispensable for the photosynthesis of photosynthetic organisms, and therefore they are inevitably exposed to ultraviolet radiation as well. All life forms have adapted to receive UV doses within a certain range. Unlike animals and humans, plants are fixed to one location during their development cycle, and therefore unable to leave their environmental conditions. This makes them particularly vulnerable to changes in the ambient UV irradiance levels. Plants have developed several complex internal mechanisms to protect themselves against overexposure to solar radiation (Rozema et al., 1997, Jansen et al., 1998). Their tolerance is determined by the effectiveness of those processes, which diminish the damaging effect of the radiation, and of those mechanisms, which repair the damage.

Despite the varied biological protection mechanisms of plants, exposure to UV radiation affects the growth and yield of plant species. Minor changes of the components (UV-A and UV-B) of the solar UV spectrum significantly affect plants, leading to reduced height, smaller leaf number, and decreased fresh weight (Panagopoulos et al., 1990, Li et al., 1998, Li et al., 1999, Gao et al., 2003). However, the range of responses of plants to UV varies greatly from species to species, and depends on the developmental stage of the plant as well (Li et al., 2000a, Li et al., 2000b, Dai et al., 1994, Kakani et al., 2003).

1.2. Oxidative stress

Evolution of life on Earth began in an atmosphere totally different from the atmosphere of our days, in that there was virtually no oxygen. The atmospheric oxygen appeared when certain organisms evolved the capacity to split water into oxygen and hydrogen atoms. Together with the rise of oxygen in the atmosphere, a part of the biota adapted to the presence of oxygen, and evolved towards aerobic life, but the evolution of aerobic life forms requiring oxygen for their metabolism triggered the processes of oxygen activation as well. Activated oxygen species are highly reactive powerful oxidants, oxygen toxicity relays on its conversion into reactive species (Cadenas, 1989).

Reactive oxygen species (ROS) are products of plant metabolism. All aerobic organisms are equipped with a highly effective network of either enzymatic or non-

enzymatic defense and ROS neutralizing strategies to counterbalance the toxicity and the damaging effect of the highly reactive oxygen derivatives. Under physiological conditions, the effect of various ROS is kept under tight control. When the balance between ROS production and removal is disturbed, the elevated level of active oxygen production exceeds the neutralizing capacity of the antioxidant network and oxidative damages occur (Foyer et al., 1994, Inzé and Montagu, 1995, Alscher et al., 1997, Overmyer et al., 2003). ROS may damage all cellular components: DNA, lipids and proteins, initiating serious cellular injuries, which may result in loss of function and eventually in cell death (Fig. 1.2.) (Scandalios, 2002).

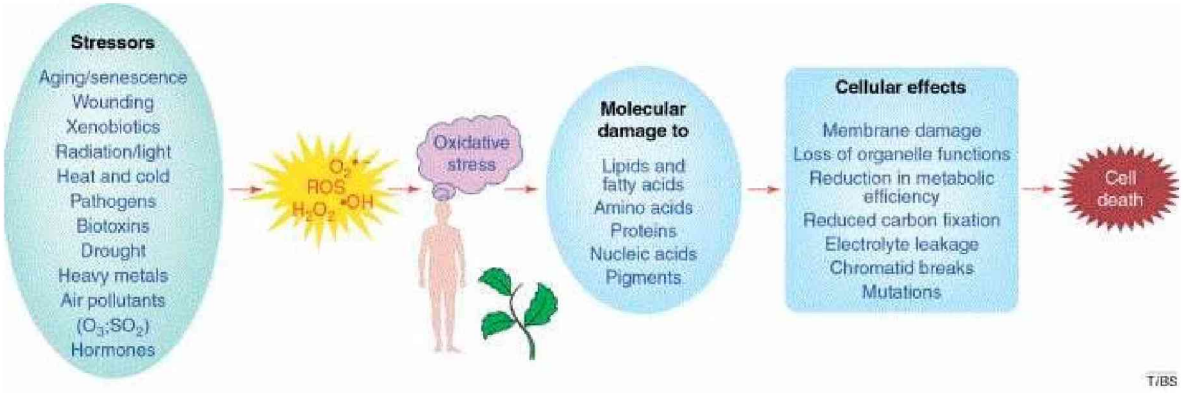

Fig. 1.2. The biological consequences of ROS mediated oxidative stress (Scandalios, 2002).

1.2.1. Chemistry of reactive oxygen species. Oxygen activation.

From the point of view of oxidative stress, the collective term of reactive oxygen species (ROS) covers not just the radical-type derivatives, such as hydroxyl and lipidperoxyl radicals, but also charged forms, for example the superoxide anion radical, or neutral ROS, as hydrogen peroxide or singlet oxygen.

A free radical is defined as an atom or molecule containing one or more unpaired electrons on its outermost electron orbital, which can be anionic, cationic or neutral one. Radicals are easily formed by electron addition or substraction. When a covalent bond is broken by homolytic fission, both atoms remain with one of the shared electrons, becoming free radicals. This type of reaction needs energy input,

possibly provided by heat or electromagnetic radiation. All atoms and molecules tend to achieve an energetically stable state, requiring the presence of paired electrons on their outermost electron shell. Since the free radical state is energetically unfavorable, the lifetime of radicals is much shorter than that of non-radical forms therefore radicals tend to react with either another free radical, or with non-radical type molecules. The later reactions promote further radical chain reaction cascades, having relevancy in biological systems. The propagation of the chain is terminated by the reaction of two radicals. Free radical reactions requiring little energy, which initiate branched chain reactions, can be very dangerous to animals and plants (Halliwell and Gutteridge, 1985).

Oxygen activation may occur by two different mechanisms: involving either electron or energy transfer.

1.2.1.1. Oxygen reduction by electron transfer reactions (monovalent reduction)

Atmospheric molecular oxygen ($^3O_2$) in its ground state is a bi-radical having two unpaired electrons in its outer orbital with parallel spins and its reactivity results from this property (Fig. 1.3 a). Oxygen is very unlikely to participate in reactions with organic molecules, since molecules having also two unpaired electrons with parallel spins on their outer orbital, but opposite to those of the oxygen are very rare. This spin restriction favors reactions in which oxygen is monovalently reduced by electron addition (Halliwell and Gutteridge, 1985).

Superoxide anion radical ($O_2^{-\bullet}$) (Figs. 1.3 b and 1.4.) is formed by single electron addition to the ground state O_2. Though $O_2^{-\bullet}$ proved to react directly with phospholipids, proteins and DNA (Halliwell and Gutteridge, 1985), its main toxicity relays on its conversion into more damaging species, such as hydroxyl radical. By proton uptake, $O_2^{-\bullet}$ forms the perhydroxyl radical ($^{\bullet}OOH$), a powerful oxidant. The half-life of $O_2^{-\bullet}$ is in the microsecond range, and its membrane-permeability has low rates (Takahashi and Asada, 1983).

The reduction of two $O_2^{-\bullet}$ molecules, accompanied by protonation leads to hydrogen peroxide (H_2O_2) formation (Figs. 1.3 c and 1.4.). *In vivo* the decay of $O_2^{-\bullet}$ to

H_2O_2 is catalyzed by superoxide dismutases (SODs), or it can be formed through reduction by ascorbate or ferredoxin. Spontaneous dismutation has a 10^5 – times slower rate than the reactions catalyzed by SOD (Bowler et al., 1992). H_2O_2 is considered even more harmful than the $O_2^{-\bullet}$ itself, because it readily permeates membranes, being a relatively stable uncharged molecule. The lifetime of H_2O_2 is about 1 millisecond, higher than the half-life of other ROS, and is considered as an important mediator of intracellular signaling processes (Foyer et al. 1997, Van Camp and Inzé, 1998, Karpinski et al., 1999, Mackerness et al., 2001, Van Bereusegem et al., 2001, Vranová et al., 2002). The reactivity of H_2O_2 is attributed mainly to its ability to form the highly reactive hydroxyl radical ($^{\bullet}OH$) (Figs. 1.3 d and 1.4.) in the presence of a transient metal reductant (Fe^{2+} or Cu^{+}) (Haber and Weiss, 1984). Irradiation of water by UV light or ionizing radiation results in the production of $^{\bullet}OH$ radicals, although in biological systems the main $^{\bullet}OH$ source is considered to be the Haber Weiss reaction.

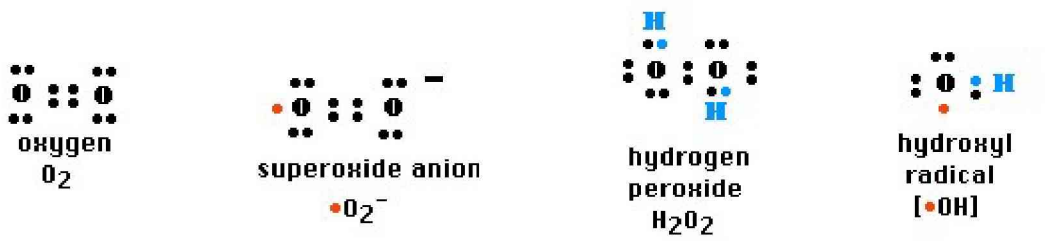

Fig. 1.3. Schematic representation of the electron structures of reactive oxygen species formed by monovalent reduction of molecular oxygen (a.) : superoxide anion radical (b.), hydrogen peroxide (c.) and hydroxyl radical (d.).

$^{\bullet}OH$ is one of the strongest oxidizing agents. Controlled *in vivo* generation of this species is responsible for the defense against pathogens (Tiedemann, 1997). The $^{\bullet}OH$ produced by cell wall peroxidases was proposed to take part in the process of cell extension (Schweikert et al., 2002). Upon exposure to various stress conditions, the generation rate of $^{\bullet}OH$ may increase. Because of its extreme reactivity this radical has very short half-life of 10^{-9}s, reacts instantaneously with molecules in its environment, with proteins, lipids or DNA. Hydroxyl radicals are too reactive to be eliminated

enzymatically, they have no scavenging enzyme and therefore their formation must be regulated to prevent damage (Halliwell and Gutteridge, 1985).

1.2.1.2. Activation of oxygen by energy transfer reactions

If ground state triplet oxygen absorbs sufficient energy to inverse the spin of one of its unpaired electrons, singlet oxygen ($^1O_2$) is formed (Fig. 1.4.). $^1O_2$ is not a free radical form of ROS and its reactivity is due to the absence of the spin restriction opposed to molecular oxygen. $^1O_2$ has also two unpaired electrons on its outer electron orbital, but these electrons have opposite spins, therefore they have high affinities to reacting with any molecule having unpaired electrons. It is an especially reactive ROS, usually produced in photosensitized reactions (type II photosensitisation) between an illuminated triplet-state dye molecule and molecular oxygen (Tanielian et al., 1984). The production of $^1O_2$ by photosensitisation is a four step process: light is absorbed by the photosensitiser and the photosensitiser triplet is formed, then trapping of the triplet state by molecular oxygen occurs and the energy is transferred from the triplet state dye to molecular oxygen. The excited triplet dye decays to ground state by this reaction.

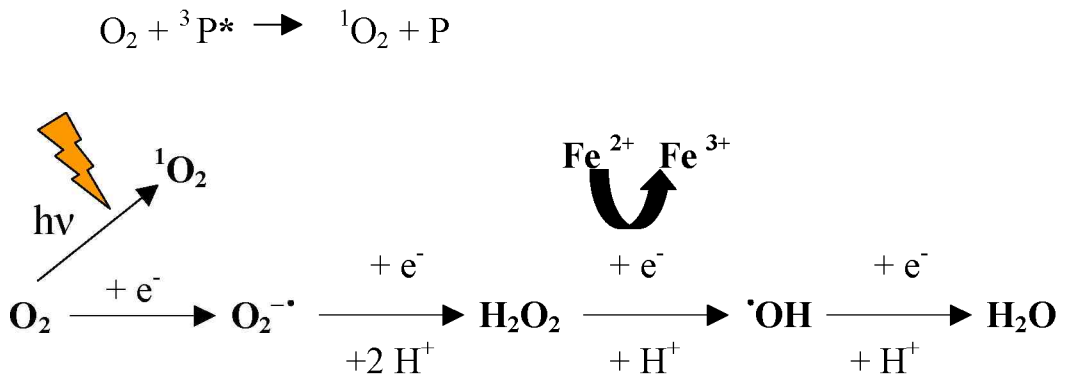

Fig 1.4. Pathways of oxygen activation either by excitation energy transfer or monovalent reduction.

1.3. Cellular production sites of reactive oxygen species

Reactive oxygen species are normally metabolic products existing in all aerobic cells and have essential functions. Their production in plants is controlled by the action of a dynamic system of different defense strategies to avoid the damaging effect of ROS. Plants have evolved different avoidance strategies, anatomical, physiological adaptation mechanisms, enzymatic and non-enzymatic defense in order to prevent damage by ROS (Halliwell, 1999). Low levels of ROS are regulated in order to carry out signaling processes and several pathways exist in plants to detoxify the ROS produced in excess, especially during stress. Oxidative stress occurs only when the interplay between the steady state ROS concentration and of their modulating enzymes is disturbed by an exogenous factor and the capacity of the antioxidant network is overwhelmed by the excess ROS. When the production of activated oxygen species is kept under tight control, they perform crucial roles in the cells.

Since plants cannot leave their ambient environment, they have to avoid various stress effects. Avoidance is an important defense strategy of plants to alleviate the effects of various stresses, by short-term anatomical changes, such as leaf movement (Nouges and Baker, 2000), curling, stomata closing (Maier-Maecker, 1999, Tabaeizadeh, 1998, Cornic, 2000, Lawlor, 2002,) and long-term genetic adaptations such as stomata hiding into special structures, by developing dense leaf hairs on the epidermis or leaf area changes. The metabolism of plants may also adapt to specific stress conditions, by the induction of the C4 and CAM-type of metabolism (Luttge, 2002, Noctor et al., 2002). The rearrangement of the photosynthetic apparatus (Mullineaux and Karpinski, 2002) is also a way of protection against photo-oxidation, for example the uncoupling of the light harvesting complexes from the photosystems (Zolla and Rinalducci, 2002) in case of excess irradiation, or rearrangement of the chloroplasts in the cell (Park et al., 1996). Chloroplasts move inside the cell in response to the intensity and direction of the incident light (Wada et al., 1993). The development of large number of smaller chloroplasts is favored instead of larger chloroplasts by the effectiveness of chloroplast rearrangement (Jeong et al., 2002). Thylakoid membrane-reorganization is an adaptive strategy to alleviate the damaging effect of heat stress (Gounaris et al., 1984). The antioxidant distribution between

bundle sheet and mesophyll cells is changed when plants are exposed to low temperature (Pastori et al., 2000), the size of antioxidant pool in maize seedlings was proved to be modified significantly when exposed to UV irradiation (Carletti et al., 2003). A wide variety of antioxidant enzymes are up-regulated under stress conditions (Panagopoulos et al., 1990, Costa et al., 2002, De Gara et al., 2003).

Those cellular compartments, where the activation of oxygen is possible, have the potential to become sources of ROS. Therefore chloroplasts, mitochondria, the endoplasmatic reticulum and the cell walls are sites of oxygen activation.

Since our work was focused only on the study of the effect of light stress on the photosynthetic apparatus, at the level of ROS production, we present only the chloroplast localized processes in more details, and give only a brief overview of other cellular ROS-generating processes.

1.3.1. Chloroplasts as major sources of ROS formation

Oxygenic photosynthesis is one of the major sources of active oxygen evolution in plant cells, by maintaining high oxygen concentrations in the environment of the photosynthetic electron transport. At the level of electron transport, agents with high oxidizing and reducing potential are formed, which may promote ROS formation. Since the electron transport system is embedded into lipid membranes, the probability of peroxidation reactions of the unsaturated fatty acids is high. Several sites of ROS formation have been identified at the level of electron transport.

1.3.1.1. Overview of the oxygenic photosynthesis

The photosynthetic membranes of plants convert the energy of solar radiation into chemical energy of ATP and NADPH, which are later used in the energy-requiring biochemical processes of CO_2 reduction to carbohydrates. The first step of photosynthesis is the absorption of light energy of the photosynthetically usable (photosynthetically active radiation, PAR) part of the solar irradiation by the chlorophyll and carotenoid containing antenna complexes (Kühlbrandt, 1994), which rapidly transfer energy to the reaction centers that initiate photochemical reactions

(Anderson and Styring, 1991). The absorbed quanta are transferred with approximately 90 % efficiency from the antenna system to the reaction center complexes, due to the organization of the pigments and their binding proteins (Kühlbrandt et al., 1994). The energy transformation step takes place within the reaction centers, where the primary photochemical reaction, the charge separation occurs between P_{680} and pheophytin (Pheo), leading to P_{680}^{+}/$Pheo^{-}$ charge pair. The redox components of the electron transport chain, redox active tyrosine, P_{680} reaction center chlorophyll dimer, pheophytin, and the plastoquinone acceptors Q_A and Q_B are bound to the the key-reaction center proteins of PSII, D1 and D2 (Barber et al., 1997, Barber, 1998, Barber and Kuhlbrandt, 1999, Zouni et al., 2001, Rutherford and Faller, 2001). The electron of $Pheo^{-}$ resulting from the primary charge separation is transferred to a permanently bound plastoquinone acceptor, the Q_A (Fig. 1.5.).

Q_A is a single-electron acceptor, from which the electron is transferred to the mobile Q_B plastoquinone acceptor, which works as two electron acceptor. Upon receiving a second electron, Q_B becomes fully reduced and protonated in two turnovers of the reaction center. Photosystem II (PSII) complex drives two chemical reactions: the oxidation of water and subsequent reduction of plastoquinone (Fig. 1.5.). The electron transferred to Q_A is substituted with other electrons from the activity of the water-oxidizing complex (Fig. 1.5.). Photosystem II is the only known protein complex that can oxidize water, resulting in oxygen evolution to the atmosphere. Water oxidation requires two molecules of water and involves thus four turnovers of the reaction center. The results of the process are: one oxygen molecule, four protons and four electrons.

Electrons are further transferred from the plastoquinone acceptors to the cytochrome b_6/f complex, from where with the participation of a mobile plastocyanin molecule, localized at the lumenal side of the thylakoid membrane, are transferred to Photosystem I (PSI) complex (Fromme et al., 2001). In the PS I reaction center the primary electron donor is a chlorophyll *a* dimer, P_{700}, the acceptors are A_0, a chlorophyll monomer, a phylloquinone molecule, A_1, and a Fe_4S_4 cluster. PSI further reduces ferredoxin, localized at the stromal side of the thylakoids. Ferredoxin reduces NADP, providing electrons for NADPH production (Fig. 1.5.).

The two photosystems overall contribute to the formation of proton gardient, electrochemical potential between the stromal and lumenal sides of the thylakoid

membranes, which by the functioning of the ATP-synthase complex leads to ATP formation. The chemical energy carriers, NADPH and ATP formed during the light-reactions of the photosynthesis are utilized by Calvin-cycle, for carbon assimilation. Ribulose biphosphate carboxylase-oxidase (Rubisco) is the key enzyme of the Calvin cycle, catalyzes the incorporation of CO_2 into ribulose-1,5-diphosphate.

In natural environments, both the intensity and the spectral composition of the ambient light fluctuate with time. The amount of energy reaching the photosystems is regulated by the distribution of the light harvesting pigment-protein complexes around the photosystems. If the spectral quality or the flux of the received light changes, a protein kinase phosphorylates the apoproteins of the light-harvesting LHCII complex. Upon phosphorylation, LHCII is uncoupled from PSII and acts instead as the light-harvesting antenna for PSI. Activation of an LHCII kinase therefore decreases absorption of light by PSII and increases absorption of light by PSI (Allen, 1981, Bennett, 1983, Allen, 1992, Allen, 1995, Allen and Nilsson, 1997). The harvesting of light energy is a strongly regulated process (Horton et al., 1996). The uncoupling of the LHCII antennas from PSII complexes has a very important protective role, by regulating the amount of light energy reaching the reaction center complexes. It is a very important mechanism in the effective utilization of light energy.

The electron transport components show lateral heterogeneity in their distribution in the thylakoid membranes. Functional PSII complexes are mainly localized in the stacked grana-regions of thylakoid membranes, while the majority of PSI complexes and the ATP-ase complexes are located in the stroma-thylakoids (Anderson, 1981, Anderson, 1982, Arvidsson et al., 1999, Allen and Forsberg, 2001).

Although light is essential for photosynthesis, it may as well become a stress factor. When the intensity of the light is higher than the utilizing capacity of the photosystems, strong oxidizing and reducing agents are formed, which promote the evolution of damaging ROS.

1.3.1.2. Singlet oxygen

Excess irradiation impairs the functioning of the photosynthetic electron transport and leads to the accumulation of excited chlorophyll triplets (Telfer and

Barber, 1989, Vass et al., 1992, Vass and Styring, 1992, Vass and Styring, 1993), $^1O_2$ is formed in photosensitised reaction between the excited chlorophyll triplet and molecular oxygen (Durrant et al., 1990, Macpherson et al., 1993, Telfer et al., 1994).

Plants prevent the production of $^1O_2$ by decreasing the probability of triplet chlorophyll formation or by eliminating the already formed triplet. When linear electron flow function is intact, chlorophyll molecules in triplet state do not accumulate. Plants usually minimize the possibility of triplet formation by dissipating the excess energy as heat, accompanied by a decline in the chlorophyll fluorescence yield, called non-photochemical quenching of chlorophyll fluorescence. The proton gradient formed under high intensity illumination leads to the activation of the xantophyll cycle, in which violaxanthin deepoxidation is effectuated by violaxanthin-deepoxidase enzyme to zeaxanthin through anteraxanthin (Gilmore and Yamamoto, 1993, Pfündel and Bilger, 1994, Demmig-Adams and Adams, 1992, Demmig-Adams and Adams, 1996). The reverse process of the cycle occurs under low light, when antheraxanthin and zeaxanthin are epoxidised by zeaxanthin-epoxidase to violaxanthin (Ruban et al., 2002). Violaxanthin-deepoxidase is localized at the lumenal side of the thylakoid and it is activated at a pH value below 6.5.

In the reaction center carotenoids are known to quench chlorophyll triplet states by triplet–triplet energy transfer, dissipating the potentially lethal excitation energy to the surroundings by intersystem crossing to the ground state (Young and Frank, 1996, Demmig-Adams, 1990), thus preventing the formation of toxic $^1O_2$. Carotenoids may confer protection to the reaction centers by directly quenching $^1O_2$ as well. Some studies hypothesize that beta-carotenoids are connected to the D1 protein turnover mechanism as well (Trebst and Depka, 1997, Depka et al., 1998).

Singlet oxygen has no specific scavenging enzyme, therefore it is neutralized by chloroplast localized $^1O_2$ quenchers, such as are ascorbate or tocopherol (Knox and Dodge, 1985, Trebst et al., 2002). Tocopherols are localized in the thylakoid membranes of the chloroplasts, being general antioxidants for membrane stability protection. The *in planta* concentration of tocopherols is light-regulated. Ascorbate is an effective $^1O_2$ scavenger and takes part in the regeneration of the membrane-bound antioxidants, such as tocopherol and reacts with superoxide, perhydroxyl and hydroxyl radicals as well (Halliwell and Gutteridge, 1985, Foyer et al., 1994).

For all scavengers it is extremely important to be localized near the site of ROS production, in order to neutralize them efficiently.

1.3.1.3. Superoxide

The reduction of molecular oxygen to superoxide is a characteristic of the illuminated functional thylakoids. When NADP is not available at the donor side of PS I, the electron derived from the photosynthetic electron transport chain may be intercepted by molecular oxygen, which is photoreduced to superoxide (Asada, 1992a). This process is known as the Mehler reaction (Mehler, 1951a, Mehler, 1951b). Most of the superoxide produced in the thylakoid membranes is oxidized back to molecular oxygen probably via plastocyanin or f-cytochrome mediated pathway (Asada, 1992a). This ROS shows little permeability towards lipid-bilayers, permeability coefficient of the phospholipid bilayer for $O_2^{-\bullet}$ was estimated to be $2x10^{-6}$cm s^{-1} at pH 7.3 and 25 °C (Takahashi and Asada, 1983). Membrane-localized superoxide anions may have longer half-life, in the range of several microseconds, compared to those evolved in aqueous phase (Takahashi and Asada, 1988).

Within the cells, superoxide dismutases (SODs) constitute the first line of defense against superoxide (Alscher et al., 2002). SODs are a family of metallo-enzymes, which catalyze the dismutation of $O_2^{-\bullet}$ into H_2O_2 and O_2 (McCord and Fridovich, 1969a, McCord and Fridovich, 1969b). SODs are present in all cell compartments where $O_2^{-\bullet}$ evolution is possible. Since phospholipid membranes are not permeable for $O_2^{-\bullet}$ (Takahashi and Asada, 1983) SODs have to be present near the site of ROS formation. Based on their metal cofactors, in eucaryotic cells three classes of SODs are distinguished: CuZnSOD present in the chloroplasts, peroxisomes and in cytosol, FeSOD is localized in the chloroplasts, MnSOD which is located in the mitochondria and in peroxisomes (Del Rio et al., 1983, Bowler et al., 1992). Superoxide has been involved in the mechanism of various oxidative stresses, for example temperature stress, senescence processes, water stress, herbicide-induced stress, stress induced by air pollutants and in photooxidative processes under chilling temperatures (McRae and Thompson, 1983, Hodgson and Raison, 1991). $O_2^{-\bullet}$ was hypothesized to be involved in the mechanism of light stress as well, which will be discussed in details in Chapter 4., as being in the main focus of our studies.

1.3.1.4. Hydrogen peroxide

Hydrogen peroxide in chloroplasts is generated by the dismutation of two $O_2^{-\bullet}$ molecules to H_2O_2 and O_2, catalyzed by superoxide dismutases. Hydrogen peroxide has the longest lifetime among ROS, in the millisecond range, therefore it can readily permeate membranes and was considered as the ideal candidate as a signal molecule (Van Camp and Inzé, 1998). Catalases (CAT) are heme-containing enzymes, which catalyze the decomposition of H_2O_2 into water and oxygen. Although catalases are not active in the chloroplasts, they are indispensable for ROS detoxification during stress, when high levels of ROS are produced (Willekens, et al., 1997).

The H_2O_2 derived from the $O_2^{-\bullet}$ produced in the Mehler reaction (Mehler, 1951a, Mehler, 1951b) is reduced by ascorbate-peroxidase (APX) to water (Fig 1.6 a), requiring ascorbate as a substrate (Asada et al., 1999) in the water-water cycle. APX is located in the stroma-thylakoid and the function of this enzyme is assured by a large, millimolar ascorbate pool (Asada, 1992b). The ascorbate-glutathione cycle is an important mechanism of ROS neutralization during normal metabolism but particularly during stress. Ascorbate is oxidized through ascorbate peroxidase (APX) activity to monodehydro-ascorbate radical (MDA). From MDA dehydroascorbic acid (DHA) is formed. Both MDA and DHA can be reduced to ascorbate by monodehydroascorbate reductase (MDAR) and dehydroascorbate reductase (DHAR) respectively (Asada, 1999). DHA reduction is coupled with the oxidation of the reduced form of glutathione (GSH) (Noctor and Foyer, 1998). GSH is a water-soluble tripeptide, containing a sulfhydryl group, and the oxidized product is glutathione disulfide (GSSG), in which a disulfide bond joins two molecules. The re-reduction of the GSSG is only possible in the presence of NAD(P)H. Glutathione, found in chloroplasts in 1-5 mM concentration is thus essential for the functioning of ascorbate peroxidase (Noctor and Foyer, 1998) (Fig. 1.6 b).

H_2O_2 produced in the cytosol is neutralized by the activity of glutathione-peroxidase (GPX) (Dixon et al., 1998). Reduced glutathione is oxidized to GSSG by H_2O_2, catalyzed by GPX. Oxidized glutathione is reduced back to GSH in a reaction catalyzed by glutathione reductase (GR). The reducing power for this reaction is supplied by NAD(P)H (Fig. 1.6 c.).

The balance between the superoxide-dismutase, ascorbate peroxidase and catalase activity in cells is critical for determining the steady state levels of $O_2^{-\bullet}$ and H_2O_2 (Bowler et al., 1992). This balance is effective in preventing the formation of the highly toxic hydroxyl radical in Fenton's reaction, catalyzed by metal ions (Asada and Takahashi, 1987). The cooperation of the antioxidants in cascades is advantageous, because they are constantly regenerated (for example ascorbate from MDA, and GSH from GSSG) and they can scavenge again the free radicals.

H_2O_2 is involved in the mechanism of a large variety of stress conditions, may act as a signal molecule because has a lifetime long enough for free diffusion and as being an uncharged molecule is able to penetrate membranes. H_2O_2 molecules were proved to be involved in the mechanism of water stress, herbicide induced stress, and are believed to be key regulators of many oxidative processes (Prasad et al., 1994, Foyer et al., 1997, Van Bereusegem et al., 2001). The possible involvement of H_2O_2 in the mechanism of light stress will be discussed in Chapter 4.

1.3.1.5. Hydroxyl radicals

$^{\bullet}OH$ is a biologically relevant radical, since it is the most damaging ROS with the shortest lifetime in the range of picoseconds. The high reactivity of $^{\bullet}OH$ was attributed to the lack of specific scavenging enzyme and to its short lifetime. Plants can only protect themselves from $^{\bullet}OH$-induced oxidative damage by the prevention of its formation, therefore the potential precursors, superoxide and hydrogen peroxide are neutralized. $^{\bullet}OH$ formation may be prevented by sequestrating components such as iron, which could catalyze $^{\bullet}OH$ evolving reactions. It was shown, that transgenic tobacco plants, which overexpressed alfalfa ferritin in vegetative tissues, retained photosynthetic function upon free radical toxicity generated by excess iron or paraquat treatment longer than control plants. The ferritin accumulating plants exhibited tolerance to necrotic damage caused by viral and fungal infections as well. Ferritin may protect plant cells from oxidative damage induced by a wide range of stresses by lowering intracellular iron and thus hydroxyl radical concentrations (Deák et al., 1999).

$^{\bullet}OH$ radical was proved to be involved in various stress mechanisms, among which its role in light stress will be discussed in Chapter 4.

1.3.1.6. Lipidperoxyl radicals

Biological membranes are organized structures composed of lipid bilayers incorporating structural and functional proteins. Biomembranes regulate the flow of materials and information between different regions of cells and between a cell and its environment. The membrane damage induced by the attack of various ROS on the lipid or protein moieties can be highly deleterious. $^{\bullet}OH$ may initiate radical chain reactions with organic molecules, particularly with polyunsaturated fatty acids of membrane lipids. In this reaction, a lipid radical is stabilized by molecular rearrangement, therefore a conjugated diene is formed, which is able to react with molecular oxygen further, yielding peroxyl radical ($ROO^{\bullet}$) (Cadenas, 1989, Buettner, 1993). The peroxyl radical itself may abstract hydrogen from an other unsaturated fatty acid, and the reaction propagates, which may be terminated by the reaction of two radicals (Wagner et al., 1994, Girotti, 2001). Tocopherol is a lipophylic antioxidant and it is synthesized in the chloroplasts, functions as a chain breaking antioxidant, preventing lipid peroxidation. Upon reacting with lipid peroxides, alpha-chromanoxyl radical is formed, this latter one being less reactive than the original lipidperoxyl radical. The alpha-chromanoxyl radical is oxidized back to vitamin E by ascorbate and NADP (Halliwell and Gutteridge, 1999).

1.3.2. Cellular ROS sources other than chloroplasts

Since mitochondria also possess electron transport chains, the leakage of electrons and activation of oxygen becomes likely in this cell compartment as well. Most oxygen is consumed in mitochondria by the cytochrome-c oxidase and oxygen is reduced at the site of alternative oxidase as well. NADH dehydrogenase was shown to be involved in the synthesis of $O_2^{-\bullet}$ and H_2O_2 in mitochondria (Møller, 2001). Detoxification reactions by cytochromes, especially by cytochrome P_{450} in the endoplasmic reticulum may also lead to $O_2^{-\bullet}$ generation (Halliwell and

Gutteridge, 1985) and peroxisomes were shown to be sites of H_2O_2 production. Lipid catabolism, the beta-oxidation of fatty acids yields H_2O_2, purine decomposition involves the presence of $O_2^{-\bullet}$. Glycolate-oxidase produces H_2O_2 in a two-step electron transfer reaction from glycolate to oxygen (Del Rio et al., 1998).

The activity of NADPH oxidase in the plasma membrane leads to $O_2^{-\bullet}$generation and NADH oxidase has also been identified to produce ROS (Morré et al., 1988). It is activated by auxin, and its role is proposed to be in cell wall acidification and auxin-dependent elongation. As sources of H_2O_2 the pH-dependent cell wall peroxidases, amine oxidases have been proposed in the apoplast (Bolwell and Wojtaszek, 1997).

Reactive oxygen species are considered in a variety of roles: as primary elicitors of damage or as important mediators of cellular damage. Lately their role as signal transduction molecules has also been shown. They have critical function in incompatible plant-pathogen interactions in plant defense responses. Studies have hypothesized that H_2O_2 and $O_2^{-\bullet}$may act as both local and systemic signals in pathogen defense (Bolwell and Wojtaszek, 1997). Reactive oxygen species have important regulating role in the process of programmed cell death, are produced in response to a variety of abiotic stresses, such as extreme temperature, UV irradiation, ozone exposure, osmotic stress or drought (Prasad et al., 1994, Mackerness et al., 2001). They may induce at the same time the regulation of certain genes (Desikan et al., 2001, Mackerness, 2000) and may as well activate protein-kinase cascades (Hirt, 1997). Several of the plant stress responses overlap, suggesting common signalling factors, with ROS (Foyer et al., 1997) and nitric oxide (Durner et al., 1998, Durner and Klessig, 1999) being the most likely candidates. ROS play a central role in the coordination of plant responses and are involved in acclimation responses (Prasad et al., 1994) and cross-talk (Bowler and Fluhr, 2000), where the response to one stress confers greater resistance to a second similar exposure, or greater resistance to exposure to another stress. For example, sub-lethal dose of ozone or UV irradiation conferred increased resistance to virulent pathogen infection (Sharma et al., 1996). Transgenic tobacco plants expressing alfalfa aldose/aldehyde reductase enzyme were considerably more tolerant to oxidative damage caused by paraquat and heavy metal

stress. These plants were also more resistant to drought stress (Oberschall et al., 2000).

ROS perform a wide array of roles in plant cells, and there is an apparent controversy in their roles. ROS are necessary for the survival of the plants, performing signal transduction and gene-activating processes, but they can as well be lethal when they are overproduced, due to the disturbance in the balance between their production and removal. The study of the roles of ROS in plants' life and their damaging effect is an important field of plant stress physiology.

1.4. Stress by excess photosynthetically active radiation

For plant survival light is essential, since it is the driving force of photosynthesis. Plants utilize the photosynthetically active radiation (PAR: 400-700 nm) wavelength range of the sunlight. Under lower PAR fluxes the received photon energy does not exceed the energy utilizing capacity of the chloroplasts and the rate of ROS generation is low and kept under tight control by the ROS scavenging molecules. Light itself may become a stress factor for plants when over-saturates the photosynthetic light reactions, by initiating processes which lead to serious structural and functional damage of the photosynthetic machinery.

The intensity of light reaching the Earth's surface is not constant, shows intense seasonal and diurnal variations, and is influenced by different factors. Under field conditions leaves are often exposed to high light intensities close to 2000 μmol $m^{-2}s^{-1}$, thus photoinhibition by excess irradiation is a very common process. When PAR intensity is higher, or the antioxidant network is impaired by environmental stress conditions, the balance between the pro-oxidant - antioxidant status of the cell is disturbed and ROS production increases beyond the capacity of the antioxidant network to cope with it. Under photoinhibitory conditions, photosystem II is preferentially damaged (Powles, 1984, Barber and Andersson, 1992, Barber, 1994, Aro et al., 1993). Photoinhibitory damage may occur through two different mechanisms: either by acceptor side-induced or by donor side-induced processes.

1.4.1. Acceptor-side induced photoinhibition

The acceptor-side induced photoinhibition occurs under saturating intensity illumination and aerobic conditions. This process results in decreased photosynthetic oxygen evolution (Powles, 1984). In acceptor side-induced photoinhibition the inhibition of the electron transfer from Q_A to Q_B was attributed to the lack of reducible plastoquinone molecules, since the plastoquinone pool and the Q_B became fully reduced (Ohad et al., 1990, Vass et al., 1992). When the plastoquinone pool is fully reduced, relatively stable double reduced Q_A molecules are formed. Q_A^{2-} is non-physiological, is only formed under photoinhibition. After protonation, it leaves the binding site and thus promotes triplet chlorophyll formation (Styring et al., 1990, Durrant et al., 1990, Vass et al., 1992, Vass and Styring, 1992, Vass and Styring, 1993, Barber and Andersson, 1992). The triplet-state reaction center chlorophyll ($^3P_{680}$) decays to ground state in the presence of molecular O_2 by energy transfer reactions, promoting $^1O_2$ formation. The highly reactive $^1O_2$ damages the protein environment, alters the D1 core protein of PSII (Aro et al., 1990, Durrant et al., 1990, Vass et al., 1992, Vass and Styring, 1993, De Las Rivas et al., 1993, Mishra et al., 1993, Macpherson et al., 1993, Telfer et al., 1994, Hideg et al., 1994 a, Hideg et al., 1994 b, Kettuunen et al., 1996).

D1 protein degradation is a two-step process: first the D1 protein is damaged by photochemical events its conformation is changed, which in the second step is recognized and degraded by proteases. The steps of the proteolysis are GTP and ATP dependent (Aro et al., 1992, Spetea et al., 1999, Spetea et al., 2000). Characteristic fragments of D1 protein degradation are 23 kDa N-terminal and 10 kDa C-terminal products (Greenberg et al., 1987, Cánovas and Barber, 1993). After selective degradation of the D1 reaction center protein of PS II, more general membrane and protein damage occurs (Melis, 1999, Barber and Andersson, 1992). Other studies identified 24 kDa and 16 kDa C-terminal, and 18 kDa N-terminal fragments (De Las Rivas et al., 1992, Kettuunen et al., 1996). Due to this process PSII is disintegrated (Hundal et al., 1990, Barbato et al., 1991, Barbato et al., 1992).

The antenna proteins of the light harvesting complexes are severely damaged under photoinhibitory conditions. Singlet oxygen takes part in the degradation of the

antenna complexes to monomeric state, as a physiological defense response of the plant (Rinalducci et al., 2004).

1.4.2. Donor-side induced photoinhibition

Unlike the acceptor side-induced process, donor side-induced photoinhibition occurs under anaerobic conditions, and lower PAR intensities. This mechanism is the characteristic of donor side impaired thylakoids, when photoinhibitory illumination was preceded by inactivation of the water-oxidizing complex (Blubaugh et al., 1991). Strong, long-lived oxidants are produced by the primary charge separation (Telfer and Barber, 1989, Aro et al., 1993). Under donor side-induced photoinhibition the main D1 degradation fragments were determined to be 24 kDa C-terminal and 9 kDa N-terminal fragments, at the lumen exposed loop of the protein (Barbato et al., 1991, Barbato et al., 1992).

In vivo studies showed that photoinhibitory irradiances damage PSI as well, especially when stress factors are present together (for example excess light and chilling temperatures) (Tjus et al., 1998, Tjus et al., 1999, Sonoike and Terashima, 1994). Under these conditions, both PSI and PSII were vulnerable to photoinhibition in thylakoid membranes and chloroplasts (Inoue et al., 1986, Sonoike, 1995). Damage may occur even at ambient temperatures in isolated systems. PSI is more protected and less vulnerable to photoinhibition under non-chilling temperatures *in vivo*, than PSII. During the thylakoid isolation some protectants, which act *in vivo*, are lost. The combination of light with other stress conditions (for example extreme temperature or UV-B irradiation) may lessen the effectiveness of the protecting energy dissipating pathways as well the ROS neutralizing capacity of antioxidants. In stressed plants the ROS level increases.

Although photoinhibition damages the photosynthetic electron transport, plants survive photoinhibitory damage through complex repair processes, involving degradation and *de novo* synthesis of the reaction center proteins. This is a very fast and dynamic mechanism, since the halftime of D1 protein turnover can be as short as 30 minutes. D1 protein turns over much faster than any other subunit of photosystem II. The mechanism of D1 protein repair implies proteolytic cleavage of the damaged protein, its removal, de novo synthesis, reinsertion in the membrane, and replacement

of the damaged protein with a newly synthesized one (Kyle et al., 1984, Mattoo et al., 1984, Adir et al., 1990, Hundal et al., 1990, Aro and Andersson, 1993, Sundby et al., 1993). When PSII components are damaged, the PSII complexes diffuse out from the grana- to the stroma-tylakoids, where they are disassembled, and the damaged D1 proteins are later replaced with new, functional proteins (Aro and Andersson, 1993).

Plants have developed several molecular mechanisms to control the amount of energy reaching to the reaction centers. Excess radiation energy is dissipated through the xantophyll cycle (Demmig Adams, 1990, Demmig-Adams and Adams, 1996, Horton et al., 1996). Besides dissipating the excess energy, the state of the LHCII also regulates the amount of light energy reaching the reaction centers (Fork and Satoh, 1986). When LHCII proteins undergo phosphorylation (Gal and Ohad, 1997, Allen and Nilsson, 1997) the antenna is detached from PSII, diffuses into the stroma-thylakoid, decreasing the light harvesting capacity of PSII. Carotenoids located in the reaction centers minimize the damaging effect of the possible ROS production, either by direct triplet chlorophyll quenching or by scavenging of the deleterious singlet oxygen. The cyclic electron flow around PSII alleviates the potential damage, decreasing the accumulation of agents with high oxidative potential (Barber and de Las Rivas, 1993). The PSII/PSI ratio is regulated at the level of gene expression in thylakoids (Allen, 1993, Pfannschmidt et al., 1999, Pfannschmidt et al., 2003).

In the mechanism of both acceptor side-, and donor side-induced photoinhibition various ROS were involved, when the balance between the effectiveness of the protective mechanisms and ROS yielding reactions was disturbed. Highly toxic species are formed, when excited pigments, such as triplet excited chlorophyll molecules take part in energy-transfer reactions to oxygen, or if electron leakage from the electron transfer pathway to oxygen becomes possible. At the level of ROS production, photoinhibition is an intensely studied process. Reactive oxygen species are very important in many biological processes, but their extremely short lifetime makes them hard to detect. Several methods have been developed to identify ROS *in vitro*, but their *in vivo* detection meets several technical difficulties. Photoinhibition induced protein damage was found to be accompanied by hydroxyl radical formation (Hideg et al., 1994a) in the donor side-induced mechanism and by $^1O_2$ (Hideg et al., 1994a, Krasnovsky, 1994, Telfer et al., 1994) evolution in the

acceptor side-induced photoinhibition *in vitro*, by various detection methods. *In vivo* $^1O_2$ evolution was also in the focus of several studies (Hideg et al., 1998, Hideg et al., 2000b, Hideg et al., 2001), and even the induction of superoxide radical production was hypothesized *in vivo* (Fryer et al., 2002), but not *in vitro*. Superoxide radicals were not detected by EPR spectroscopy as promoters of photoinhibitory damage in spinach thylakoids (Hideg et al., 1995), though they have been supposed to participate in photoinhibition as products of electron transport to oxygen both in functioning (Miyao, 1994) and in donor-side impaired PSII (Chen et al., 1995), and recently in PSI (Tjus et al., 2001). The involvement of ROS other than singlet oxygen and superoxide in the mechanism of photoinhibition was also studied. Isolated Ca^{2+} and Cl^- depleted PSII particles with functional water splitting complex produced $^{\bullet}OH$ radicals and superoxide upon illumination on the acceptor side, and Cl^- depleted ones additionally produced $^{\bullet}OH$ originating from H_2O_2 on the donor side of PSII (Arató et al., 2004).

Due to the lack of consensus between the different *in vitro* and *in vivo* studies our goal was to establish *in vivo*, by using a direct detection method adapted for plant stress studies, the nature ROS types other than singlet oxygen, if any, involved in the mechanism of photoinhibition.

1.5. Stress by ultraviolet radiation

Photosynthetic organisms need sunlight and therefore they are also exposed to the UV photons of the solar radiation. The depletion of the ozone layer - which selectively absorbs part of the UV-B radiation - is a source of concerns about the biological impact of the increased solar UV fluxes on the biota (Kerr et al., 1993). In general, biological damage is stronger at shorter wavelengths, thus a minor increase in the total UV-B irradiation may cause significant damage to living systems (Tevini, 1988, Caldwell et al., 2003). In this way the increase in the UV/PAR ratio of solar radiation received may become a stress factor for plants.

Ultraviolet-B radiation (280–320 nm) is an environmental challenge affecting a number of metabolic functions through the generation of reactive oxygen species. Higher plant species show a wide variety in their response to elevated UV-B

radiation. UV stress has many direct and indirect effects on plants: it may cause plant morphogenetic effects, which can in turn modify the architecture of plants and the structure of the vegetation. UV-B radiation may alter pigment composition, influences the adaptive mechanisms of plants and alters on long term the biomass production (Sullivan and Teramura, 1990, Teramura and Sullivan, 1990, Teramura and Sullivan, 1994). Of much importance is the response of agriculturally important plant species, for example cotton was proved to loose fiber quality upon UV-B exposure (Gao et al., 2003).

Although plants can tolerate lower levels of UV radiation, above a certain threshold it induces active oxygen mediated oxidative stress, leading to severe functional disorders. However, the tolerance threshold is species-dependent and the effectiveness of acclimation mechanisms versus the damaging processes is also influenced by the developmental stage of the plants, younger leaves are less damaged than older ones (Mackerness et al., 1998).

High intensity UV-B irradiation damages the majority of essential cellular constituents. UV-B targets nucleic acids in plant cells, resulting in a multitude of DNA photoproducts, mainly cyclobutane-pyrimidine dimers, and to a lesser extent pyrimidine (6-4)-pyrimidone dimers (Britt, 1996, Pang and Hays, 1991). The UV-B induced DNA damages are repaired via light-dependent photo-reactivation (Britt, 1996), by the action of photolyase enzymes (Waterworth et al., 2002). Amino acids and proteins are also prone to damage by UV radiation, due to the strong tyrosine, tryptophane, phenylalanine absorption in the UV region (Vladimirov et al., 1970). Photolysis of cysteine residues results in the breaking of the disulfide bonds, which stabilize the tertiary structure of proteins (Creed et al., 1984). Therefore, UV-B irradiation may alter the function of proteins and the activity of the enzymes by modifying their structure. The key-enzyme of carbon fixation in plants, Rubisco (Strid et al., 1990), the ATP-ase (Murphy, 1983, Zhang et al., 1994) and the violaxanthin deepoxidase (Pfündel et al., 1992) are damaged by UV radiation via cysteine modification. Lipids, especially phospho- and glycolipids with isolated or conjugated double bonds are prone to UV induced photochemical modification under aerobic conditions (Panagopoulos et al., 1990, Kramer et al., 1991). Thus, UV-B irradiation damages membranes, and the lipid-peroxyl radicals formed in this process may initiate further radical reaction cascades.

1.5.1. The effects of UV-B radiation on photosynthesis

Almost all redox- and protein components of the photosynthetic electron transport are sensitive to UV-B (Vass, 1996). The impairment of the photosystems is dose dependent, preferentially PSII (Bormann, 1989, Strid et al., 1990) is damaged, PSI being only affected by higher intensities (Brandle et al., 1977). Due to UV-stress, reduction in dry weight and total chlorophyll was also reported (Fiscus and Booker, 1995).

The action sites of UV-B damage have been hypothesized to be the manganese cluster of the water-oxidizing complex, accompanied by damage of the Q_A and Q_B, and of the redoxactive Tyr_Z and Tyr_D (Greenberg et al., 1989, Renger et al., 1989, Vass et al.,1996). Although the majority of redox and protein components are damaged, the predominantly UV-B sensitive site of PSII is the water oxidizing complex, rather than the acceptor side (Vass et al., 1996, Spetea et al., 1996). The core proteins of PSII, D1 and D2 are degraded to specific fragments: D1 is cleaved into a 20 kDa C-terminal and a 12-13 kDa N-terminal fragment, different from those appearing when the plant is exposed to excess PAR, indicating different degradation patterns (Friso et al., 1994a). The production of these fragments has been detected in isolated membranes (Friso et al., 1994a), and in isolated reaction centers (Friso et al., 1995). Because the primary cleavage site of D1 is located close to the Mn binding site, the primary sensitizer of D1 damage is considered to be the water-oxidizing complex, but direct UV-B damage to the protein matrix may also occur. A quinone-independent pathway has been hypothesized for the fragmentation of the D2 protein, because D2 loss was also observed in PSII reaction-center complexes lacking quinone acceptors (Spetea et al., 1996). The protein environment in the vicinity of the Mn cluster may also be damaged by free radicals. Since the dominating free radical species in UV-B irradiated PSII preparations have been found to be hydroxyl and carbon-centerd radicals (Hideg and Vass, 1996), these may act as inducers of D1 damage. Most of the studies which investigated the effect of UV-B irradiation on PSI concluded that compared to damage of PSII, PSI is rather unaffected (Brandle et al., 1977). This difference in the sensitivity of the two photosystems to UV-B irradiation may reside in the fact, that the water-oxidizing complex is linked to PSII and the

redoxacive tyrosines are also part of the PSII complex. The cytochrome b_6/f complex is mainly unaffected by UV-irradiation (Strid et al., 1990).

In an environmentally relevant background of photosynthetically active radiation, the UV-B (but not the UV-A) induced degradation of the core proteins D1 and D2 was synergistically accelerated (Jansen et al., 1996). The counteraction of UV radiation with PAR may have damaging effect on the repair mechanisms of the cell as well: the recovery from photodamage may be hampered by the UV-B induced destruction of unsaturated membrane lipids (Kramer et al., 1991). Low intensities of UV radiation and low PAR levels may act synergistically enhancing photodamage of PSII by inhibiting the D1 repair cycle (Jansen et al., 1996).

UV-B irradiation may affect the efficiency of light harvesting as well, the light harvesting complex LHCII, which is responsible for the absorbtion of light and energy transfer to the reaction centers is sensitive to UV-B irradiation. LHCII functionally disconnects from PSII in UV-B exposed thylakoids, and UV-B radiation decreases the mRNA transcription level of the *cab* gene, responsible for the synthesis of the chlorophyll a/b binding proteins of LHCII (Jordan et al., 1991). The excess energy dissipating mechanisms of plants may also be obstructed by UV-B induced damage to the violaxanthine-deepoxidase, which may lead to inoperative xantophyll cycle (Pfündel et al., 1992).

1.5.2. UV-B radiation induced reactive oxygen species

UV-B may impair the function of proteins or the defense system of the plant by the inactivation of the radical scavenging enzymes (Strid, 1993). ROS induction is known to be the early plant response to UV-B exposure. High levels of UV-B radiation induce lipid peroxidation and membrane damage by the action of various reactive oxygen species (Takeuchi et al., 1995). In isolated thylakoid membranes, UV-B exposure triggered hydroxyl radical generation was detected by EPR spectroscopy, but the presence of carbon centerd (methyl-like), and peroxyl radicals (Hideg and Vass, 1996, Hideg et al. 1999) were also reported. Singlet oxygen was not found in the same preparation. UV-B induced D1 protein degradation was assigned to hydroxyl radicals (Hideg et al. 1999). Several indirect *in vitro* and *in vivo* studies also point the oxidative nature of UV-B stress, and hypothesize the possible production of

ROS other than hydroxyl and carbon-centered radicals. Long UV-B treatments of about 6–30 h induced stress related genes in SOD sprayed leaves (Mackerness et al., 1998, Mackerness et al., 2001). The induction of superoxide radical evolution was assumed in these *Arabidopsis thaliana* leaves. UV-B treatment activated the plants' own superoxide dismutase enzymes in higher plants (Rao and Ormrod, 1995), as well as in *Chlorella* (Malanga and Puntarulo, 1995). These data suggested increased $O_2^{-\bullet}$ production under UV-B stress under various experimental conditions. UV-B radiation triggered the rise of ultra-weak luminescence in *Brassica napus* leaves, an indicator of oxidative membrane damage (Cen and Björn, 1994). Upon UV-B exposure, increased amount of ascorbate radicals was also detected *in vivo* (Hideg et al., 1997).

1.5.3. UV defense mechanisms

Although ultraviolet radiation may induce severe morphological and physiological disorders, plants may acclimate to lower levels of UV-B by various morphological and functional changes, which favor their survival. As a whole-plant response leaf curling and thickening was reported (Bornman and Vogelman, 1991). Thickening of the epidermal layer increases the UV absorbtion pathway and has also been reported as a UV response (de Lucia et al., 1992). The induction of stomata closure to regulate the gas-exchange, redistribution of chlorophyll or hypocotyl elongation (Kim et al., 1998) are also important mechanisms of adaptation to low UV irradiation. Lower doses of UV-B (but not UV-A radiation) radiation caused tendril coiling in *Pisum sativum* (Brosché and Strid, 2000). These morphological changes induced by lower levels of UV-B are important in the adaptation process (Rozema et al., 1997).

Plants have various sensitivity to UV irradiation, certain species have adapted more successfully to higher UV fluences than others. Tolerance and acclimation to UV-B mainly depends on the balance between the damaging reactions and antioxidant efficiency or repair responses. Acclimation is a complex process, which involves various signalling pathways (Mackerness et al., 2001). Plants respond to increased UV irradiation by down-regulation of photosynthetic genes (Jordan et al., 1991) and up-regulation of those genes, which are associated with the defense against stress.

Induction of flavonoid biosynthesis is one of the most extensively characterized plant responses to UV-B irradiation (Jansen et al., 1998). For example the expression of calchone synthase, which is the key enzyme of flavonoid biosynthesis was found to increase within a few hours after the exposure to UV-B (Chappel and Hahlbrock, 1984). Low UV fluences stimulate the up-regulation of antioxidant- and flavonoid biosynthetic genes of the phenylpropanoid pathway, which result in the accumulation of flavonoids and sinapic esters (Day and Vogelmann, 1995).

Plants protect themselves from the harmful radiation by synthetizing flavonoids, which accumulate mainly in the upper epidermal cell layer of leaves, and act as internal filters and by making adjustments to the antioxidant systems at both cell and whole organism level. Flavonoids are believed to act not just as UV-screens, but are effective antioxidants as well (Bornman, 1989, Takeuchi et al., 1996, Rozema et al., 2002). The use of transgenic plants is a powerful tool in plant stress studies. Plants having reduced ability to screen out the UV radiation show increased DNA damage, the accumulation of cyclobutane pyrimidine dimers increased (Mazza et al., 2000). *Arabidopsis* plants lacking phenolic UV-screens were more sensitive to UV irradiation than wild type ones (Landry et al., 1995).

In *Vicia faba* it was shown that two flavonoids particularly responded to enhanced UV-B. Quercetin and kaempferol were UV-B inducible, both being mainly located in epidermal cells. In addition to UV-screening, quercetin may also act as an antioxidant. (Rozema et al., 2002). Other studies suggest that carotenoids and flavonoids may also be involved in plant UV-B photoprotection (Frederick and Lubin, 1988). Different alkaloid-type compounds, such as polyamines may also contribute to UV tolerance. It was found, that there is positive correlation between the tolerance to UV-B and the elevated level of polyamines in soybean (Kramer et al., 1991).

Low levels of UV-B irradiation lead to a reinforcement of the antioxidant system as one of the plants' adaptive responses. Glutathione showed enhanced turnover under UV-B irradiation, but no net change in its concentration (Masi et al., 2002). Following UV-B exposure, the tocopherol content was lower in maize seedlings pointing to the membrane environment as a primary target of UV-B radiation. On the other hand, the water-soluble antioxidant content was largely unaffected (Carletti et al., 2003). Radicals formed through lipid peroxidation in thylakoid membranes due to UV-B irradiation are scavenged effectively by alpha-

tocopherol (DeLong and Steffen, 1998). In *Spirodella* exposed to supplemental UV-B, the activity of scavengers increased very fast, as an early defense response. Scavenger activity decreased in the frame of a few days, but the already achieved tolerance did not become altered, suggesting the replacement of the original early mechanism, by an other one, believed to be the accumulation of UV-screening pigments (Jansen, 1998).

Proline accumulation in plants exposed to UV irradiation may also protect cells against peroxidation processes (Pardha Saradhi et al., 1995).

ROS induction, known as one of the early effects of exposure to high UV-B irradiation, leads to lipid peroxidation and membrane damages. Before adequeate shielding by flavonoids is achieved, these oxidizing agents have to be counteracted by antioxidants and protective pigments to prevent cellular damage. A chain reaction is proposed as response of maize plants to supplemental UV-B irradiation: as first step, while the synthesis of screening pigments in the epidermis proceeds, thylakoid membranes are oxidatively damaged. Then radicals are counteracted by the antioxidant system. Once concentrations of the UV-absorbing compounds in the epidermis were sufficient, antioxidant responses were no longer observable, showing that maize was able to prevent oxidative stress by UV-B irradiation by UV-screening (Carletti et al., 2003).

All low intensity UV-B irradiation induced plant adaptive responses are regulated by a widely studied, complex signalling mechanism. UV-B signaling pathways involve the participation of various ROS in plant tissues (Mackerness et al., 2000, Mackerness et al., 2001). Singlet oxygen has also been involved as a signalling molecule in the UV-induced pathogen-related gene induction mechanism (Green and Fluhr, 1995).

1.5.4 The effect of UV-A radiation on plants

While the damaging mechanism of UV-B radiation is in the focus of several studies, less information is available on the effect of UV-A, although the intensity of solar UV-A is many times higher than that of UV-B. Unlike UV-B, UV-A intensity is not attenuated by penetration through the atmosphere. The difference in the action site of UV-A and UV-B in photosynthesis has been intensely discussed, attributing

smaller damaging effect to the longer wavelength (UV-A) irradiation, than to the higher photon-energy UV-B (Turcsányi and Vass, 2000). Various plant responses to UV irradiation are in agreement on a lesser effect of the same dose of UV-A as compared of UV-B. UV-A stress inhibited approximately 5-10 times less the growth of oat plants than UV-B (Flint and Caldwell, 2003), and 2-3 times less UV-A induced DNA damage was shown in alfalfa seedlings, than in UV-B irradiated ones (Quaite et al., 1992). UV-A was found to be approximately 90% less efficient in inhibiting photosynthesis of *Rumex* leaves (Rundel, 1983) and the photosynthetic efficiency was lowered less in UV-A treated isolated chloroplasts (Jones and Kok, 1966) than in the corresponding UV-B treated ones. UV-A affected photosynthesis of isolated thylakoids (Turcsányi and Vass, 2000, Vass et al., 2002) and of green algae (White and Jahnke, 2002) in a similar way, as UV-B, although the extent of damage was not as intense as in the case of UV-B. UV-A was found less effective to cause radical-related symptoms than UV-B (Hideg et al., 1997, Cen and Björn, 1994).

UV-A has also been shown to inhibit plant growth, to accelarate leaf senescence and to impair PSII electron flow. In isolated thylakoids, UV-A irradiation damaged PSII, both at the donor and the acceptor side, via a mechanism similar to that induced by UV-B irradiation (Turcsányi and Vass, 2000). UV-A irradiation was shown to have no effect on the induction of stress related genes in SOD sprayed leaves (Mackerness et al., 1998, 2001).

Under field conditions stresses are usually present at the same time: for example, PAR may interact with both UV-B and UV-A, or high PAR fluxes are accompanied by high temperatures. The combination of stress factors damage the plants differently, as compared to the damages induced by stresses acting alone. Sometimes the combination of various stress factors may aide or hamper damage, antioxidant or repair mechanisms. Non-photoinhibitory levels of visible light acting simultaneously with UV-irradiation can ameliorate the UV-B effect (Warner and Caldwell, 1983).

Our work aimed to investigate in UV-stressed leaves the ROS production, to study the oxidative nature of UV-stress. We also aimed to compare the ROS generating efficiency of various UV-A and UV-B wavelengths in irradiated leaves, in

order to understanding the mechanism of UV induced damage. An other goal of our study was to compare the mechanism of stress by UV irradiation and photoinhibition at the level of ROS evolution.

2. AIMS OF THE STUDY

Since there is a lack of consensus regarding the nature of reactive oxygen species production induced by light stress, various ROS have been involved in the mechanism of both stress by excess photosynthetically active radiation and ultraviolet irradiation. The aims of our work were:

1. We aimed to introduce a sensitive, specific method for direct *in vivo* ROS detection, in plant stress studies. Therefore, we developed further a recently introduced technique, ROS detection by double (fluorescent and spin) sensors. Our aim was to characterize and to apply the sensors *in vivo*. We aimed to find sensors for ROS other than the previously studied $^1O_2$.

2. By applying a double sensor reactive with both singlet oxygen and superoxide, we aimed to investigate whether photoinhibition *in vivo* induced superoxide production, besides the singlet oxygen already detected in previous studies of our group. We aimed to extend our studies to *in vivo* applications.

3. Our other goal was to reveal whether singlet oxygen and superoxide were involved in UV stress: how various UV wavelengths activated the production of various ROS, whether there was a difference in the ability of UV-A and UV-B to promote the production of ROS in *vitro* and *in vivo*?

3. MATERIALS AND METHODS

3.1. Thylakoid isolation

Thylakoid membranes were isolated from fresh market spinach and used on the day of purchase. Leaves were washed, their main vessels were cut off and the remaining tissue was homogenized in HEPES buffer (40 mM, pH 7.5) containing 400 mM sucrose, 15 mM NaCl, 5 mM $MgCl_2$, 2 mM Na-EDTA, 5 mM Na-ascorbate and 1 g/l BSA (Takahashi and Asada, 1982). The homogenate was filtered through a three layer gauze filter and two layers of tissue-paper, in order to filter out the bigger chloroplast-fragments and centrifuged at 8000 x g for 20 minutes at 4°C. The supernatant was discarded, and the pellet was resuspended in a HEPES buffer (40 mM, pH 7.5), containing 400 mM sucrose, 15 mM NaCl and 5 mM $MgCl_3$. The resuspension was performed by gently separating the thylakoids from the deposited starch with a brush. The resuspended pellet was centrifuged again at 8000 x g for 20 minutes at 4°C, and the supernatant was discarded. The pellet was suspended in the above buffer and stored at - 80°C until use. All suspension steps were performed in dim green light.

3.2. Chlorophyll content determination

Chlorophyll content of the isolated thylakoid membranes was determined in 80% acetone (Arnon, 1949). Various volumes of thylakoids were diluted in 80% acetone. Absorption of each sample was determined at 645 nm and 662 nm. Chl(a) and Chl(b) concentrations were calculated as:

Chl (a) = $(12.7 \times A_{662} - 2.69 \times A_{645}) \times$ dilution factor

Chl (a+b) = $(8.02 \times A_{662} + 20.2 \times A_{645}) \times$ dilution factor

The obtained values were averaged and the concentration was given in µg/ml units.

3.3. Chlorophyll extraction in detergent

For experiments with free chlorophyll, it was extracted from isolated thylakoid membranes with TritonX-100 detergent. Thylakoids of known chlorophyll concentration were suspended in a Na-phosphate buffer (50 mM, pH 7.2), containing 10% Triton X-100. This mixture was stirred for 30 minutes at room temperature in the dark, then centrifuged at 6000 x g for 10 minutes. Extracted chlorophyll was present in the supernatant fraction, which was stored at -80°C until use.

3.4. Oxygen polarography

Photoinhibition and UV irradiation induced electron transport loss in isolated thylakoids was estimated from the decrease in oxygen evolution, expressed as percentage loss, compared to untreated samples.

Photosynthetic oxygen evolution of thylakoid samples (20 μg/ml chlorophyll, 1ml) was measured with a Clark-type oxygen electrode. First, a baseline signal was recorded while keeping the sample in the dark, for 2 minutes. The thylakoid suspension was then illuminated with saturating intensity PAR (1000 μmol m^{-2} s^{-1}) in the presence of an electron acceptor, and the extent of oxygen evolution was recorded for 3-4 minutes. As acceptor, we used 3 mM 2,5-dimethyl-p-benzoquinone (DMBQ).

The electrode was calibrated by adding $Na_2S_2O_4$ to 1 ml distilled water and oxygen evolution was calculated assuming 0.120 μM oxygen dissolved in 1 ml water.

3.5. Variable chlorophyll fluorescence

The effect of photoinhibition and UV irradiation on the photosynthesis of various leaves was estimated from the relative decrease in their variable chlorophyll fluorescence. The extent of damage was expressed as percentage loss, as compared to non-irradiated, but already infiltrated leaves.

Maximum quantum yield parameters of PSII, F_v/F_m, and the electron transport rate, $\Delta F/F_m'$ (Genty et al., 1989), were measured with either a PAM-100 or a portable mini-PAM chlorophyll fluorometer (Walz, Effeltrich, Germany). F_v/F_m was

determined in leaves dark adapted for 15 min. $\Delta F/F_m'$ was measured under low intensity actinic light of 30 μmol m^{-2} s^{-1}. Typical F_v/F_m and $\Delta F/F_m'$ values of spinach leaf segments before the application of either photoinhibition by excess PAR or UV irradiation were of 0.81 and 0.44, respectively. The infiltration process lowered these parameters (Hideg et al., 1998, Hideg et al., 2002a). F_v/F_m and $\Delta F/F_m'$ was lowered to 88% and 75% by vacuum infiltration and to 90% and 85% by pinhole infiltration. The presence of the ROS sensors didn't affect these parameters.

3.6. Plant material

For *in vivo* ROS detection under stress conditions, various plants were used.

All stress experiments were performed on either whole leaves or on freshly cut leaf segments.

Mature spinach (*Spinacia oleracea*) leaves were purchased from a local breeder and used on the same day. The plant material was transported to the laboratory in bundles with roots, in a moistened sponge. *Arabidopsis thaliana* plants were grown in greenhouse at 22-23ºC and 50-60 μmol m^{-2} s^{-1} PAR, 16 h light/8 h dark. Plants were used 7 weeks after sowing.

Transgenic tobacco (*Nicotiana tabacum*) lines used in this study were obtained from collaborators, from the laboratory of Prof. Kozi Asada (Fukuyama University, Japan). The studied lines lacked either the chloroplast localized, or the cytosol localized superoxide dismutase (CuZn SOD) enzyme. These ANT4 and ANT3 plants, respectively, were compared to control (SR1) ones in their response to ultraviolet irradiation. Tobacco plants were grown in the greenhouse under 50-70 μmol m^{-2} s^{-1} PAR, 16 h light/8 h dark, at 22-25° C for 6 weeks from sowing.

3.7. Fluorescent sensors. Tools of ROS detection.

Reactive oxygen species have short lifetimes and are present in extremely low concentrations in plant samples. Therefore, there is a need for special and very sensitive methods to identify them. EPR techniques are suitable for *in vitro*, isolated thylakoid membrane studies (Hideg et al., 1994a, Hideg et al., 1994b, Hideg et al.,

1995), but *in vivo* ROS detection by EPR meets several technical difficulties, due to the interference of the high water content of leaves and microwaves. Applying fluorescent probes for *in vivo* studies, we can avoid the difficulties raised by the EPR ROS detection.

Fluorescent double sensors were designed and synthesized for our ROS experiments in the laboratory of Organic and Medicinal Chemistry at the University of Pécs. These double (spin and fluorescent) ROS sensors consist of a fluorophore group and a nitroxide precursor moiety (Kálai et al., 1998, Hankovsky et al., 2001). They are more stable in leaves than the nitroxide spin traps alone (Hideg et al., 1998).

The fluorescence of ROS double sensors is intense, but they are EPR silent. When these sensors react with ROS, the spin trap moiety is converted into a nitroxide radical and this reaction results in partial quenching of the sensor's fluorescence. The nitroxide form of the sensor is also EPR active (Green et al., 1990). This way, the reaction of the sensor with ROS can be monitored either by fluorescence quenching or by following the appearing of the EPR signal characteristic to the nitroxide. This principle was realised in a dansyl-based $^1O_2$ sensor, DanePy. This ROS sensor was successfully applied in detecting $^1O_2$ *in vitro* and *in vivo* (Kálai et al., 1998, Hideg et al., 1998, Hideg et al., 2000a, Hideg et al., 2000b, Hideg et al., 2001).

In the following section of the thesis, we also introduce and characterize potential double ROS sensors other than DanePy, which were later applied for stress-induced ROS detection in leaves. ROS detection was based on the fluorescence quenching of the sensor.

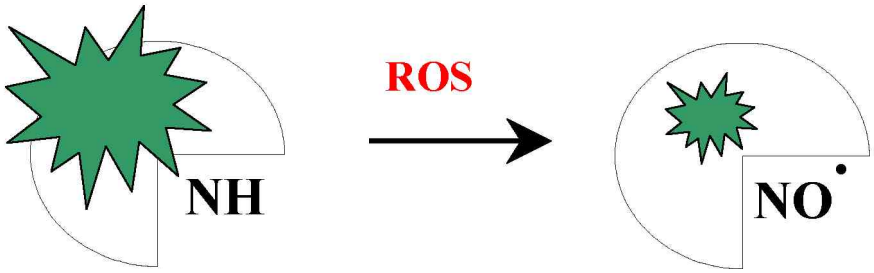

Fig. 3.1.: The principle of ROS detection with fluorescent sensors. The reaction of the sensor with specific ROS led to the formation of relatively stable nitroxide radical, and resulted in partial quenching of the originial fluorescence of the sensor.

Three of the fluorescent sensors applied in this study have a dansyl-group as fluorophore (Fig. 3.2.), and one contains rhodamine (Fig. 3.3.).

The applied dansyl based sensors are the following (Fig. 3.2.):

5-Dimethylamino-naphthalene-1-sulfonic acid (2-diethylamino-ethyl)-(2,2,5,5-tetramethyl-2,5-dihydro-1*H*-pyrrol-3-ylmethyl)-amide (DanePy);

5-Dimethylamino-naphthalene-1-sulfonic acid (2,2,5,5-tetramethyl-2,5-dihydro-1*H*-pyrrol-3-ylmethyl)-amide (HO-1889NH)

2-Methyl-1-oxy-3,4-dihydro-2*H*-pyrrole-2-carboxylic-acid [2-(5-dimethylamino-naphthalene-1-sulfonylamino)-ethyl]-amide (L-2204)

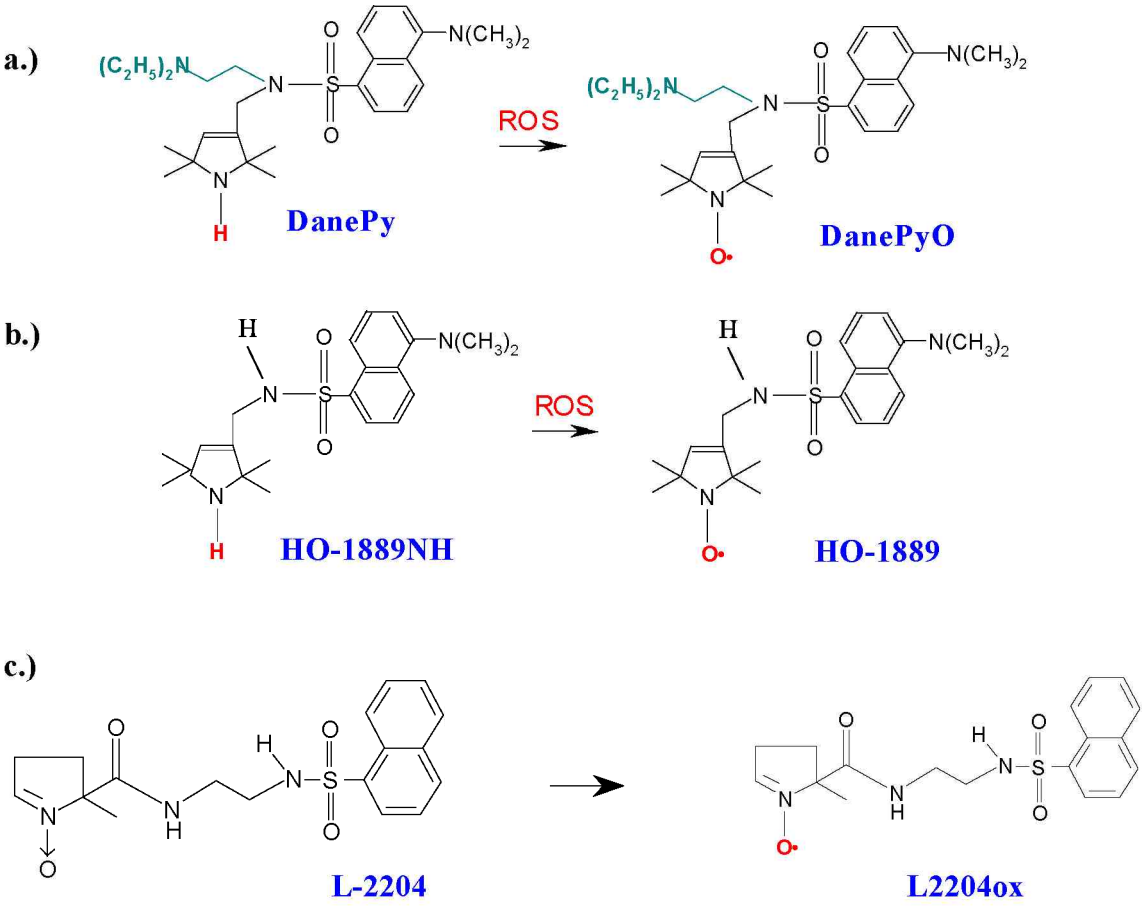

Fig. 3.2.: The dansyl-based double ROS sensors and their synthesized oxidised pair applied in this study: DanePy and DanePyO a.), HO-1889NH and HO-1889 b.), and L-2204 and L-2204ox c.).

HO-1889NH and DanePy have similar structures. HO-1889NH only lacks one side chain attached to the group linking the fluorescent moiety to the trap group. In L-2204, the fluorophore is combined with a free radical trap instead of the tetramethyl-pyrrole moiety. The influence of the differences in the molecular structure of the sensors on their specificity towards various ROS was investigated.

The rhodamine-based sensor applied in this study was HO-2941 (3-N-(2,2,5,5-tetramethyl-2,5-dihydro-1 H-pyrrol-3-carboxoamidopropyl) sulforhodamine), shown in Fig. 3.3. :

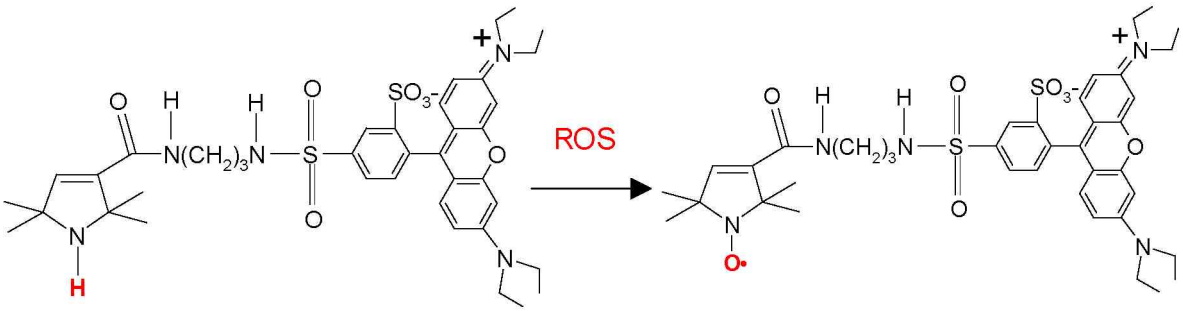

HO-2941 **HO-2942**

Fig. 3.3.: The rhodamine-based double sensor, and its oxidized pair applied in this study: HO-2941 and HO-2942.

3.7.1. Physicochemical characterization of traps

Double sensors have to fulfill several conditions in order to be applicable for *in vivo* ROS detection studies: they have to be sensitive to one or more types of ROS and have to be stable in the studied system. It is important that the applied sensors are able to reach the site of ROS production.

Before being applied in stress experiments both dansyl-type and rhodamine-based ROS sensors were tested for *in vitro* stability and in plant samples, as well as for selectivity.

Fluorescence emission spectra of the ROS sensors were recorded at room temperature, with a Quanta Master QM-1 (Photon Technology Int. Inc., USA) spectrofluorimeter. For specificity and stability tests as well as for *in vitro* studies

both emission and excitation slits were 1 nm. Optimal excitation wavelengths were 340 nm for DanePy and HO-1889NH, 360 nm for L-2204 and 533 nm for the rhodamine-based HO-2941. Fluorescence emission spectra were recorded in the 400-650 nm or 550-650 nm ranges for dansyl or rhodamine based sensors, respectively.

To define the maximal ROS quenching ability, emission spectra of the sensors were compared to the spectra of their chemically synthetized nitroxide pairs. Both DanePy and HO-1889NH were capable of more than 80% fluorescence quenching therefore they are suitable tools for effective ROS detection (Fig. 3.4.).

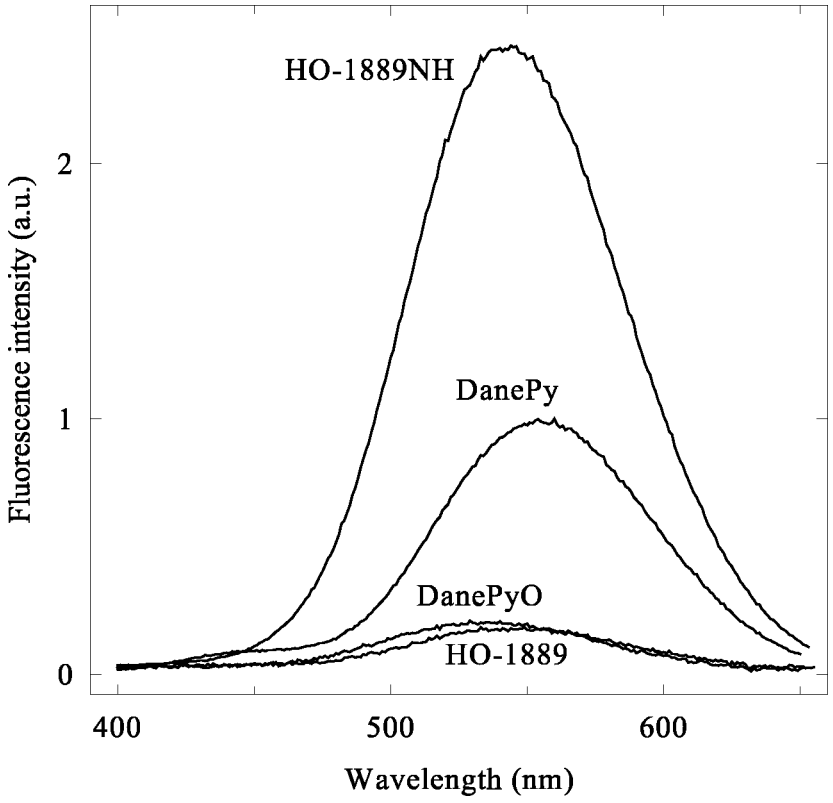

Fig. 3.4.: 340 nm excited 400 - 650 nm fluorescence emission spectra of 200 μM DanePy and HO-1889NH and of their corresponding synthetized nitroxide pairs, DanePyO and HO-1889 in Na-phosphate buffer (pH=7.2).

The stability of the traps was investigated in a 50 mM Na-phosphate (pH 7.2) buffer, as a first step of physicochemical characterization.

Reactivities of DanePy, HO-1889NH, L-2204 and HO-2941 for ROS were characterized by following their fluorescence quenching when chemically generated active oxygen species were added to their solutions (see page 54. for Table 1). Upon conversion of the trap group into nitroxide radical by ROS, the fluorescence of the sensors decreased (Fig. 3.1.). The fluorophore groups of both types of sensors, dansyl chloride and rhodamine chloride were tested without the putative ROS traps, as controls. The fluorescence of these compounds did not quench upon ROS addition, therefore the recorded fluorescence intensity loss of each sensor was attributed to the reaction of the trap moiety with ROS.

For these experiments, stock solutions of the sensors were prepared in 96% ethanol, then further diluted in sodium-phosphate buffer. The final concentration of ethanol in all samples was less than 5%.

Before chemical ROS generation, the fluorescence emission spectra of the sensors (200 μM) were recorded as reference.

$^1O_2$ was generated from 50 μM RoseBengal or from 50 μmol Triton-extracted chlorophyll by illuminating these solution for 10 minutes with 500 μmol m^{-2} s^{-1} PAR from a KL-1500 (DMP, Switzerland) lamp through an optical fiber. Warming of the samples was avoided by the use of the optical fiber. Dyes generated $^1O_2$ in a type II photodynamic reaction (Redmond and Gamlin, 1999, Caspi et al., 2000).

$O_2^{-\bullet}$ was produced by the illumination of 60 μM riboflavine for 10 minutes under the above illuminating conditions (Cunningham et al., 1985).

$^\bullet OH$ was generated from the reaction of 200 μM H_2O_2 and 200 μM Fe(II)-sulphate, in Fenton's reaction (Haber and Weiss, 1984):

$$Fe^{2+} + H_2O_2 \rightarrow Fe^{3+} + OH^- + {}^\bullet OH$$

Iron ions without H_2O_2 – neither in Fe (II) (from ammonium ferrous sulphate), nor in Fe (III) (from $FeCl_3$) form - did not influence the fluorescence of the tested ROS sensors (Hankovszky et al., 2001). In this way, the effect of the reaction mixture can be attributed to hydroxyl radicals.

When RoseBengal, detergent extracted chlorophyll or riboflavin was present in the sample, the reference spectrum was composed of the sensor's and photosensitizer dye's emission, excited at the optimum excitation wavelength of the sensor.

After addition of the chemically generated ROS to the solution of the sensor, the fluorescence emission spectrum of the sensor was recorded again. ROS detection was based on the decrease of sensor fluorescence (Kálai et al., 1998). The difference between the two fluorescence emission intensities (fluorescence quenching) represented the ROS scavenging ability of the respective sensor and was given as %. The conversion of the sensor into oxidized form is irreversible (Bilski et al., 2003).

As controls, the chemically synthesized nitroxide (oxidized) forms of the sensors were also tested for reactivity to the above ROS. These were not affected by ROS addition, therefore fluorescence decays of the sensors were attributed to ROS and not to other factors, such as illumination or reactions of ROS with the fluorophore moiety.

3.7.2. Detecting the ROS sensors' fluorescence in leaves. Infiltration

For *in vivo* ROS detection we infiltrated leaf segments with either 1 mM DanePy or 1 mM HO-1889NH in water solution. Two different infiltration approaches were used for getting the sensor into the leaves: the leaves were either infiltrated with the solution of the sensor by vacuum infiltration, or by introducing it into the leaf through a pinhole.

Vacuum infiltration was done inside a plastic syringe. Small segments of leaf samples were placed inside the syringe from the back, and it was closed. The syringe was then filled with 1,5-2 ml of one of the ROS sensors (1 mM water solution, containing less than 10 % ethanol) within 15-20 s. After removing the air, the plunger was pulled rapidly while the nozzle was kept closed.

The other infiltration approach, through a pinhole derived from the adaptation of a method usually used for infecting leaves with pathogens. The solution of the sensor was forced into the leaf tissue through a pinhole made on the adaxial side by a plastic syringe without needle. A sharp and thin pin made the pinhole without punching through the leaf (Hideg et al., 2002a). This way the infiltrated area was about 1.5 cm^2 depending on the proximity of vascular tissue (for details see Fig. 4.6. on page 63). The excess solution of the sensor was removed from the surface of the leaves with a tissue paper.

In order to allow the diffusion of the sensor within the infiltrated leaves, they were kept in dark for 5-10 minutes, before the reference spectrum was recorded.

As compared to other methods, infiltration through a pinhole provided the most uniform distribution of the sensor in the leaf, and decreased photosynthetic electron transport parameters of the infiltrated segment the less, by only about 10-15 % (Hideg et al., 2002a).

Stress-induced ROS production in the leaves previously infiltrated with any of the sensors was studied by various fluorescence detection methods: by spectrofluorimetry, fluorescence imaging and confocal laser scanning microscopy.

3.7.2.1. Spectrofluorimetry

From the sensor-infiltrated area of the leaf a 15 x 5 mm segment was cut off and fixed on a homemade metal sample holder. To avoid drying of the sample during the experiments, the leaf segment was placed on a wet tissue-paper stripe. The sample was than covered with a quartz plate, which ensured proper humidity environment for the sample, and also immobilised it.

The sample holder on which the leaf segment was fixed, was placed into the spectrofluorimeter, facing 45° angles to both excitation and emission axis (Fig. 3.6.). Two crossed polarizers (set to 90° polarization angles) were applied to exclude artefacts from reflection or light scattering, one at the excitation and another one at the emission side. All spectrofluorimetry measurements were carried out with a Quanta Master QM-1spectrofluorometer (Photon Technology International – PTI, Inc. U.S.A.).

In leaf experiments the excitation and emission slits were both opened to 4 nm. Five spectra were averaged from the same sample, in order to improve the signal-noise ratio.

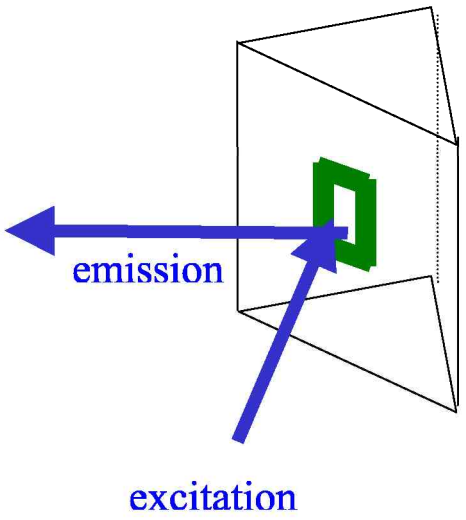

Fig. 3.6. Scheme of the irradiation setup in leaf-experiments. The leaf segment was placed on the sample holder, facing 45° angles to both excitation and emission axis.

For each spectrum, 10 data points in the vicinity of the 532-535 nm maximum value were averaged. Fluorescence quenching of the sensor in the leaf pointed the presence of ROS (Hideg et al., 1998). Aside from the amplitude decrease of the fluorescence emission spectrum no other spectral parameters changed upon reaction of the sensor with ROS.

In order to be suitable for *in vivo* experiments, the ROS sensors have to be fairly stabile in the studied systems. All sensors were tested for stability in leaves. In these experiments, infiltrated leaves were kept in dark, and fluorescence of the sensors was checked periodically.

Each infiltration results in different absolute sensor fluorescence intensity. Various absolute fluorescence intensity values can be obtained in different plant species.

ROS sensors are not perfectly stable in leaves (Hideg et al., 1998). Due to this slight instability, all data were corrected with stability changes of the sensor during the time of the experiments.

Since the dansyl-based sensors are excitable in the UV range (by 340 nm), their fluorescence emission maximum overlaps with the 515-550 nm UV induced

blue-green intrinsic fluorescence of leaves (Chapelle et al., 1984, Chapelle et al., 1991, Lang and Lichtenthaler, 1991, Lichtenthaler and Schweiger, 1998). Changes in the blue-green auto-fluorescence levels of leaves are good, although unspecific indicators of plant stress (Hideg et al., 2002b). Upon exposing leaves to UV radiation, their BGF level changes have also to be taken into account when monitoring the fluorescence quenching of the ROS sensors *in vivo*. Therefore, in plant stress experiments the relative fluorescence emission intensities of the sensors were corrected in the BGF background for all time points of the experiments.

After corrections, ROS production was given as the percentage loss in the sensors' fluorescence as compared to the fluorescence emission measured before the application of the stress to the leaf.

3.7.2.2. Fluorescence imaging

Fluorescence images were recorded on detached leaves positioned flat on black paper, with their adaxial sides up. Fluorescence was followed using an Epi-LightUV FA500 monochrome CCD camera imaging system (AISIN Taitec, Kosmos Kenkyo Inc., Japan). The excitation was 310 nm (10 nm bandwidth) and emission was detected through a BG18 (410-640 nm) band pass filter. Fluorescence images were collected using the instrument's image capture facility.

In an other set of experiments, a Leica MZ FL III Fluorescence Microscope (Leica Microsystems, Tokyo, Japan) was used, with 1.5 magnification. Excitation was from a broad band UV source, from a Supercure 203S source (San-Ei Electric Co., Japan) through a UG11+DUG11 band pass filter combination (295-375 nm). Fluorescence emission was detected through a BG18 (410-640 nm) band pass filter by a digital image analysing system (Pixera Viewfinder 3.5, Pixera Corp., USA). Images were acquired using identical focus settings.

For quantitative analysis, individual images were converted to greyscale and ROS-induced fluorescence quenching was evaluated the UTHSCSA ImageTool freeware (University of Texas Health Science Center, San Antonio, Texas, USA, available on the Internet by anonymous FTP from ftp://maxrad6.uthscsa.edu).

3.7.2.3 . Confocal LSM studies

For micro-localization studies, leaf cuttings (6 x 6 mm) including the area infiltrated with the ROS sensor were sandwiched between two UV-transparent microscope cover glass layers and measured using a confocal laser scanning system (LSM 510, Karl Zeiss, Germany) in combination with an inverted microscope (Axiovert 100 M, Karl Zeiss, Germany). Adaxial sides of the leaf segments faced the 351 nm Ar laser excitation (80 mW, ENTCII-653, Coherent Enterprise, Santa California, USA). Fluorescence emission was observed through 515-550 nm filters for green (sensor) and above 650 nm for red (chlorophyll) fluorescence. Fluorescence emission was collected from a 115 x 115 μm area. Images were scanned at 0.8 s per frame, averaging 4 images.

In order to study the localisation of the ROS sensor inside the leaf, the intensity distributions of the green ROS sensor fluorescence and of red chlorophyll fluorescence were compared along the same line on the same image in unstressed leaves. For characterising stress-induced changes of green fluorescence we compared the intensity distributions at various stages of the treatment.

Fluorescence imaging and LSM experiments were done by Dr. Éva Hideg at Fukuyama University, Japan, in collaboration with Prof. Kozi Asada (Hideg et al., 2002). All other measurements were carried out at Szeged, by the author.

3.8. Stress conditions

3.8.1. Photoinhibition

The production of various ROS was studied in both isolated thylakoid membranes, and *in vivo*, in leaf samples exposed to photoinhibition by excess PAR.

3.8.1.1. Photoinhibition of thylakoid membranes

Isolated thylakoid membranes were diluted in 50 mM NaH_2PO_4: Na_2HPO_4 buffer (pH 7.2) to 20 μg/ml final chlorophyll concentrations. The sensor's solution was added to the thylakoid and the fluorescence emission spectrum of the ROS sensor

was recorded, while continuously stirring the sample to avoid precipitation of the membranes. Each sample contained less than 5% ethanol.

After recording a reference emission spectrum of the sensor, photoinhibition was carried out inside the spectrofluorimeter. The content of the cuvette was exposed to 1500 μMm^{-2} s^{-1} PAR, through an optical fiber from a KL-1500 (DMP-Switzerland) lamp, while being continuously stirred. This illumination process did not warm the samples. Thylakoid membranes were irradiated for 30 minutes and the fluorescence intensity of the sensor was checked periodically after 0, 10, 20 and 30 minutes of irradiation.

3.8.1.2. Photoinhibition of leaf samples

Leaves were infiltrated with the 1 mM water solution of one of the ROS sensors (see Chapter 3.7.) and were fixed to the metal sample holder. A reference fluorescence emission spectrum of the sensor was recorded. The fixed leaf-segment was exposed to 1800 μMm^{-2} s^{-1} intensity PAR illumination for 30 minutes through an optical fiber from a KL-1500 (DMP-Switzerland) lamp. The fluorescence intensity of the ROS sensor was checked periodically.

Photoinhibition of leaf samples was carried out inside the spectrofluorimeter and the leaf segment fixed to the sample holder was not moved during the duration of the experiment. Alternating fluorescence measurements and illumination sequences were carried out by turning the tourette of the sample-holder between measurements.

3.8.2. Stress by UV irradiation

Reactive oxygen production induced by UV stress by was studied in isolated thylakoids and *in vivo*, in leaves.

3.8.2.1. UV-A and UV-B irradiation of thylakoid membranes

Thylakoid membranes were diluted in 50 mM NaH_2PO_4: Na_2HPO_4 buffer (pH=7.2). Final chlorophyll concentration of the samples was of 20 µg/ml. The solution of the ROS sensors was added according to the method described in

Chapter 3.8.1.1. A reference fluorescence emission spectrum of the sensor was recorded, than thylakoids were irradiated in the presence of the ROS sensor with 27 μmol m^{-2} s^{-1} UV-B from a VL-215M lamp, having bandwidth of 295-320 nm with maximal emission at 312 nm (Vilbert-Lourmat, France). A cellulose acetate filter (Courtaulds Chemicals, U.K.) was used to exclude UV-C. In an other set of experiments, thylakoid membranes were irradiated with UV-A irradiation from a broadband 345-385 nm, 365 nm centered UV-lamp (Vilber Lourmat, VL-215L) of 35 μmol m^{-2} s^{-1}. The intensity of the UV irradiation was measured with a Cole-Parmer radiometer, equipped with either a 312 nm or a 365 nm sensor.

Samples were continuously stirred while being irradiated in order to avoid the precipitation of the membranes. During the 60 minutes UV-irradiation the fluorescence emission of the ROS sensor was checked periodically.

To compare the ability of various UV wavelengths to induce differential ROS production, thylakoids were exposed to quasi-monochromatic (±8 nm around central wavelength) UV irradiation in the range of 280-390 nm in the presence of one of the ROS sensors. The lamp of the spectrofluorimeter was used as quasi-monochromatic UV source. Photon flux was determined with ferrioxalate actinometry (see Chapter 3.10.).

3.8.2.2. UV-irradiation of leaf samples

In vivo reactive oxygen evolution in UV-stressed leaves was studied by applying different irradiation protocols.

1. To avoid having to keep the ROS sensor in the leaf for longer times, UV-B irradiation was applied in two sequences. *Arabidopsis thaliana* leaves were infiltrated with the solution of either DanePy or HO-1889NH. After recording a reference emission spectrum, infiltrated leaves were irradiated with 27 μmolm^{-2} s^{-1} UV-B, from a VL-215M lamp, for 30 minutes. During the stress treatment the fluorescence emission of the sensor was measured periodically (Fig. 3.7 a). In a second set of experiments leaves were first exposed to 27 μmolm^{-2} s^{-1} UV-B for 30 minutes, without infiltration. Pre-irradiated leaves were than infiltrated with one of the double

sensors and a reference spectrum was recorded. Leaves were then exposed again to UV-B radiation for 30 more minutes (Fig. 3.7 b). The fluorescence emission of the ROS sensor was recorded every 10 minutes during the second set of UV-B exposure. In total, the stress treatment lasted for one hour but the sensor was only infiltrated at halftime of the treatment.

ROS production between the 30th and 60th minutes of UV-B irradiation was estimated by comparing changes of the sensor fluorescence to the reference spectrum measured at the 30th minute of the stress treatment. Since the absolute fluorescence intensity value of the sensor in the leaf is different in each infiltration, the two sets of intensity data had to be combined. In this process the first reference point of the second series was normalised to the last data of the first series.

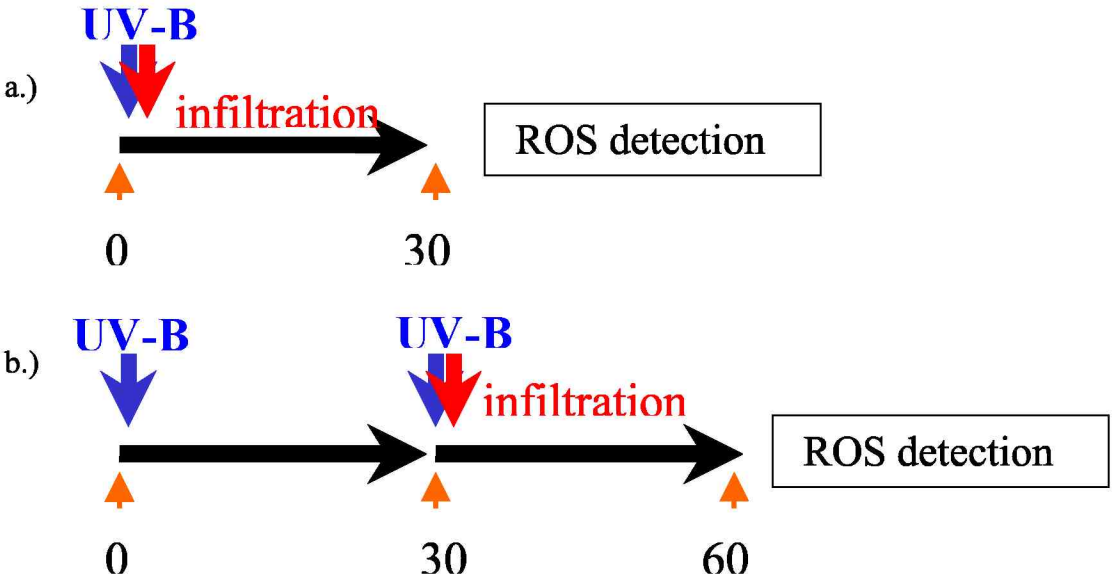

Fig. 3.7.: Time-course of UV-B stress in Arabidopsis thaliana leaves infiltrated with one of the ROS sensors and irradiated for 30 minutes a.), or in leaves pre-treated for 30 minutes with UV-B irradiation and irradiated again after infiltration for 30 more minutes b.).

2. For comparing the ability of various UV spectral components to generate ROS *in vivo*, spinach leaves were infiltrated with the solution of either DanePy or HO-1889NH and irradiated with equal quanta of quasi-monochromatic (approximately ± 8 nm around central wavelength) UV in the range of 280 – 390 nm. The stress treatment was carried out inside the spectrofluorimeter, using as UV source the lamp of the fluorometer.

As stress treatment, leaves were irradiated with 2 x 10^{22} photons of the selected wavelength. Irradiation times to achieve these doses were ranging from 15 to 30 minutes. Treatment times needed to provide 2 x 10^{22} photons of each selected wavelength were determined by ferrioxalate actinometry (See Chapter 3.10.).

3. ANT3 and ANT4 transgenic and SR1 tobacco plants were exposed to the above dose of UV irradiation only at two selected wavelengths: 290 nm and 360 nm.

After recording a reference spectrum, the fluorescence intensities of the sensors were checked several times during the irradiation as well. Fluorescence emission spectra of the sensors were recorded with 4 nm wide excitation and emission side slits. UV irradiation of the samples was carried out using 16 nm wide excitation slit. Since the emission of the ROS sensor was checked periodically during the UV stress-treatment, the opening of the excitation side slit was changed frequently. The accuracy of the settings was controlled using a perylene-containing standard, provided by the spectrofluorimeter manufacturer. Data acquisition was complete in two minutes, and due to the reduced slit size, the 340 nm excitation applied for the fluorescence measurements did not cause any additional ROS production. All measurement and irradiation sequences were carried out without moving the leaf sample.

In all UV stress experiments, fluorescence data were corrected for the changes of the UV-inducible blue-green intrinsic fluorescence of leaves (Chapelle et al., 1984). Maximum of the 340 nm-excited emission spectra of the dansyl-based sensors were around 532-535 nm, which in leaves overlapped with the UV-induced blue-green auto-fluorescence. With adequate infiltration, this intrinsic fluorescence in the

515-550 nm spectral region was usually kept less than 10-30% of the sensors' fluorescence.

3.9. Other ROS detecting methods

3.9.1. Hydrogen peroxide detection by histochemical staining

Stress induced H_2O_2 production was studied in the ANT3, ANT4 transgenic and SR1 wild type tobacco plants by a histochemical staining method (Thordal-Christensen et al., 1997). Tobacco leaves were exposed to 27 μmol m^{-2} s^{-1} UV-B from a VL-215M lamp. After the stress treatment leaves were immersed into a 2 mg/ml 3,3'-diaminobenzidine (DAB) solution and kept in dark, while gently stirring the samples on a swinging table for 2 hours. This procedure ensures uniform distribution of the solution on the leaf surface. Stock solution of 50 mg/ml DAB was prepared in 1N HCl then it was further diluted to 2 mg/ml in milliQ water. The reaction of DAB with H_2O_2 was based on endogenous peroxidase activity of the leaves resulting in brownish colour of the tissue where the H_2O_2 was present. After 2 hours of DAB treatment, chlorophyll was removed from the leaves by boiling them in 96 % ethanol for 10 minutes in a water bath. After taking pictures of the stained leaves, they were further stored in 96 % ethanol, the H_2O_2-DAB complex being very stabile, the colour persisted for longer times.

3.9.2. Superoxide detection by cytochrome-c reduction in thylakoid membranes

In order to compare the $O_2^{-\bullet}$ generating ability of equal doses of various UV wavelengths, the reduction of 20 μM cytochrome-c was followed in thylakoids (20 μg/ml chlorophyll) exposed to UV radiation. The absorbance changes of cytochrome-c were monitored at 550 nm. Absorbance changes were detected both in the presence of 0.5 units of catalase, in order to neutralize H_2O_2, if present and without the enzyme (Vandewalle and Petersen, 1987).

3.10. Ferrioxalate actinometry

Ferrioxalate actinometry (Hatchard and Parker, 1956) was carried out using 6 mM $K_3Fe(C_2O_4)_3$ in 50 mM sulphuric acid. Potassium ferrioxalate was prepared by adding three parts of potassium oxalate (1.5 M) to one part of ferric chloride (1.5 M). The resulting precipitate was re-crystallized three times with water and dried. After being exposed to UV radiation in the spectrofluorimeter, the $K_3Fe(C_2O_4)_3$ solution was diluted with 1 g L^{-1} 1,10-phenantroline and 0.5 M sodium acetate buffer (2:2:1 V:V:V), and kept in the dark for 30 min until the development of the colorimetric complex. The absorbance of the resulting Fe-(1,10-phenantroline)$_3$ $^{2+}$ was measured at 510 nm and compared with a reference (ferrioxalate without irradiation) solution. UV photon flux (photons min^{-1}) was calculated assuming a constant quantum yield for the reduction of iron ions over the 200-400 nm photoactive wavelength range (Lee and Seliger, 1964, Björn, 1971). Irradiation times corresponding to 2 x 10^{22} photons were found to be between 15 – 30 minutes, depending on wavelength of the applied UV irradiation. UV treatments, all representing the same total accumulated dose (the same number of photons) corresponded to approximately 18 – 36 mmoles m^{-2} s^{-1} photon flux and to a 28 – 45 kJ m^{-2} irradiance.

3.11. Statistics

In vitro sensor tests were repeated five times each, averaged and standard deviations were calculated.

PSII activity of thylakoid membranes was measured by recording oxygen evolution before and after the application of the stress. Each experiment was repeated five times, averaged and the standard deviations were calculated.

Fluorescence emission maxima of the applied ROS sensors were calculated from the average of 10 data points around the 532-535 nm maxima of the dansyl-based sensors and 582-585 nm maxima of the rhodamine-based sensor, in order to avoid artefacts from scattering. Each spectrum was an average of 4 scans. ROS sensor fluorescence quenching data were calculated from 3-4 independent spectra.

T-tests were performed on fluorescence quenching data of the ROS sensors and loss of variable chlorophyll fluorescence data, in order to establish the correlation between these data in the UV-irradiated plant samples.

Mean values and standard deviations of the $\Delta F/F_m'$ were calculated from 3-4 repetitions.

4. RESULTS AND DISCUSSION

The number of studies focussed on light stress in plants is vast (see Barber and Andersson, 1992, Aro and Andersson, 1993, Vass, 1996, Caldwell et al., 2003). Both photoinhibition and stress by UV irradiation have been studied ***in vitro*** and ***in vivo***, with a vide variety of methods. Although many methods are available to detect ***in vitro*** oxidative stress, direct ***in vivo*** applications are limited, as the methods used ***in vitro*** meet several technical difficulties when applied in whole-plant studies. Therefore, direct ***in vivo*** ROS detection is a key factor in plant oxidative stress studies. There is an increasing need for a new ROS identifying technique, applicable for ***in vivo*** direct oxidative stress detection. To overcome the detection difficulties raised in the ***in vivo*** adaptation of the methods used for ***in vitro*** studies, double fluorescent and spin ROS sensors have been introduced.

In this chapter we report experiments in which we used and improved a recently developed technique suitable to detect stress-induced ROS production in different plant systems ***in vivo***. One of the double sensors, DanePy has already been successfully applied to detect $^1O_2$ (Kálai et al., 1998, Hideg et al., 2000a, Hideg et al., 2000b, Hideg et al., 2001).

In this thesis we present and characterize other double sensors, reactive to ROS other than $^1O_2$, which were suitable to be applied ***in vivo***, for detecting light stress induced ROS. These sensors were characterized and applied in stress experiments in parallel with DanePy.

4.1. Physico-chemical characterization of fluorescent sensors

Although DanePy proved to be a good $^1O_2$ sensor for ***in vivo*** studies, as previous studies of our group showed (Kálai et al., 1998, Hideg et al., 2000a, Hideg et al., 2000b, Hideg et al., 2001), there was further need to find a fluorescent ROS sensor specific to ROS types other than $^1O_2$. Therefore, as a first phase of our studies, other potential ROS sensors were characterized.

Testing a new compound is a complex process. A fluorescent ROS sensor has to meet several criteria in order to be applicable in biological experiments. It has to be

stable in the sample, its fluorescence emission and excitation spectrum should not overlap with that of the studied biological material. It should be selective to a few ROS, preferably to one from among the species of interest. Before applying a fluorescent ROS sensor in stress induced ***in vivo*** ROS detection, it has to be characterized from physical and chemical points of view: optimal parameters should be found for fluorescence detection and selectivity has to be investigated. The identification of the micro-localization of the sensor in the leaf, and its stability in the studied system are also important.

Reactivity of the sensors was investigated ***in vitro***, by the addition of chemically generated ROS. When the tested sensor proved to be reactive to one or more ROS, its ***in vitro*** and ***in vivo*** stability was checked. Following these, the sensor's localization in the plant tissue had to be studied. The last step in this process was the actual ***in vivo*** application of the sensor, under the studied stress conditions.

4.1.1. Specifity

Four potential double sensors were selected, three of which had a dansyl group as fluorophore. From the dansyl-based sensors two had a tetramethyl-pyrrole moiety to trap ROS (DanePy and HO-1889NH), and in L-2204 the tetramethyl-pyrrole group was substituted with a free radical trap (Fig. 2.2.). In the fourth sensor the tetramethyl-pyrrole group was combined with a rhodamine fluorophore (HO-2941) (Fig. 2.3.).

Photosensitization of various dye molecules, such as Rose Bengal or free chlorophyll produces $^1O_2$ in a type II photodynamic reaction. Type II photodynamic $^1O_2$ generation has a wide array of medical applications, in cancer photodynamic therapy (Ochsner, 1997). Although both Rose Bengal and free chlorophyll generate $^1O_2$ when illuminated, some studies hypothesize that photosensitized free chlorophyll is not a pure $^1O_2$ source, other radicals may also be evolved (Harbour and Bolton, 1978). The fluorescence quenching of the sensors was followed upon their reaction with $^1O_2$ generated from one of the above sources (an example of characteristic quenching is presented in Fig. 4.1.). It was found, that the reaction of the sensors with $^1O_2$ generated from either Rose Bengal or free chlorophyll photosensitization led to different fluorescence quenching. Fig. 4.2. illustrates the differences in L-2204 fluorescence quenching upon the reaction of the sensor with $^1O_2$ derived from two

different sources. The fluorescence loss of the sensor was more intense when $^1O_2$ was generated from detergent-extracted chlorophyll, than from photosensitised Rose Bengal. This finding supports the earlier suggestion that illuminated chlorophyll is not a pure $^1O_2$ source, other radicals may also be generated by this reaction (Harbour and Bolton, 1978).

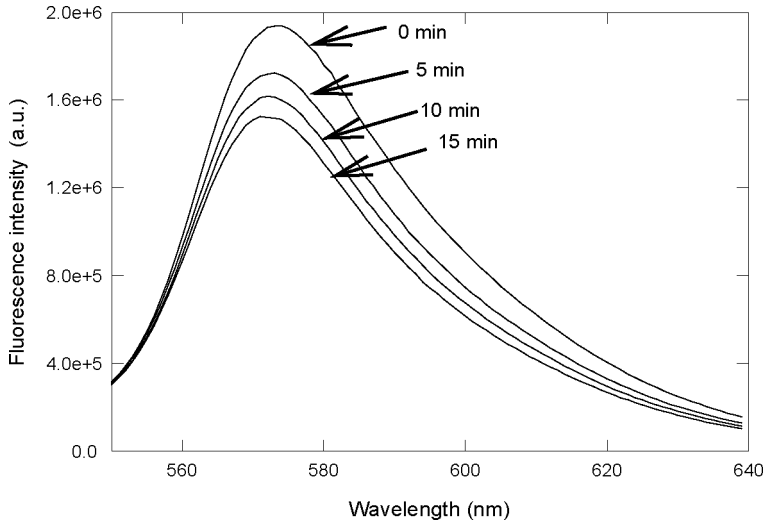

Fig. 4.1.: Fluorescence intensity loss of HO-1889NH in Na-phosphate buffer (pH=7.2) induced by singlet oxygen generated from illuminated Rose Bengal (For experimental details see Chapter 3.7.1.).

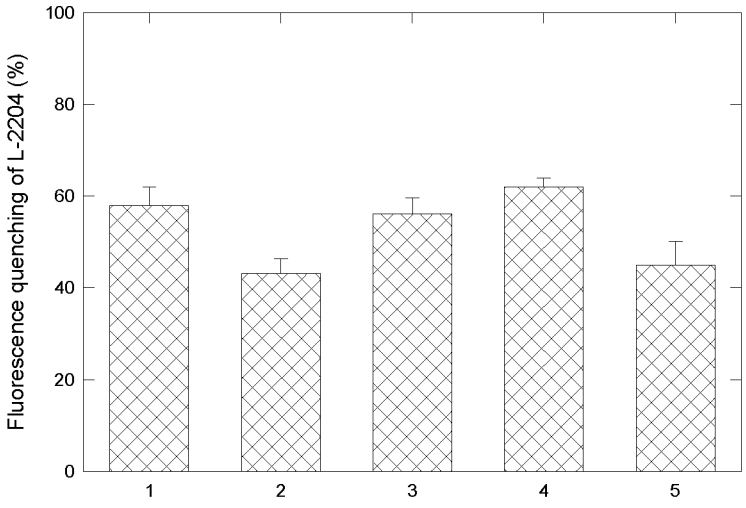

Fig. 4.2.: L-2204 reactivity towards ROS generated from various chemical sources: $^1O_2$ from illuminated chlorophyll (1) or Rose Bengal (2); H_2O_2 (3); $^{\bullet}OH$ (4); $O_2^{-\bullet}$ (5).

Table 1. presents the relative changes in the fluorescence emission of all characterized fluorescent sensors upon their reaction with various ROS.

Although the molecules of DanePy and HO-1889NH were very similar, having identical tetramethyl-pyrrolle moieties and identical fluorescent groups (Fig. 2.2.), it was found, that by modifying the molecular structure only by substituting one side-chain attached to the group linking the fluorophore with the trap with hydrogen, the sensor's selectivity significantly changed. This minor difference in the molecular structure of the two sensors conferred difference in their reactivity to ROS. HO-1889NH was sensitive not only to $^1O_2$ (Fig. 4.1.) , as DanePy (Kálai et al., 1998), but to $O_2^{-\bullet}$ as well (Table 1.). However its reactivity to $^1O_2$ was not as high as of DanePy. Fluorescence of the two sensors was not quenched by either $^\bullet OH$ or by H_2O_2 (Table 1.). L-2204 proved to be unspecific, fluorescence quenching occurred upon its reaction with $^1O_2$, $O_2^{-\bullet}$, $^\bullet OH$ as well as with H_2O_2 (Fig. 4.2. and Table 1). For this reason, we did not use L-2204 in the ***in vivo*** plants stress studies described here. Nevertheless, L-2204 may be used in detecting general oxidative stress, in different systems.

The rhodamine-based HO-2941 (Table 1) showed moderate reactivity to $^1O_2$ only, and practically no response to either H_2O_2 or $^\bullet OH$. We tested this sensor as an alternative to the UV-excitable dansyl-based compounds. Although its ROS induced quenching was smaller, than that of the dansyl-based sensors, HO-2941 was also studied ***in vivo***.

	No addition	$^1O_2$	$O_2^{-\bullet}$	H_2O_2	$^\bullet OH$
DanePy	100 %	35 %	93 %	97 %	98 %
HO-1889NH	100 %	60 %	65 %	98 %	96 %
L-2204	100 %	47 %	45 %	52 %	55 %
HO-2941	100 %	81 %	98 %	95 %	102 %

Table 1: Relative changes in the fluorescence emission of the ROS sensors upon reacting with various ROS from chemical sources.

Although the fluorescence of HO-1889NH is much more intense than that of the DanePy and as Fig. 3.4 shows its maximal quenching ability is higher than that of the DanePy (see Fig. 3.4, page 38), the sensitivity towards $^1O_2$ of this sensor is smaller than that of DanePy.

All sensors proved to be very stabile ***in vitro*** in dark for hours. In order to be applicable for stress-induced ***in vivo*** ROS detection, the ROS trapping ability and the fluorescence parameters of the sensors should not be altered by the stress condition itself. Therefore all fluorescent sensors were tested for their sensitivity to excess light or UV irradiation. None the above characteristics were altered by the applied irradiation.

The fluorophores of the characterized sensors were investigated as controls. Neither dansyl-chloride, nor rhodamine-chloride showed reactivity to any ROS, their fluorescence was not quenched. Because the fluorophore itself is not reactive to any of the studied ROS the fluorescence quenching of the complete sensor can be attributed only to the reaction of the trap group with ROS. The structural moiety, which is responsible for the sensor's activity is the amine-centre in the tetramethyl-pyrrole ring (Bilski et al., 2003).

4.1.2. *In vivo* characterization of fluorescent ROS sensors

4.1.2.1. *In vivo* stability of fluorescent ROS sensors

ROS sensors' stability in the studied system is a prerequisite of their application in plant stress studies. Therefore, when considering ***in vivo*** applications, it is crucial to investigate the stability and the micro-localization of the sensors in leaves.

DanePy, HO-1889NH and HO-2941 were investigated for ***in vivo*** stability. 1 mM aqueous solutions of the sensors were infiltrated into tobacco leaves and their dark stability was followed for all time points of the upcoming stress experiments. These sensors were not perfectly stable ***in vivo***, therefore, fluorescence quenching data had to be corrected for their slight instability. The mechanism behind this stress-unrelated instability can probably be attributed to physical factors, such as diffusion of the sensor in the leaf, or to chemical processes, since the metabolism of the sensor in the leaf is not yet known. The amine centre in the tetramethyl-pyrrole ring can be oxidized by other oxidants in addition to $^1O_2$, for example by endo-peroxides, which

can be formed in biological systems from the reaction of $^1O_2$ with different substrates (Albro et al., 1997, Bilski et al., 2003).

4.1.2.2. Micro-localization of florescent sensors in leaves

The micro-localization of the sensors in the leaf is also of interest when we use them as tools of ***in vivo*** stress-induced ROS detection.

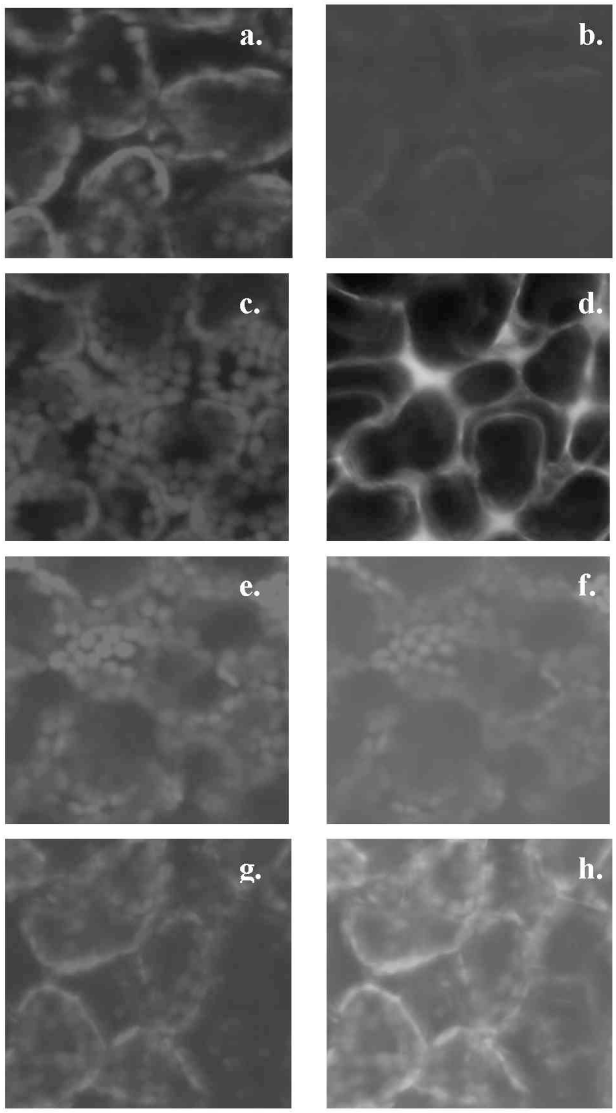

Fig. 4.3.: LSM images of 351 nm excited red (λ>650 nm) chlorophyll fluorescence (a.), (c.), (e.), (g.) detected in spinach leaves infiltrated with distilled water (a.), HO-2941(c.), DanePy(e.), HO-1889NH (g.). Green (505< λ<550 nm) fluorescence emission was detected in distilled-water infiltrated (a.), DanePy (f.) and HO-1889NH (h.) infiltrated leaves. Yellow fluorescence (560< λ<615 nm) of HO-2941 emission is showed by panel (d.)

Since our studies were focused on the investigation of the effect of light stress on the photosynthesis of plants at the level of ROS production, micro-localization studies investigated especially the question whether the characterized ROS sensors penetrated to the chloroplasts or not. For this reason LSM imaging studies were performed to localize the sensors in the infiltrated spinach leaves.

Confocal laser scanning microscopy is a non-invasive technique, which gives the possibility of higher resolution monitoring of the fluorescence changes of the sensors inside inner layers of the leaf, in mesophyll cells. We compared the localization of the 351 nm UV excited red chlorophyll fluorescence emission above 650 nm (Figs. 4.3 a, c, e, g and 4.4 a, c), which identified chloroplasts, with the 515-550 nm dansyl-based ROS sensor fluorescence emission (Figs. 4.3 f, h and 4.4 b, d) and the 560-615 nm yellow rhodamine-based ROS sensor fluorescence (Fig. 4.3. d).

Images show, that the 515-550 nm DanePy fluorescence was co-localized with the red chlorophyll fluorescence, emitted from the chloroplasts (Figs. 4.3 e, f and 4.4 a, b) .

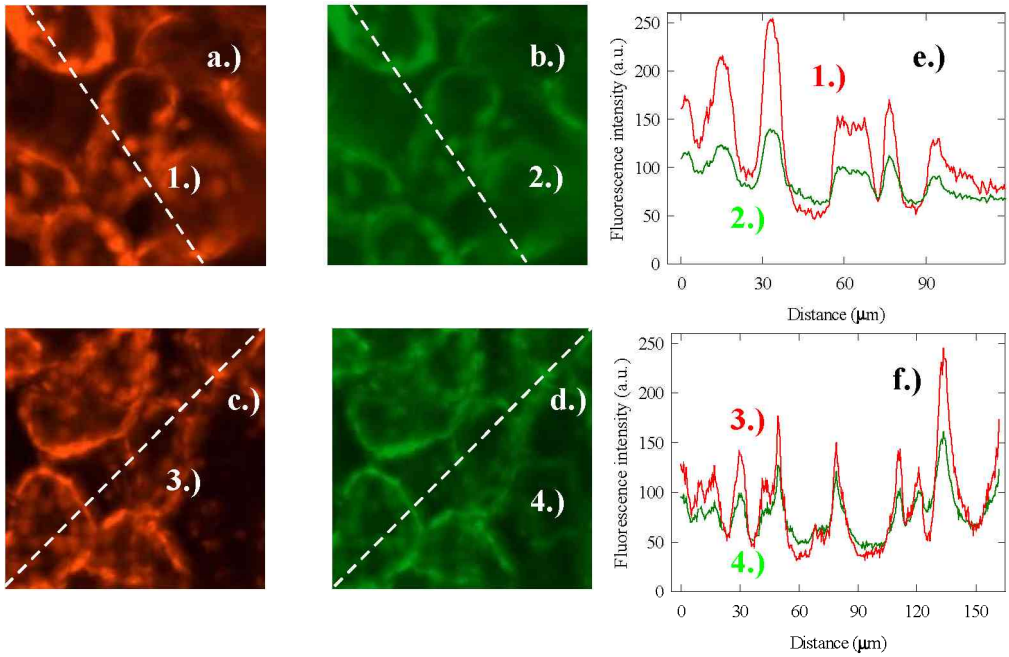

*Fig. 4.4. LSM images of 351 nm excited red (λ>650 nm) chlorophyll fluorescence (a,c) and green fluorescence (515<λ<550 nm)(b,d) detected in spinach leaves infiltrated with aqueous solutions (<10 % ethanol) of either DanePy (a,b) or HO-1889NH (c,d). Graphs (e,f) compare intensities of red and green fluorescence along the diagonal lines (1,2) shown on the images. Image size is 115*115 μm.*

Comparison of the intensity distribution of green fluorescence from DanePy with that of the red chlorophyll fluorescence (Fig. 4.4 e.) showed that DanePy penetrated to the chloroplasts (Figs. 4.4 a, b, e). Intensity profile of the green fluorescence at the local minima between peaks was above zero (Fig. 4.4 e), which represented the emission of the sensor in the symplastic or apoplastic compartment, and the UV-inducible leaf autofluorescence. The ratio between the DanePy fluorescence detected from chloroplasts and from the symplast does not necessarily reflect quantitative distributions of the sensors, because the fluorescence yield of the sensor may depend on its environment, on whether is localized in membrane-phase or in aqueous environment. The above results support the previous finding, when the localization of DanePy inside the chloroplasts was shown in ***Arabidopsis thaliana*** leaves (Hideg et al., 2001). The fluorescence of HO-1889NH also coincided with the red chlorophyll fluorescence (Figs. 4.3 g, h and 4.4 c, d), as of DanePy. The intensity profile of HO-1889NH green fluorescence was compared to the red chlorophyll fluorescence, which identified chloroplasts (Fig. 4.4 f). As in the case of DanePy, the intensity profile of the green fluorescence at the local minima between peaks was found also to be above zero (Fig. 4.4 f). Since HO-1889NH was localized in the chloroplasts, the sensor with double-reactivity was also suitable for ***in vivo*** stress-photosynthesis related ROS detection studies. On the other hand, the 560-615 nm yellow fluorescence from HO-2941 was not co-localized with the red chlorophyll fluorescence (Figs. 4.3 c, d). Since HO-2941 did not penetrate into the chloroplasts, its ***in vivo*** applications in photosynthesis-related stress studies was limited. The rhodamine-based sensor may be used in experiments focusing on other than chloroplast-localized events, for example when information about the $^1O_2$ production in other cell compartments is needed. Because photosynthesis-related ***in vivo*** ROS production was our main interest, HO-2941 was not applied in further studies. Although, images (Figs. 4.3. and 4.4.) confirm the co-localization of both DanePy and HO-1889NH fluorescence with the chlorophyll fluorescence, the sensors are present in other cell compartments as well.

4.1.2.3. The *in vivo* ROS sensor fluorescence overlaps with the UV-induced blue-green auto-fluorescence (BGF) of leaves

Both DanePy and HO-1889NH were excitable by 340 nm UV irradiation, and their fluorescence was emitted in the 400-620 nm region, with emission maxima around 530-550 nm.

Apart from the red chlorophyll fluorescence, ultraviolet excitation of plant leaves also results in blue-green intrinsic fluorescence (BGF) emission in the 450-550 nm region. The identity, the distribution and the localization of those molecules, which emit in this spectral region is intensely discussed in several studies (Chapelle et al., 1984, Goulas et al., 1990, Chapelle et al., 1991, Cerovic et al., 1993, Lichtenthaler and Schweiger, 1998, Johnson et al., 2000, Hideg et al., 2002b). This intrinsic fluorescence probably originates from a variety of sources. BGF has been attributed mainly to the cell wall bound ferulic acid (Morales et al., 1996, Lichtenthaler and Schweiger, 1998), but flavonoids (Hideg et al., 2002b) and phenols, such as quercetin, kaempferol and coumaric acids, and even NADPH (Cerovic et al., 1993) are also believed to contribute to the overall blue-green fluorescence emission of the UV excited plant leaves. Abiotic stresses induce changes in the BGF levels of leaves. BGF is considerably enhanced in UV-treated leaves (Hideg et al., 2002b) correlating with the increased polyphenolics synthesis in the exposed leaves (Sullivan and Teramura, 1990). These compounds are part of the plant's defense system, acting either as UV screens or functioning as antioxidants. BGF emission was not observed in chloroplasts of barley leaves (Hideg, 2002), although other studies report such emission in different plant species (Chapelle et al., 1991) or in isolated chloroplasts (Latouche et al., 2000). The UV-inducible BGF was low in leaves infiltrated with distilled water without the ROS sensors (Fig. 4.3 b).

Spectrofluorimeter measurements showed that the fluorescence emission maxima of both dansyl-based ROS sensors overlapped with the UV-inducible BGF of leaves (Fig. 4.5.). Although UV irradiation induced certain enhancement of the BGF in stressed leaves, adequate infiltration provided much higher levels of ROS sensor fluorescence emission than that of the BGF emission (Fig. 4.5.). Moreover losses in the sensor's fluorescence were many times higher, than the BGF changes. Figure 4.3 a. shows the LSM image of a spinach leaf infiltrated with water. The 351 nm excited

red chlorophyll fluorescence from Fig. 4.3 a. was compared to the UV-excited green fluorescence of leaves shown in panel b). The UV-excited green fluorescence of the leaves was low compared to that of either DanePy (Fig. 4.3 f) or HO-1889NH (Fig. 4.3 h). Therefore, adequate infiltration leads to much higher fluorescence emission from the sensor than the intrinsic leaf fluorescence (Fig. 4.5.). Even though these changes of the BGF of stressed leaves are small, ROS sensor fluorescence quenching data were always corrected for the UV-excited BGF modifications.

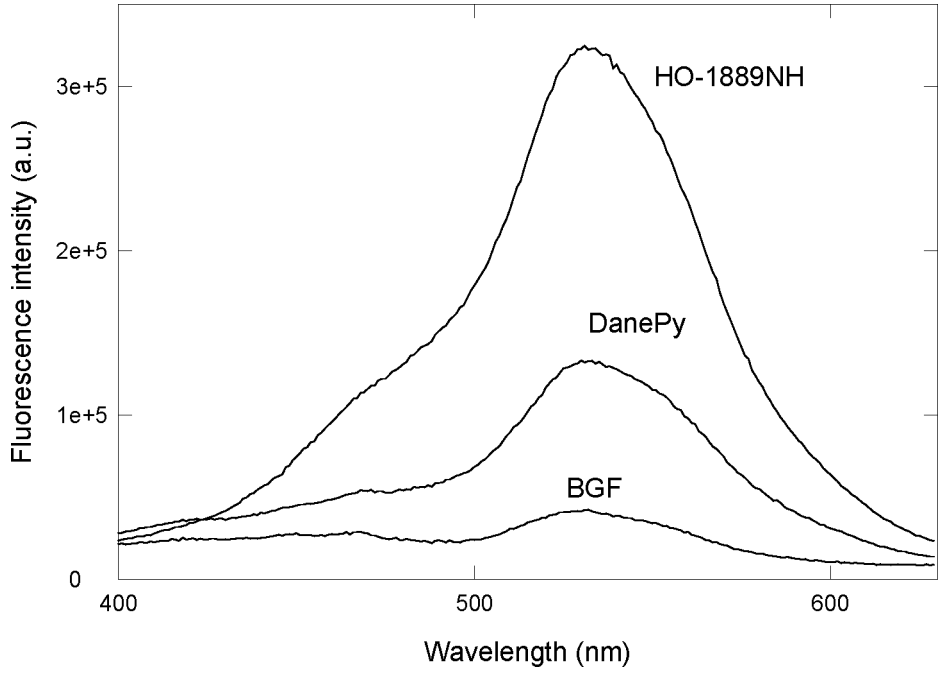

Fig. 4.5.: 340 nm induced fluorescence emission spectra of spinach leaves infiltrated with 1 mM aqueous solutions (containing less than 10 % ethanol) of DanePy or HO-1889NH, and blue-green (BGF) emission of a spinach leaf infiltrated with distilled water.

4.1.2.4. The distribution of fluorescent sensors in leaves

The choice of the infiltration method significantly affected the distribution of the sensor in the leaf. Infiltrating methods were selected in order to ensure optimal

distribution of the sensor in the leaf, but having as little effect on the photosynthetic activity of the studied plant as possible.

Previous studies showed that even though floating the leaf on the solution of the sensor did not affect photosynthetic parameters severely, only weak sensor fluorescence was detectable due to the poor uptake of the sensor, which was mainly localized in the petiole and in the vascular tissue of the leaf. Vacuum infiltration did not assure homogenous distribution of the sensor in the leaves, a large amount of the ROS sensor was deposited in the petiole, and photosynthetic activity was lowered by about 20 % (Hideg et al., 2002a). Therefore a new, less damaging infiltration method was introduced, in which the solution of the ROS sensor was forced into the leaves through a pinhole.

By applying infiltration through a pinhole the distribution of the sensor in the leaf was more uniform, than it could have been achieved by other methods. A small area of DanePy infiltrated leaf is shown in Fig 4.6. The infiltrated area was usually about 1.5 cm^2, depending on the proximity of vascular tissue, which prevented the further distribution of the sensor. This type of infiltration process decreased PSII activity by less than 10 %, to a smaller extent than vacuum infiltration (20 %) (Hideg et al., 2002a). PSII activities were not altered by the ROS sensors themselves in any of the mentioned infiltration methods: the loss of variable chlorophyll fluorescence occurred due to the infiltration rather than to the presence of the sensors (Hideg et al., 2002a).

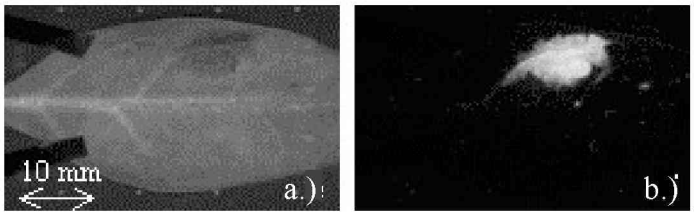

Fig. 4.6.: Photographic image of a tobacco leaf infiltrated through a pinhole: the infiltrated area is darker in the picture a.) and the distribution of DanePy: 310 nm excited 410-640 nm fluorescence emission image of the same leaf b.).

Due to the infiltration, the UV-excited intrinsic BGF intensity was enhanced. Various infiltration techniques led to different enhancement of the BGF in the infiltrated leaves compared to those, which were not infiltrated. BGF intensity was more enhanced in vacuum infiltrated leaves than in those infiltrated through a pinhole.

The amount of sensor taken up by different leaves of distinct plant species is a very important factor. Infiltration through a pinhole is the suitable technique when larger, softer leaves of dicotyledous species are the object of the study, while monocotyledous species are hard to infiltrate by this method. For example young spinach leaves are infiltrated more efficiently with double sensors than wheat leaves (unpublished data). The concentration of the sensors in the mesophyll cells cannot be exactly quantified. Despite of their high fluorescence emission intensities in leaves and of their potential to be quenched by ROS almost totally, compared to their original fluorescence, double ROS sensors can only be used for relative fluorescence change estimations, due to their variability in absolute intensity. Although exact ROS concentration values in leaves cannot be quantified, the ROS-inducing effects of various stress conditions can be compared.

Summarizing the above findings, we concluded, that whenever possible, infiltration through a pinhole was favourable for ***in vivo*** stress studies. Nevertheless, fluorescence data had to be corrected for sensor stability and, in the case of UV stress experiments, for the changes of the intrinsic blue-green fluorescence of the leaf as well.

4.2. Stress by excess photosynthetically active radiation

The mechanism of photoinhibition is one of the most extensively studied stress mechanisms in plant science. It is generally accepted, that the primary target of photoinhibition is the photosystem II (Barber and Andersson, 1992). Photoinhibitory damage occurs, when photosynthetically active samples are irradiated under aerobic conditions by excess photosynthetically active radiation. Excess PAR impairs PSII electron transport, which is followed by selective degradation of the D1 reaction centre protein, and by more general lipid and protein damage (Aro et al., 1993). The nature of reactive oxygen species involved in the mechanism of high light intensity induced damage is still an open question. The light-induced loss of Q_A in

photoinhibited reaction centers allows the formation of triplet excited reaction centre chlorophylls with high probability (Vass and Styring, 1992, Telfer et al., 1994). In this model, the evolution of $^1O_2$ was presumed from the interaction of excited chlorophyll molecules with the oxygen, present abundantly in chloroplasts (Vass et al., 1992, Vass and Styring, 1993). Previous ***in vitro*** and ***in vivo*** experiments revealed that $^1O_2$ indeed was the main ROS product of the acceptor side- induced photoinhibition (Macpherson et al., 1993, Hideg et al., 1994a, Hideg et al., 1994b, Hideg et al., 1998, Hideg et al., 2001). The involvement of $O_2^{-\bullet}$ radicals in the mechanism of photoinhibition has also been hypothesized in certain studies (Kyle, 1987, Miyao, 1994, Fryer et al., 2002) although the formation of these species was not proved in spinach thylakoids (Hideg et al., 1995). There is still no consensus on the nature of photoinhibition induced ROS in leaves. We extended our studies to the application of dansyl-based double sensors to investigate photoinhibition by excess PAR at the level of ROS production.

In the present study we investigated whether there was any detectable $O_2^{-\bullet}$ production in photoinhibited thylakoids or in leaves exposed to excess PAR, by using fluorescent ROS sensors.

4.2.1. Photoinhibition of thylakoid membranes

The parallel use of the $^1O_2$ reactive DanePy and of the $^1O_2$ and $O_2^{-\bullet}$ reactive HO-1889NH was a good opportunity to obtain information about the $O_2^{-\bullet}$ produced in photoinhibited thylakoid samples. Isolated thylakoid membranes were exposed to 1500 μmol $m^{-2}s^{-1}$ PAR for 30 minutes in the presence of either DanePy or HO-1889NH. The fluorescence of DanePy decreased by 40 % meanwhile HO-1889NH fluorescence was quenched by only 10 % (Fig. 4.7.). The oxygen evolving capacity of the thylakoid membranes decreased to 60 % of the original activity during the photoinhibition.

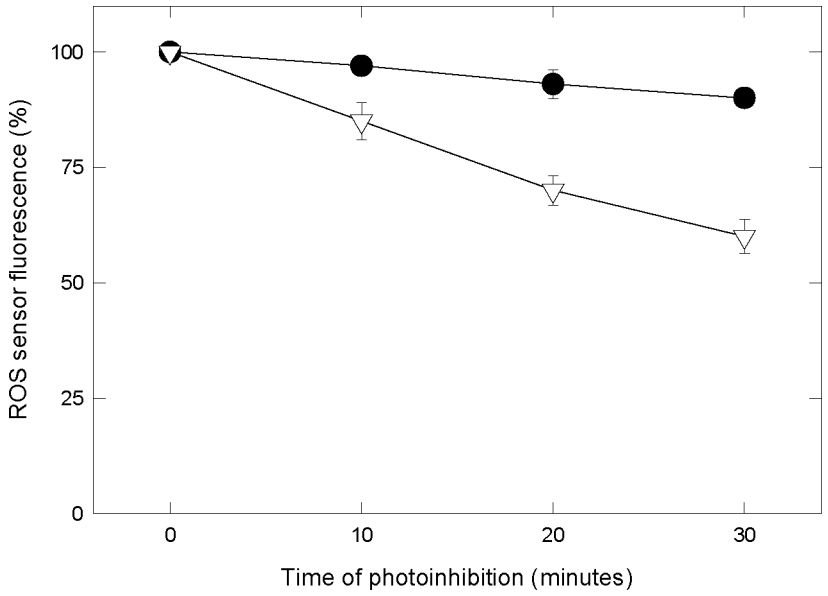

Fig. 4.7.: Fluorescence quenching of DanePy (triangles) and HO-1889NH (circles) in thylakoid membranes exposed to 1500 μmol m^{-2} s^{-1} PAR for 30 minutes.

Based on these findings, our results support the model hypothesizing singlet oxygen as the main promoter of photoinhibitory damage in isolated thylakoid membranes. $O_2^{-\bullet}$ radicals were not detected by trapping ROS with fluorescent sensors.

4.2.2. Reactive oxygen species produced in photoinhibited leaves

Details of the photoinhibition induced damaging processes in PSII are still not fully understood. ***In vivo*** singlet oxygen evolution was proved in photoinhibited leaves by fluorescence spectroscopy (Kálai et al., 1998, Hideg et al., 1998), and the site of $^1O_2$ evolution was identified to be in the chloroplasts by imaging techniques (Hideg et al., 2001). By using double sensors in photoinhibited thylakoids the presence of $O_2^{-\bullet}$ could not be detected, but a few studies hypothesize $O_2^{-\bullet}$ and other ROS evolution in photoinhibited leaves (Fryer et al., 2002). By introducing the $^1O_2$ and $O_2^{-\bullet}$ reactive ROS sensor, HO-1889NH, we studied whether there was any $O_2^{-\bullet}$ production in photoinhibited leaves. DanePy was used in parallel with the new sensor to detect light stress induced ***in vivo*** ROS production.

Both DanePy (Hideg et al., 2001) and HO-1889NH (Barta et al., 2002) penetrated into the chloroplasts of leaves (Figs. 4.3 e, f, g, h and 4.4 a, b, c, d), and their initial fluorescence had the potential to be quenched by more than 80 % upon reaction with their target ROS, as assumed from the difference in the fluorescence intensities of the sensors and of their nitroxide pairs (Fig. 3.4.). Therefore, by applying these sensors, more detailed information was obtained about the ROS evolution under stress by excess PAR.

Arabidopsis thaliana leaves were infiltrated with either DanePy or with HO-1889NH and irradiated with 1800 μmol $m^{-2}s^{-1}$ PAR for 30 minutes (Fig. 4.8.). Leaves were vacuum-infiltrated because the morphology of ***Arabidopsis*** leaves did not allow pinhole infiltration, as being very small.

By recording the fluorescence of the sensor every 10 minutes during the stress treatment, it was shown, that the fluorescence of the sensors was quenched progressively as the stress treatment proceeded. The fluorescence quenching of the ROS sensors is an accumulative process: the extent of quench at a given time point during the photoinhibition is characteristic to the total ROS production until that time. In this way, ROS evolution is characterized by the increase of quenching during relatively short, 10 minutes intervals.

Fig. 4.8. illustrates the progressive fluorescence quenching of both ROS sensors in the photoinhibited leaves. During 30 minutes of photoinhibition the fluorescence of DanePy decreased to almost half compared to its original intensity, suggesting intense $^1O_2$ evolution. The above findings supported previous results, which showed $^1O_2$ production in photoinhibited broad bean and ***Arabidopsis*** leaves (Hideg et al., 1998, Hideg et al., 2001).

Although $O_2^{-\bullet}$ radicals were not identified ***in vitro*** in photoinhibited isolated thylakoid membranes, when HO-1889NH infiltrated ***Arabidopsis*** leaves were exposed to 1800 μmol m^{-2} s^{-1} PAR for 30 minutes, the fluorescence of this sensor decreased significantly. HO-1889NH fluorescence quenching was higher than that of DanePy under identical conditions. Therefore assuming $O_2^{-\bullet}$ production under the above stress conditions seemed feasible. Vacuum infiltration itself caused about 10-15 % decrease in the photosynthetic electron transport of the leaves, but the applied photoinhibitory treatment decreased the variable chlorophyll fluorescence by 50%.

Fluorescence spectroscopy gives information about the total fluorescence of the sensor originated from a small, approximately 1 x 8 mm portion of the leaf segment, while LSM imaging is a technique with higher resolution, the monitoring of ROS sensor fluorescence changes becomes possible at the level of cells.

In order to study the origin of $O_2^{-\bullet}$ in photoinhibited leaves, confocal laser scanning microscopy experiments were carried out.

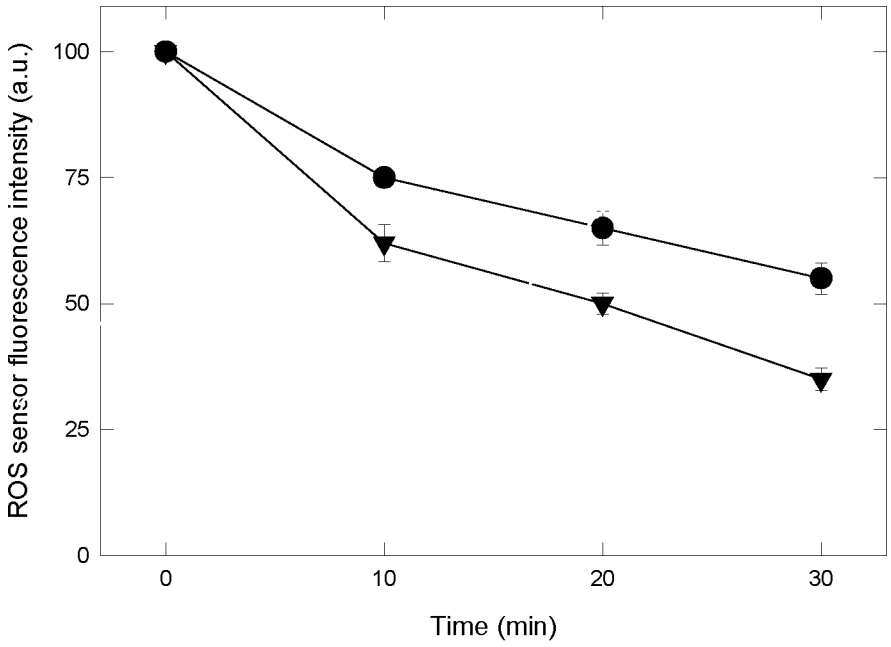

Fig. 4.8. Fluorescence quenching of DanePy (circles) and of HO-1889NH (triangles) in Arabidopsis thaliana leaves exposed to photoinhibition by 1800 µmol m^{-2} s^{-1} PAR for 30 minutes.

Spinach leaves were infiltrated with either DanePy or HO-1889NH and exposed to 1800 µmol m^{-2} s^{-1} PAR for 45 minutes (Figs. 4.9. and 4.10.). To follow the progress of photoinhibition during the treatment, LSM images were taken at 0, 15, 30 and 45 minutes in both cases. The 351 nm UV-induced green DanePy fluorescence gradually decreased as the time of the photoinhibition progressed and by the end of the treatment almost completely disappeared (Fig. 4.9 e, f, g, h). Green fluorescence

was entirely emitted from the sensor, since the UV-induced intrinsic BGF intensity was low in leaves under our experimental conditions (Fig. 4.3. b). Fluorescence intensity profiles of the 515-550 nm emissions were plotted along diagonal lines on the LSM pictures (Fig. 4.9.). These plots showed, that the originally high intensity peaks corresponding to the green DanePy fluorescence in the chloroplasts gradually decreased during the 45 minutes of the treatment. These plots, which confirmed the visual information, showed that DanePy fluorescence was quenched in the chloroplasts, by photoinhibition-induced $^1O_2$. These findings supported the earlier results, which proved $^1O_2$ production in photoinhibited leaves (Hideg et al., 2001).

When infiltrated into spinach leaves, the fluorescence emission of HO-1889NH was quenched by photoinhibition-induced ROS similarly to that of DanePy. LSM images and the HO-1889NH fluorescence intensity profiles showed that the fluorescence of this ROS sensor was also quenched progressively in the chloroplasts as the time of the photoinhibition treatment progressed (Fig. 4.10.). HO-1889NH fluorescence decreased to smaller extent, by approximately 50 % only than the fluorescence of DanePy under identical conditions (Fig. 4.9.). It is also of interest that HO-1889NH fluorescence was detected from outside chloroplasts as well only the yield of the sensor may depend on its environment.

As control, the common fluorescent group of both applied sensor molecules, dansyl-chloride was also tested. It was found, that the fluorescence of dansyl-chloride was not quenched by photoinhibition-induced ROS (Hideg et al., 1998).

In order to follow photoinhibition-induced ROS production in whole leaves quantitatively, spinach leaves were infiltrated with either DanePy or HO-1889NH through a pinhole and were exposed to irradiation by 1800 μmol m^{-2} s^{-1} PAR for 75 minutes. 75 minutes of photoinhibition resulted in more than 90 % inactivation of the photosynthetic electron transport. 295-375 nm UV-excited 410-640 nm fluorescence emission image of the infiltrated area was taken after the infiltration as reference (Figs. 4.11 c and 4.12 a), then the sensors' fluorescence was monitored during the time-course of the photoinhibition by acquiring fluorescence images during the treatment. Exposure to excess PAR resulted in gradual quenching of DanePy fluorescence (Fig. 4.11.), to less than 25 % of its original intensity by the end of the treatment.

On the other hand, HO-1889NH fluorescence was not quenched as extensively as that of DanePy, by approximately 50 % only of the original fluorescence in leaves

exposed to the same 75 minutes photoinhibition. The electron transport activity of the studied leaves decreased by the end of the treatment to less than 10 % (Fig. 4.13.). Both DanePy and HO-1889NH fluorescence quenching during the above photoinhibitory treatment were plotted in function of the photosynthetic activity loss of the leaves (Fig. 4. 11 and 4.12).

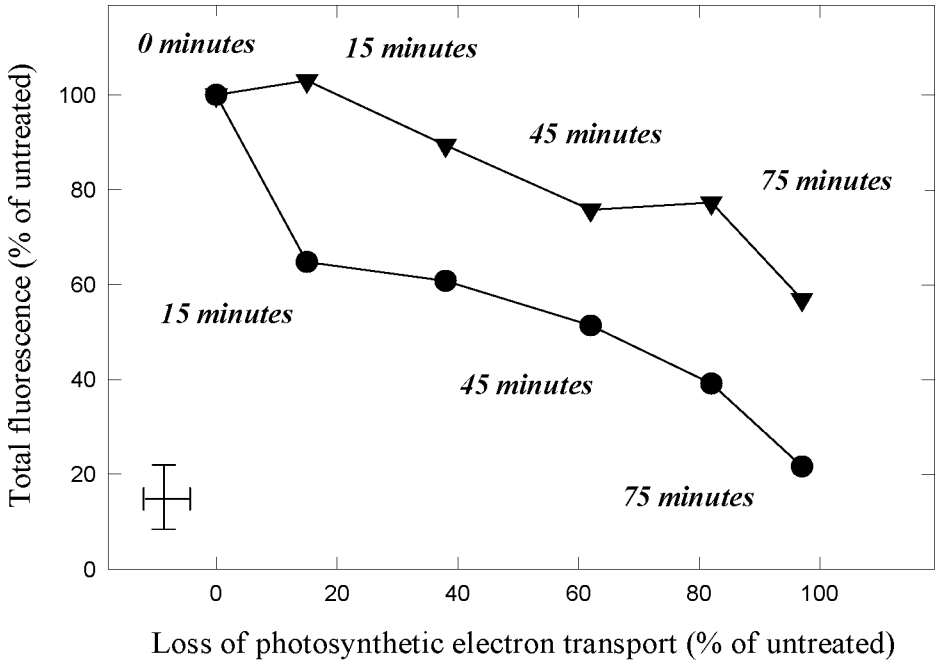

Fig. 4.13.: DanePy (circles) and HO-1889NH (triangles) fluorescence quenching in spinach leaves exposed photoinhibition by 1800 µmol m^{-2} s^{-1} PAR for 75 minutes. Data points were calculated from the images of Figs. 4.11 and 4.12. Typical errors in the ROS fluorescence loss and loss of the photosynthetic yield parameter were calculated from three different experiments, and are shown as vertical and horizontal error bars in the left corner of the figure.

Although the fluorescence of the $^1O_2$ and $O_2^{-\bullet}$ reactive HO-1889NH decreased significantly in the photoinhibited leaves, its quenching was attributed to trapping photoinhibition-induced singlet oxygen only, since the fluorescence decrease of this sensor proved to be less extensive than that of the $^1O_2$ reactive DanePy (Fig. 4.13.). The above data, the LSM and fluorescence microscopy images supported the

conclusion, that the fluorescence quenching of both sensors occurred mainly in the chloroplasts due to their reaction with the photoinhibition-induced $^1O_2$, the contribution of $O_2^{-\bullet}$ was minor. The former conclusion was supported by the extent of DanePy fluorescence quenching in photoinhibited thylakoids as well, the fluorescence of the $^1O_2$ and $O_2^{-\bullet}$ reactive sensor quenched by 10 % only (see Fig. 4.7.). However, the higher fluorescence quenching of HO-1889NH than that of DanePy in ***Arabidopsis thaliana*** leaves (see Fig. 4.8.) suggested the contribution of both $^1O_2$ and $O_2^{-\bullet}$ in photoinhibition. The nature of this process is yet unknown and needs further investigation, but was not the aim of the current thesis.

4.3. Stress by UV-radiation.

The nature of ultraviolet-radiation elicited oxidative stress at the level of photosynthesis is an intensely discussed process. Above a certain threshold UV radiation inhibits photosynthesis, by a mechanism different than the inhibition by excess PAR. PSII electron transport is inactivated by UV radiation, and D1 core protein is damaged (Renger et al., 1989, Vass et al., 1999). D1 degradation products are different than the fragments detected upon photoinhibition (Greenberg et al., 1989, Friso et al., 1994a), and the degradation of the D2 protein was also proved (Friso et al., 1994b). There are indirect evidences of UV-induced ROS production: UV irradiation induces the up-regulation of free radical scavenging enzymes (Foyer et al., 1994, Rao and Ormrod, 1995), the accumulation of ascorbate free radicals (Hideg et al., 1997), and the increase of oxidative membrane damage-related ultraweak luminescence (Cen and Björn, 1994). ***In vitro*** studies proved the induction of hydroxyl radical, peroxyl- and carbon centered radical evolution in UV-B irradiated thylakoid membranes (Hideg and Vass, 1996). The UV-B induced D1 degradation was associated with hydroxyl radicals (Hideg et al., 1999). Other studies hypothesized $O_2^{-\bullet}$ production in UV-B stressed leaves (Mackerness et al., 1998, Mackerness et al., 2001). The UV-A induced mechanism is generally considered to be similar, but a few orders of magnitude less effective than that of the UV-B irradiation (Turcsányi and Vass, 2000, White et al., 2002, Quaite et al., 1992).

Because of the lack of consensus and direct ***in vivo*** ROS data in plant leaves, our aim was to study UV-induced ROS evolution using double sensors both ***in vitro*** and ***in vivo***.

4.3.1. Reactive oxygen species detection in thylakoid membranes exposed to UV-irradiation.

The possible role of $^1O_2$ and $O_2^{-\bullet}$ in the mechanism of damage induced by UV-stress was investigated in isolated thylakoid membranes.

Thylakoids were exposed to either broadband (emission maximum at 365 nm) of 35 μmol m^{-2} s^{-1} UV-A, or broadband (emission maximum at 312 nm) 27 μmol m^{-2} s^{-1} UV-B irradiation in the presence of DanePy or HO-1889NH for 60 minutes (for details see Chapter 3.8.2.1.). Although the oxygen evolving capacity of the membranes decreased almost completely by the end of the treatment, neither DanePy nor HO-1889NH fluorescence was quenched by more than 5-10 %, which was less than the 10% uncertainty of the measurements. Since the 345-385 nm UV-A and the 295-320 nm broadband UV-B irradiation did not elicit $^1O_2$ and $O_2^{-\bullet}$ production detectable by double sensors under these conditions, it was assumed, that the source of ROS production may either be selectively activated by other wavelength UV range or certain components needed for the ROS production may be localized outside the thylakoid membranes. In order to follow the wavelength dependency of the $^1O_2$ and $O_2^{-\bullet}$ production in isolated thylakoids HO-1889NH fluorescence decrease was studied in thylakoids exposed to quasi-monochromatic UV irradiation of various wavelengths. Irradiation doses were adjusted to induce the same 60 % loss of the oxygen evolving capacity for all applied wavelengths by using different irradiation times, ranging from 20 to 50 minutes. Only minor HO-1889NH fluorescence quenching of about 10 % was detected for any wavelength in the 290 - 390 nm interval (Fig. 4.14.). In control experiments it was checked that the fluorescence of the sensors was not altered by the applied UV irradiation of any wavelength (data not shown). Therefore, significant $O_2^{-\bullet}$ production was not detected in thylakoids with HO-1889NH.

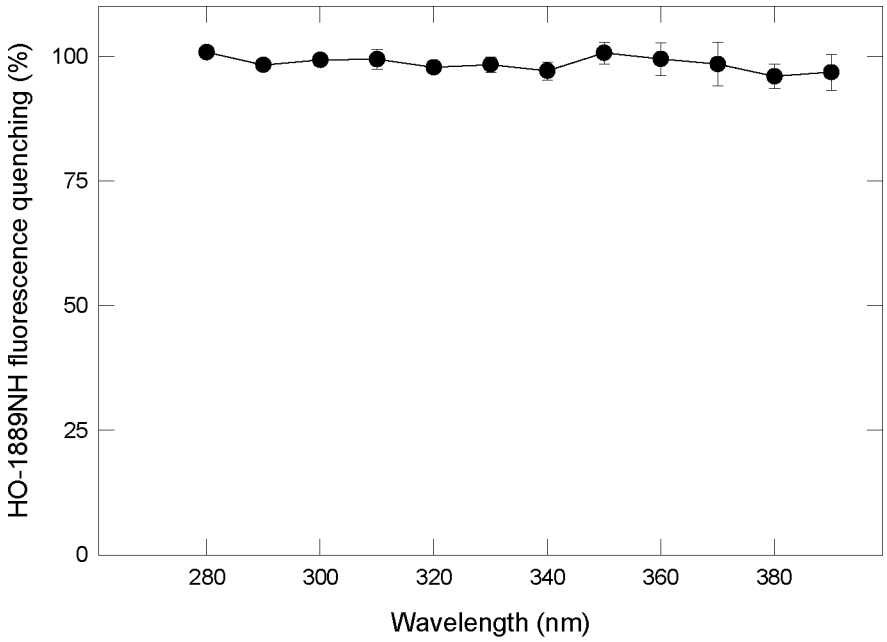

Fig. 4.14. HO-1889NH fluorescence quenching in thylakoids (20µg/ml) exposed to quasi-monochromatic UV-radiation of 280 to 390 nm.

To verify the absence of $O_2^{-\bullet}$ in the UV stressed thylakoids, a different detection approach was applied.

From among the numerous spectrophotometrical assays available, the detection of superoxide-induced 550 nm absorbance change of ferricytochrome-c were used (Takahashi and Asada, 1988). Thylakoid samples were irradiated with quasi-monochromatic UV radiation as above in the presence of cytochrome-c. $O_2^{-\bullet}$ evolution was quantified by the cytochrome-c absorbance changes at 550 nm. Superoxide-inducible cytochrome-c reduction was small at any of the applied UV wavelengths, slightly higher in the 370-390 nm range (Fig. 3.15.). Cytochrome-c absorbance changes were monitored in the presence of added catalase as well. Catalase was added in order to neutralize H_2O_2, which may have been produced in UV-treated thylakoid membranes. Hydrogen peroxide, formed directly or as a product of superoxide dismutation, can oxidize ferrocytochrome-c at rates comparable to those at which ferricytochrome-c is reduced by superoxide. This reoxidation may affect

significantly superoxide detection. The reoxidation can be prevented by catalase addition (Vandewalle and Petersen, 1987).

Significant differences were not detected between the cytochrome-c reduction of those samples, which were treated in the presence of catalase and of those without. From the above findings we concluded, that neither UV-A nor UV-B irradiation led to detectable $O_2^{-\bullet}$ production in our thylakoid experiments.

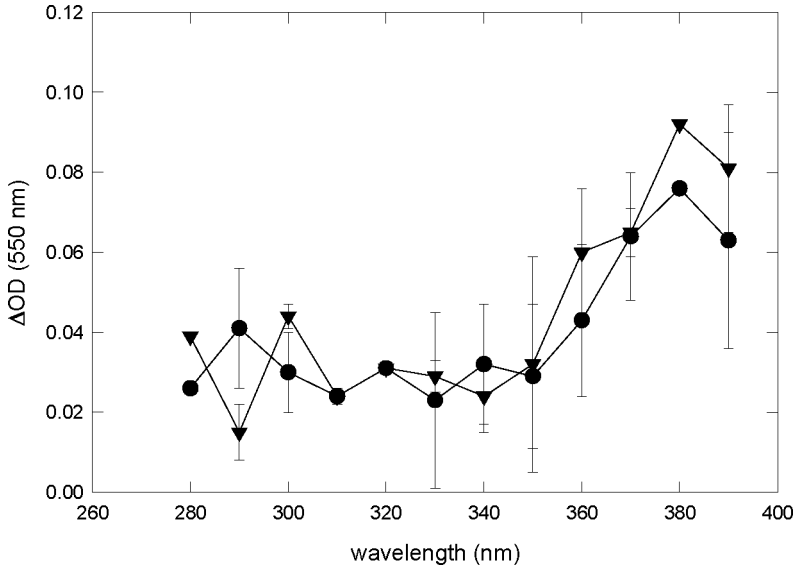

Fig. 4.15.: 550 nm absorbance changes in the of cytochrome-c in thylakoids irradiated with various wavelength UV-radiation. ΔOD at 550 nm was recorded in the presence (triangles) and in the absence (circles) of 0.5 units of catalase.

4.3.2. UV-radiation induced *in vivo* ROS production

4.3.2.1. $^1O_2$ and $O_2^{-\bullet}$ detection leaves exposed to broadband (295- 320 nm) UV-B irradiation

Because of the discrepancy between the indirect ***in vivo*** (Mackerness et al., 1998, Mackerness et al., 2001) and direct ***in vitro*** results (presented in Chapter 4.3.1.)

on the involvement $O_2^{-\bullet}$ in UV stress, our experiments were extended to direct ROS detection in UV-irradiated leaves.

Arabidopsis thaliana leaves were vacuum infiltrated with either DanePy or HO-1889NH then exposed to 27 μmol m^{-2} s^{-1} UV-B irradiation of 295- 320 nm from a broadband lamp for 60 minutes.

Although ROS sensors are stable in sodium-phosphate buffer for several hours, they are not perfectly stable in the leaves (see Chapter 4.1.2.), therefore their application in long-term stress experiments meets difficulties. The sensors may be metabolised in a yet unknown way in the leaf, therefore they were applied in short-term ***in vivo*** studies. To avoid keeping the sensor for longer time in the leaf, UV irradiation was performed in two sequences: the fluorescence emission decrease of the sensor was followed in infiltrated ***Arabidopsis*** leaves, irradiated for 30 minutes (Fig. 3.7 a), or pre-illuminated leaves were infiltrated and exposed to UV-B for 30 more minutes (Fig. 3.7 b). Variable chlorophyll fluorescence of leaves decreased during the pretreatment by approximately 30 % and the further illumination decreased photosynthetic activity by 30 % more. The extent of total ROS production during the 60 minutes UV-irradiation was evaluated by combining the two data sets: the first reference point of the pre-treated series was normalized to the last reference point of the series which did not receive UV-irradiation prior to the infiltration (Fig. 4.16.). This normalization was necessary, because the absolute fluorescence intensity achieved in each infiltration and each leaf was different. ROS production between the 30^{th} and 60^{th} minutes of UV-B irradiation was estimated by comparing changes of sensor fluorescence to the reference point recorded after the pre-treatment.

DanePy fluorescence was not quenched during the UV-B irradiation (Fig. 4.16.), although the PSII activity decreased by 60 %. On the other hand, the fluorescence of the $^1O_2$ and $O_2^{-\bullet}$ sensitive fluorescent trap HO-1889NH was extensively quenched, by 75 % during the same UV treatment (Fig. 4.16.). The correlation between the loss of photosynthetic activity in irradiated ***Arabidopsis*** leaves and the fluorescence quenching of the double-reactive HO-1889NH is opposed to the ***in vitro*** findings presented in Chapter 4.3.1.

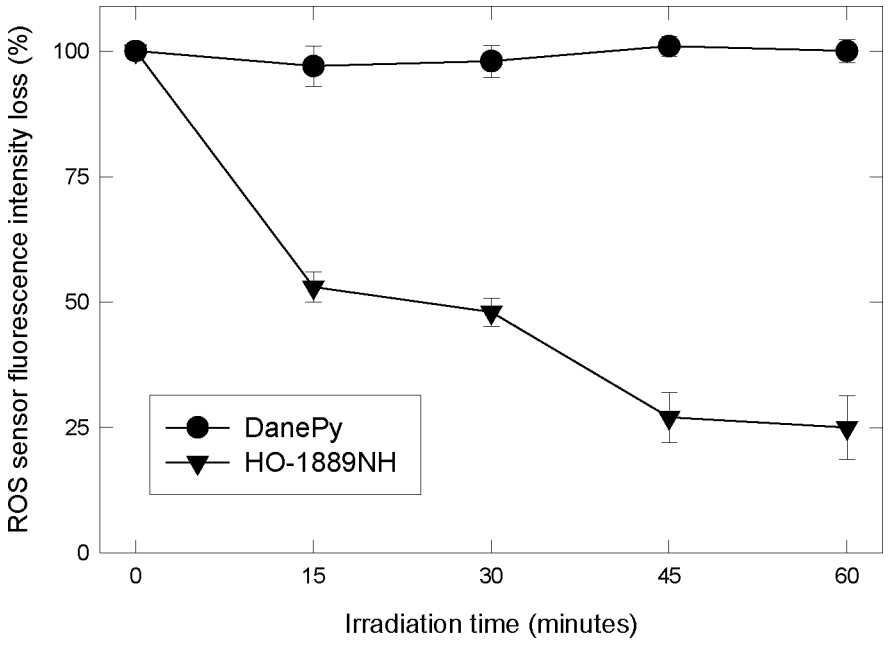

Fig.4.16.: DanePy (circles) and HO-1889NH (triangles) UV-induced fluorescence quenching in Arabidopsis thaliana leaves irradiated with 27 µmol m^{-2} s^{-1} UV-B of 295-320 nm for 60 minutes.

We could not detect $O_2^{-\bullet}$ production neither in thylakoids exposed to 295-320 nm UV-B irradiation by using fluorescent sensors, nor in thylakoids irradiated with quasi-monochromatic UV-B and UV-A of various wavelengths, by monitoring cytochrome-c absorbtion changes. The above ***in vivo*** results suggest, that the dominating ROS product of stress by UV-B irradiation in our experiment was $O_2^{-\bullet}$ and UV-B induced $^1O_2$ was not detected. The discrepancy between the ***in vitro*** thylakoid and ***in vivo*** leaf $O_2^{-\bullet}$ detection led to the conclusion, that a component necessary for the $O_2^{-\bullet}$ yielding reaction was localized outside thylakoids, and therefore $O_2^{-\bullet}$ was not detected in isolated membranes, while the mentioned factor was present in the leaves, therefore in the ***in vivo*** experiments $O_2^{-\bullet}$ production was associated with the mechanism of UV stress. This confirmed the findings of previous

indirect studies, which indicated the possibility of $O_2^{-\bullet}$ production by the activation of SOD enzymes in plants exposed to UV-B irradiation (Rao and Ormrod, 1995)

4.3.2.2. ROS production in CuZnSOD deficient leaves

Transgenic plants, carrying modifications in their expression of certain antioxidant enzyme-regulating gene, or having altered or over-expressed antioxidant production are very often used to study the oxidative nature of the damage induced by various stressors (Bowler et al., 1991, Van Camp et al., 1996, Allen et al., 1997, Shadle et al., 2003). Additional protection may be achieved against the damaging ROS (Oberschall et al., 2000). Superoxide dismutase enzymes (SODs) constitute the first line of defense against superoxide in plant cells (Bowler et al., 1992, Alscher et al., 2002). SODs catalyse the dismutation of $O_2^{-\bullet}$ into H_2O_2 and O_2 (McCord and Fridovich, 1969a and McCord and Fridovich, 1969b). Various isoforms of these enzymes are present in various cellular compartments, where the production of superoxide is possible (Mittler et al, 2002). By altering the expression of certain SOD isoenzymes in different cell compartments, valuable information may be acquired about the cellular localization of superoxide-yielding reactions.

Two SOD deficient tobacco lines were studied, in parallel with the SR1 control, in terms of UV-A and UV-B induced ROS production. ANT4 tobacco leaves lacked the chloroplast localized superoxide dismutase (CuZnSOD) iso-enzyme, while ANT3 leaves were deficient in the cytosol-localized CuZnSOD enzyme. In ANT3 leaves the cytosol- and in ANT4 leaves the chloroplast SOD activity was less than 5 % (unpublished data).

Detached leaves SR1 control plants and of ANT4 or ANT3 CuZnSOD deficient plants were infiltrated with the ROS double sensors through a pinhole. These plants were exposed to quasi-monochromatic 290 ± 8 nm UV-B or 360 ± 8 nm UV-A irradiation. Responses of the ANT4 and ANT3 plants were compared to that of SR1 in terms of photosynthesis and ROS production. $^1O_2$ and $O_2^{-\bullet}$ radicals were monitored in

the UV-stressed leaf segments by following the fluorescence quenching of the two dansyl-based ROS sensors DanePy and HO-1889NH.

The leaves were irradiated with equal photon doses. Irradiation times corresponding to $2x10^{22}$ photons were 15 and 20 minutes, for 290 and 360 nm, respectively. This experimental setup provided higher intensities than natural solar fluxes and the illumination periods were short. Direct ROS detection was possible under such conditions, because the leaves were not allowed to acclimate to the stress, and the extent of detectable damage depended on the already exiting antioxidant status and UV-screening pigment resources of the plants only.

Both DanePy and HO-1889NH fluorescence was quenched in all tobacco genotypes irradiated with 290 nm UV-B. The fluorescence decrease of HO-1889NH was larger in all genotypes as compared to that of DanePy (Fig. 4.17 a, b).

Assuming that the ***in vivo*** affinity of DanePy and HO-1889NH to $^1O_2$ was similar, owing to their identical ROS trap moiety, $O_2^{-\bullet}$ production was estimated as the difference between the ROS-induced HO-1889NH fluorescence intensity decrease minus the DanePy fluorescence loss (Fig. 4.17 c). No significant differences were found in the amount of either $^1O_2$ or $O_2^{-\bullet}$ produced in SR1, ANT3 and ANT4 plants exposed to UV-B irradiation (Fig. 4.17.), while the photosynthetic electron transport activity of all three genotypes decreased (Fig. 4.18.).

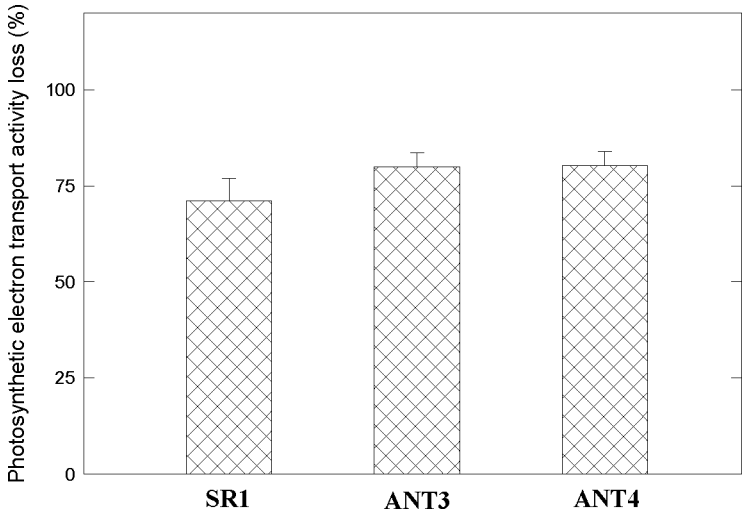

Fig. 4.18.: Variable chlorophyll fluorescence loss of SR1, ANT3 and ANT4 plants exposed to $2x10^{22}$ UV-B photons of 290±8nm.

The variable chlorophyll fluorescence decreased similarly in ANT3 and ANT4 upon the UV-B treatment, both CuZnSOD deficient plants were slightly more sensitive to UV-B radiation than the wild type (Fig. 4.18.).

Similarly, ROS sensor infiltrated ANT3, ANT4 and SR1 leaves were exposed to $2x10^{22}$ UV-A photons of 360 nm. DanePy fluorescence was not quenched significantly in any of the genotypes, thus it can be assumed that $^1O_2$ was not produced under the given experimental conditions in the UV-A irradiated leaves. Although HO-1889NH fluorescence decrease was more intense than that of the DanePy quenching, significant differences were not detected between the three genotypes (Fig 4.19.). ANT3 and ANT4 plants were more sensitive to UV-A radiation than SR1 plants, however we could not detect significant differences between the photosynthetic activity decrease of the two mutants (Fig. 4.20.).

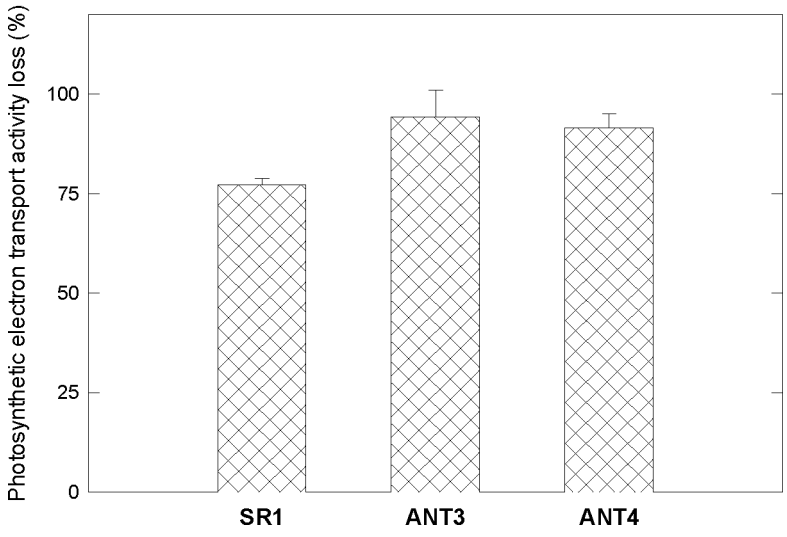

Fig. 4.20.: Variable chlorophyll fluorescence loss of SR1, ANT3 and ANT4 plants exposed to $2x10^{22}$ UV-A photons of 360±8nm.

From the above results, the contribution of both singlet oxygen and superoxide was assigned to the UV radiation elicited stress. SOD deficient leaves were more sensitive to both UV-B and UV-A radiation than controls, but there was no difference

between the loss of electron transport activity of the two SOD mutants. The extent of the detected UV-induced $O_2^{-\bullet}$ production was similar in control and mutant leaves, but the electron transport was differently deactivated in SR1 and mutant leaves, the trapped $O_2^{-\bullet}$ was assumed to be involved in the mechanism of UV induced oxidative stress. However, the question of $O_2^{-\bullet}$ being involved in a chloroplast localized or a cytosol-localized process needs further investigation in the above SOD deficient mutants.

In vitro studies assumed $^{\bullet}OH$ radical to be the first product of the UV-B induced oxidative stress in thylakoid membranes (Hideg et al., 1995). H_2O_2 decomposition catalyzed by iron ions is a potential source of $^{\bullet}OH$ radicals at the level of photosynthetic electron transport in stress exposed plants. When the electron transport is over-saturated and the NADP pool is totally reduced, electron leakage from the electron transport to oxygen becomes feasible. Through consecutive reduction steps involving H_2O_2 and Fe(II), $^{\bullet}OH$ radicals may be formed. Certain studies point the decomposition of H_2O_2 catalyzed by the iron from ferredoxin as possible $^{\bullet}OH$ radical yielding reaction (Asada, 1992a). Hydrogen peroxide has been suggested to appear as an intermediate during water-oxidation (Wydrzynski et al., 1989), thus UV-B induced decomposition of H_2O_2 could produce highly reactive hydroxyl radicals within the water oxidizing complex and promote extensive damage to the protein environment.

In vivo H_2O_2 production was studied in UV-B stressed SR1, ANT3 and ANT4 tobacco leaves, irradiated with 295-320 nm 27 μmol m^{-2} s^{-1} UV-B, for 3 hours. The UV-B treatment reduced the photosynthetic activity of the leaves by about 50 %. UV stress induced H_2O_2 evolution was visualized by a histochemical staining technique: the reaction of 3,3'-diaminobenzidine (DAB) with H_2O_2 gives a dark-brown coloured product, which can be visualized by decolouring the leaf tissue (see Materials and Methods – Chapter 3.9.1- for details). Higher amounts of DAB-detectable H_2O_2 were found in the UV-B treated ANT3 mutant, which was deficient in the cytosol localized CuZnSOD, than in the wild type SR1 and chloroplast-localized CuZnSOD deficient ANT4 tobacco (Fig. 4.21).

The UV-B induced H_2O_2 originating from a reaction localized inside the cytosol was trapped in our experiment by DAB. UV-B induced H_2O_2 evolution may

involve the presence of $O_2^{-\bullet}$ in the cytosol, as an intermediate state. In those plants which had active chloroplast localized SOD to scavenge $O_2^{-\bullet}$, the possible precursor of H_2O_2, this species was not detected by DAB-staining.

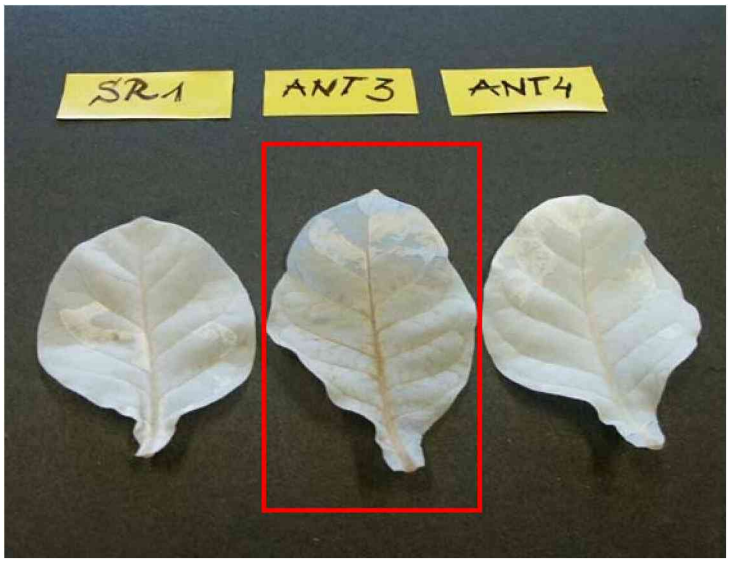

Fig. 4.21.: 3, 3'-diaminobenzidine staining of detached SR1 wild type, ANT3 chloroplast CuZn SOD deficient, and ANT4 cytosol-localized CuZn SOD deficient tobacco.

In summary, results from experiments with SOD-deficient tobacco leaves showed, that both UV-A and UV-B irradiation elicits multilevel oxidative stress. By using double sensors no significant difference could be detected in the UV-induced $^1O_2$ and $O_2^{-\bullet}$ production of the ANT3 or ANT4 and control leaves, however, SOD deficient leaves were slightly more sensitive to UV-B and UV-A irradiation than control leaves. On the other hand, the H_2O_2 detected in the cytosol-localized SOD deficient mutant pointed the importance of cytosol localized SOD in neutralizing superoxide produced upon UV-B exposure.

4.3.2.3. *In vivo* ROS detection by fluorescence microscopy

Since fluorescence spectroscopy experiments provided information only about small segments of leaf cuttings, quantitative analysis of UV-radiation induced ROS was performed on whole spinach leaves infiltrated with solutions of either DanePy or HO-1889NH through a pinhole. The infiltrated leaf segments were exposed to UV radiation of 280-360 nm from a broadband source for 60 minutes and the fluorescence loss of the ROS sensors emission was recorded through a 410 - 640 nm filter.

DanePy fluorescence was quenched during the UV treatment by only 8 %, which is less than the 10 % uncertainty of the measurements (Figs. 4.22. and 4.24.), while the rate of electron transport was lowered by approximately 90 %. Therefore, the applied broadband UV radiation did not result in significant induction of $^1O_2$ evolution in spinach leaves (Fig. 4.24.). Contrary to DanePy, the fluorescence of HO-1889NH progressively decreased as the irradiation proceeded (Fig. 4.23.). The strong, progressive quenching of HO-1889NH fluorescence indicated that the applied UV radiation promoted $O_2^{-\bullet}$ production.

Quantitative analyses of the images confirmed the visual information: in spinach leaves $O_2^{-\bullet}$ production was induced by 280 -360 nm broadband UV radiation, while $^1O_2$ evolution was not a characteristic response triggered by the combination of UV-A and UV-B radiation. These findings are in accordance with previous indirect studies, which reported the activation of SOD genes in UV treated plants (Rao and Ormrod, 1995). Superoxide evolution was detected in 290 nm and 360 nm UV irradiated control and CuZnSOD deficient tobacco plants as well (for details see Chapter 4.3.2.2.). Moreover, singlet oxygen was also detected in SOD deficient and control plants irradiated with quasi-monochromatic UV-A and UV-B radiation (for details see Chapter 4.3.2.2.).

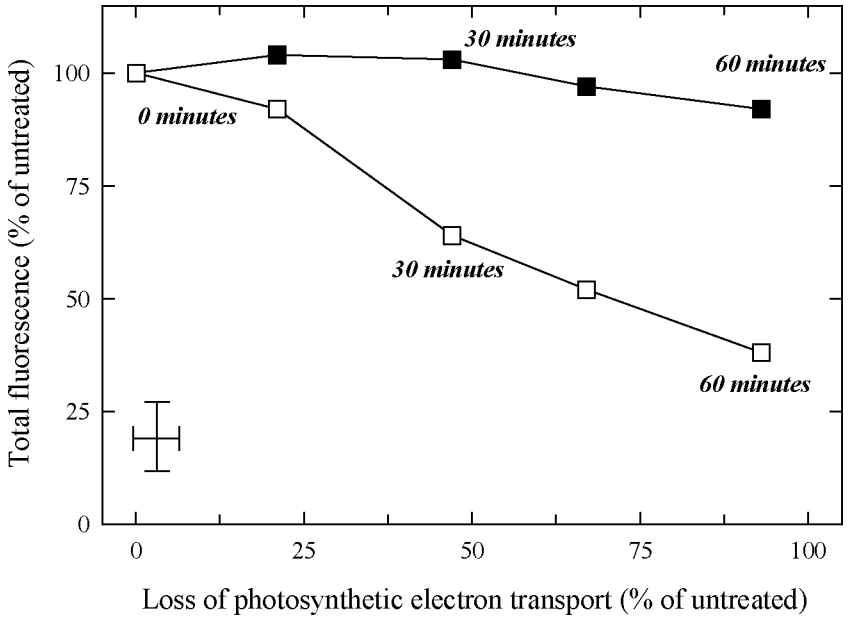

Fig. 4.24.: DanePy (full squares) and HO-1889NH (empty squares) fluorescence quenching in spinach leaves exposed to 280-360 nm UV radiation in function of photosynthetic electron transport loss. Data points were calculated from images of Figs. 4.22 and 4.23.

Since the intensity ratios of different components in the applied broadband UV lamp was not known, the wavelength dependency of UV-induced $^1O_2$ and $O_2^{-\bullet}$ production was studied in leaves, to compare the effect of stress by UV-A to that of UV-B irradiation. We examined the ROS generating ability of various wavelengths UV irradiation in the range of 280-390 nm.

4.3.2.4. *In vivo* ROS generating efficiency of various UV wavelengths

The ROS generating ability of identical fluxes of quasi-monochromatic UV radiation was studied ***in vivo***. ROS sensor infiltrated spinach leaves were irradiated with $2x10^{22}$ photons of various wavelengths ranging from 280 nm to 390 nm. Treatment times were short, between 20 and 30 minutes. The applied doses were

higher in this case as well than the natural UV intensities, corresponding to photon fluxes of about 18-36 µmoles m^{-2} s^{-1}, and irradiances of 28-45 kJ m^{-2}. The applied irradiation caused losses of variable chlorophyll fluorescence in a range between 5-30 %. It is notable, that identical dose of UV-A photons damaged the photosynthetic electron transport less than UV-B photons (Fig. 4.25.). This finding is in agreement with other studies, which considered UV-A radiation to be less effective in causing radical-mediated oxidative damage in different intact and isolated systems, than the high energy UV-B radiation (Rundel et al., 1983, Quaite et al., 1992, Flint and Caldwell, 1996, Turcsányi and Vass, 2000, Flint and Caldwell, 2003). Various UV-induced damage action spectra were suggested for DNA damage, growth retardation and photosynthetic efficiency loss (Flint and Caldwell, 2003).

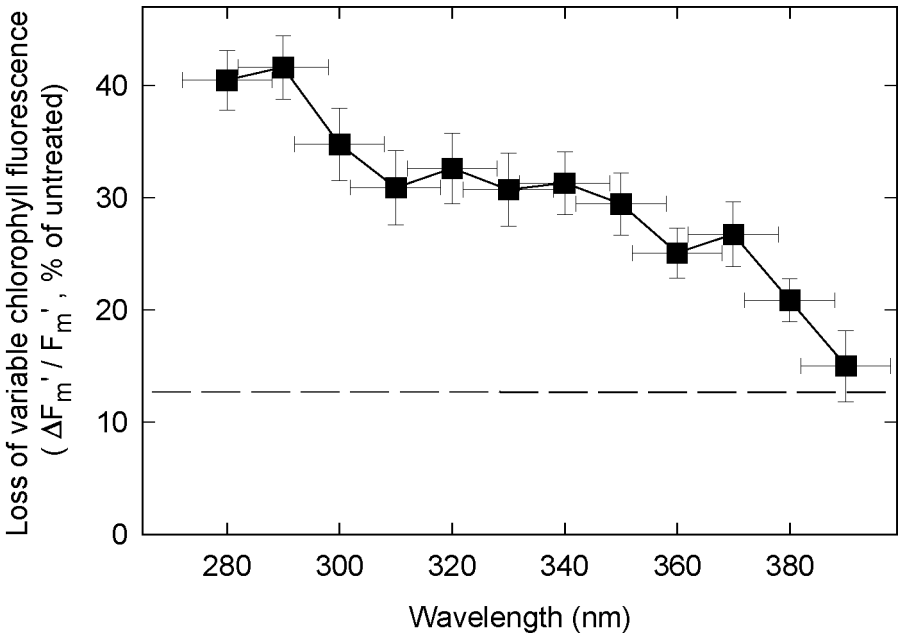

Fig. 4.25.: Loss of variable chlorophyll fluorescence of UV treated spinach leaves. The dashed line indicates the extent of photosynthetic electron transport activity loss induced by the infiltration process itself.

The extent of $^1O_2$ generating capacity of various UV-A and UV-B wavelengths was estimated from the quenching of DanePy fluorescence in the irradiated leaf samples. DanePy emission significantly decreased upon application of longer wavelength, smaller energy UV-A photons, compared to the effect of the same dose of higher energy UV-B photons (Fig. 4.26.). It was found, that the ability of 280-300 nm UV-B radiation to cause $^1O_2$ production was low (Fig. 4.26.). This finding supports previous studies which showed that the main promoters of UV-B induced oxidative damage are other molecules than singlet oxygen (Hideg et al., 1999), and our conclusions drawn from the microscopy experiments presented in this chapter (Hideg et al., 2002a). Longer wavelength UV-B irradiation, however, showed slightly higher capability to induce $^1O_2$ evolution in the irradiated spinach leaves (Fig. 4.26.). Contrary to the UV-B treatment, UV-A irradiation led to extensive DanePy fluorescence loss. This result showed, that various UV-A wavelengths, especially at 360-390 nm activate intense $^1O_2$ production in the irradiated leaves. To our knowledge, this is the first direct detection of singlet oxygen production induced by UV-A radiation.

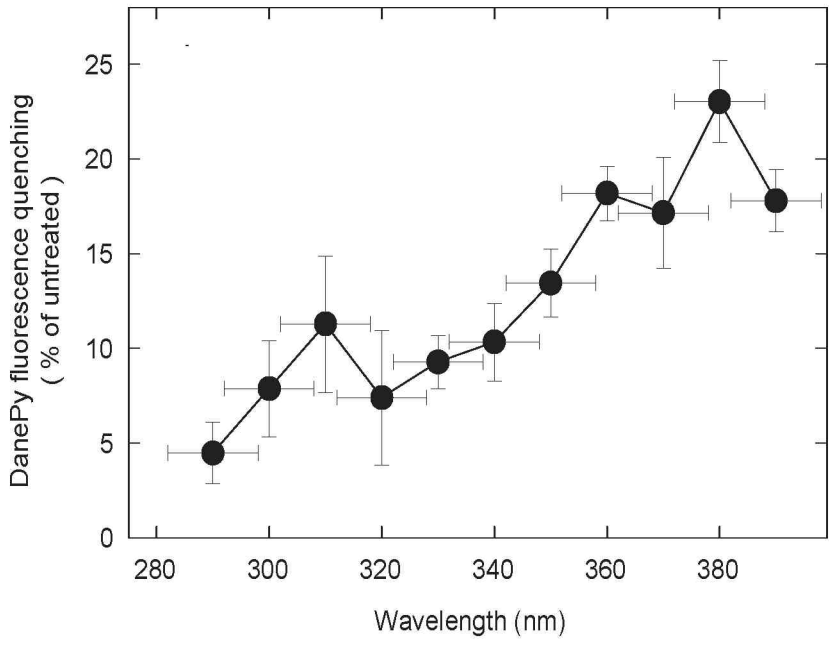

Fig. 4.26.: DanePy fluorescence quenching in spinach leaves irradiated with $2x10^{22}$ photons of various UV-A and UV-B wavelengths.

As to compare the effect of the applied UV radiation to the effect of photoinhibition, when spinach leaves were exposed to $2x10^{22}$ UV-A photons of 360±8 nm the amount of produced singlet oxygen was similar with the amount detected in leaves exposed to 1800 μmol m^{-2} s^{-1} illumination for 1 hour. The later treatment corresponded to $4 x10^{24}$ photons (data not shown).

The correlation between the pattern of DanePy fluorescence quenching at different wavelengths with the loss of photosynthetic electron transport activity of irradiated leaves is shown in Fig. 4.27. The lack of positive correlation between the various UV-A and UV-B wavelength induced $^1O_2$ evolution and photosynthetic yield loss is obvious (Fig. 4.27.). Therefore, the source of UV-A inducible $^1O_2$ is possibly localized outside of the chloroplasts. Although DanePy penetrated into the chloroplasts (Hideg et al., 2001), it was distributed in other cell compartments as well (Hideg et al., 2002a, Barta et al., 2002) and its fluorescence quenching could have occurred in other compartments as well.

The extent of HO-1889NH fluorescence quenching was similar for all applied wavelengths (Fig. 4.28.). ***In vivo*** $O_2^{-\bullet}$ evolution was estimated from the difference between the HO-1889NH and of DanePy fluorescence quenching upon their reaction with UV-induced ROS. This substraction is applicable, if we assume that the ***in vivo*** affinity of DanePy towards $^1O_2$ is similar to the reactivity of HO-1889NH. Data corrected with DanePy quenching values revealed that ***in vivo*** $O_2^{-\bullet}$ evolution was mainly a UV-B inducible reaction, shorter wavelength UV-A (320-350 nm) irradiation resulted in smaller amount of $O_2^{-\bullet}$.

The positive correlation between the UV radiation-induced electron transport damage and the amount of the produced $O_2^{-\bullet}$ supported the hypothesis of a $O_2^{-\bullet}$ production site located in, or at least close to the thylakoid membrane (Fig. 4.29.). The correlation between the two data sets was calculated by using t-test statistics, a linear fit was also calculated (Fig. 4.29.). Statistical analysis showed that data were normally distributed around the regression.

In our experiments UV-B treatment inhibited both the electron transport and prompted $O_2^{-\bullet}$ production more extensively than UV-A. The amount of detected radicals was proportional with the extent of electron transport damage, showing, that the $O_2^{-\bullet}$ production in UV irradiated leaves is connected to a chloroplast-localized

process. ***In vitro*** studies hypothesized the possibility of an UV-B induced conversion of H_2O_2 to $O_2^{-\bullet}$ (Nicole et al., 1990).

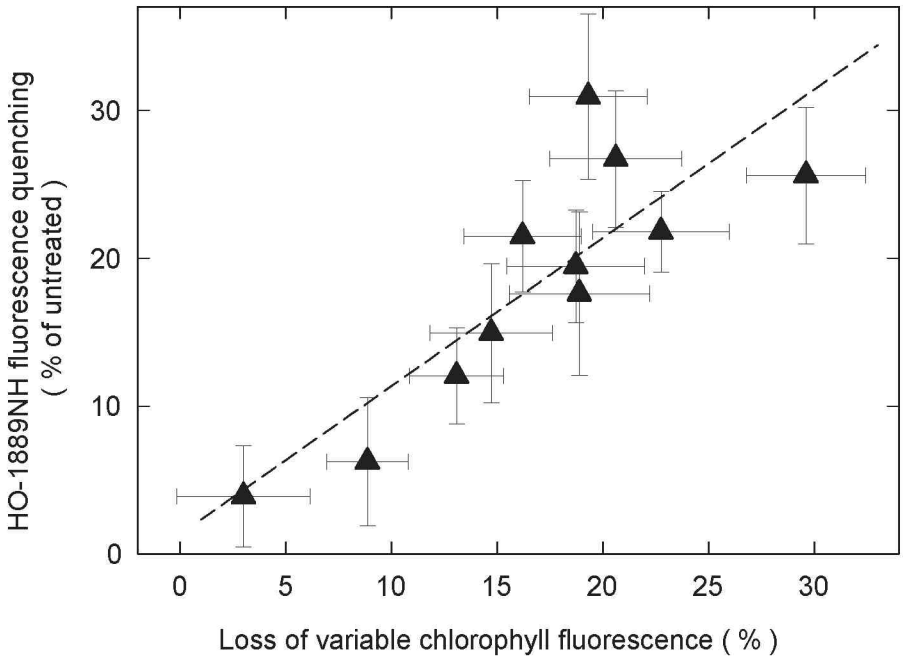

Fig. 4.29.: Correlation between the corrected HO-1889NH fluorescence loss and variable chlorophyll fluorescence decrease in spinach leaves irradiated with various wavelength UV-irradiation. Each data point represents one of the used wavelengths. The dashed line represents the weighted linear fit of the data points.

UV radiation is known to affect the activity of several antioxidant enzymes, among these the activity of the superoxide dismutase (SOD) is altered by UV-irradiation (Costa et al., 2002), therefore $O_2^{-\bullet}$ may accumulate due to the lowered scavenging efficiency of the neutralizing enzymes as well. The responses of either chloroplast-localized (ANT4) or cytosol-localized (ANT3) SOD deficient plants were compared to control ones in terms of photosynthesis and ROS production under UV-A and UV-B irradiation. In general, SOD deficient leaves were more sensitive to UV radiation than controls. Therefore, the absence of either the cytosol or the chloroplast

localized SOD led to increased UV-sensitivity of the plants. Moreover, the sensitivity of the control SR1 plants to UV radiation and the similar UV-induced ROS generation of the control and mutant plants may as well indicate damage of either cytosol or chloroplast localized SODs of the control plants.

Summarizing these findings it was concluded, that ROS production in leaves exposed to UV irradiation is not homogenous, various UV wavelengths induce the production of various ROS. Although $^1O_2$ evolution was a characteristic UV-induced physiological response, typical for irradiation by 340-390 nm, $^1O_2$ was not a product of a source localized inside the chloroplasts, because its evolution did not show correlation with the loss of photosynthetic electron transport activity. UV-B induced $O_2^{-\bullet}$ production correlated with the loss of electron transport activity, on the other hand UV-A induced $O_2^{-\bullet}$ correlated less. UV stress is a complex oxidative stress, leading to the excess production of various ROS, which may disturb the fragile balance between the removal and the production of these oxidizing species.

Our ***in vivo*** experiments support the existence of a $O_2^{-\bullet}$ yielding primary reaction localized in the chloroplasts, possibly in the thylakoid membrane. By using HO-1889NH, the $^1O_2$ and $O_2^{-\bullet}$ reactive fluorescent sensor ***in vitro*** we could not prove the evolution of $O_2^{-\bullet}$ in UV stressed thylakoid membranes. Therefore it was reasonable to assume that a component necessary for the superoxide yielding reaction ***in vivo*** was absent from our ***in vitro*** samples.

In photoinhibition and in all types of UV experiments, the sensitivity of the leaves exposed to light stress was studied in the absence of the sensors as well, in order to establish whether the used sensors may or may not act as antioxidants in the mesophyll cells. We could not detect any difference in sensitivity to the applied irradiation of the sensor-infiltrated leaves, and of those un-infiltrated (data not shown). Therefore our results support a hypothetical approach in which the presented sensors do not act as antioxidants: the trapped ROS amount is proportional with the amount of ROS, which induce damage.

Future improvements of the different ROS detecting techniques and the introduction of new sensors, possibly specific to ROS types other than $^1O_2$ and $O_2^{-\bullet}$ will give more detailed information about the pathways of ROS production initiated

by UV stress. The study of changes in the antioxidant network of plants exposed to UV stress and the monitoring the products of ROS-initiated oxidative reactions is also a path to be followed in studying the mechanism of this oxidative stress further. It is important to note, that in our experiments direct detection of stress induced ROS required the use of UV intensities higher than natural fluxes. Future improvements in the sensitivity of methods will open the possibility of studies using near-field intensity radiation as well.

5. CONCLUSIONS

1. We characterized and successfully applied a recently introduced method, ROS trapping with fluorescent probes in leaf stress experiments. We studied and characterized several new traps in plant studies and selected a new, singlet oxygen and superoxide-reactive fluorescent sensor.

The following conclusions were supported by spectrofluorimetry, laser scanning microscopy and fluorescence microscopy experiments:

2. By applying the singlet oxygen sensitive DanePy and the singlet oxygen and superoxide reactive HO-1889NH in parallel experiments in both isolated thylakoid membranes and leaves, we have shown that:

    a.) Photoinhibition promoted singlet oxygen evolution both *in vitro* and *in vivo*, with a possible minor contribution of superoxide anion radicals.

    b.) UV radiation leads to ROS production in leaves: various UV wavelengths induced the production of various ROS. To our knowledge this is the first observation of UV-A induced $^1O_2$ in leaves. $^1O_2$ evolution was characteristic to 340-390 nm irradiated leaves. The source of $^1O_2$ appears to be outside the chloroplasts. Although in isolated thylakoid membranes we were not able to report detectable levels of superoxide production, neither in experiments with a broadband source nor under and quasi-monochromatic UV irradiation, *in vivo* superoxide production was induced in spinach leaves exposed to UV-B irradiation. Superoxide production was characteristic to the UV-B wavelength region but not to UV-A. We showed the existence of a $O_2^{-\bullet}$ yielding primary reaction localized in the chloroplasts, possibly in the thylakoid membranes.

6. REFERENCES

Adir N., Shochat S. and Ohad I. (1990) Light-dependent D1 protein synthesis and translocation is regulated by reaction center II. Reaction center II serves as an acceptor for the D1 precursor., *J Biol Chem.* 265(21): 12563-12568.

Albro, P.W., Bilski, P., Corbett, J.T., Scroeder, J.L. and Chignell, C.F. (1997) Photochemical reactions and phototoxicity of sterols: novel self-perpetuating mevhanism for lipid photooxidation. *Photochem. Photobiol.* 66: 316-325.

Allen, J.F (1981) Chloroplast protein phosphorylation couples plastoquinone redox state to distribution of excitation energy between photosystems. *Nature* 291: 25–29.

Allen, J.F. (1992) Protein phosphorilation in regulation of photosynthesis. *Biochim. Biophys. Acta* 1098: 278-335.

Allen, J.F. (1993) Redox control of transcription: Sensors, response regulators, activators and repressors. *FEBS Lett.* 332, 203-207.

Allen, J.F. (1995) Thylakoid protein phosphorilation, state 1- state 2 transitions, and photosystem stoichiometry adjustment: Redox control at multiple levels of gene expression. *Physiol. Plant.* 93: 196-205.

Allen, J.F. and Nilsson, A. (1997) Redox signalling and the structural basis of regulation of photosynthesis by protein phosphorilation. *Physiol. Plant.* 93, 196-205.

Allen, J.F. and Forsberg, J. (2001) Molecular recognition in thylakoid structure and function, *Trends Plant Sci.* 6(7): 317-326.

Allen, R.D., Webb, R.P., Schake, S.A. (1997) Use of transgenic plants to study antioxidant defenses. *Free Rad. Biol. Med.* 23(3): 473-479.

Alscher, R., Donahue, J.L. and Cramer, C.L. (1997) Reactive oxygen species and antioxidants: relationship in green cells. *Phys. Plant.* 100: 224-233.

Alscher, R.G., Erturk, N. and Heath, L.S. (2002) Role of superoxide dismutases (SODs) in controlling oxidative stress in plants. *J Exp. Bot.*, 53(372): 1331-1341.

Anderson , J. M. (1981) Consequences of spatial separation of photosystem 1 and 2 in thylakoid membranes of higher plant chloroplasts. *FEBS Lett.* 124: 1–10.

Anderson , J.M. (1982) Distribution of the cytochromes of spinach chloroplasts between the appressed membranes of grana stacks and stroma-exposed thylakoid regions. *FEBS Lett.* 138: 62–66.

Anderson, B. and Styring, S. (1991) Photosystem II: molecular organization, function and acclimation. In: *Current Topics in Bioenergetics (Lee, C.P. ed)* Vol. 16, 1-81. Academic, New York, USA.

Arató,A., Bondarava, N. and Krieger-Liszkay, A. (2004) Production of reactive oxygen species in chloride- and calcium-depleted photosystem II and their involvement in photoinhibition, *Biochim. Biophys. Acta -Bioenergetics,* 1608 (2-3): 171-180.

Arnon, D.I. (1949) Copper enzymes in isolated chloroplasts. Polyphenoloxidase in Beta vulgaris. *Plant Physiol.* 24, 1-25.

Aro, E.M., Hundal, T., Carlberg, I. and Andersson, B. (1990) *In vitro* studies on light-induced inhibition of Photosystem II and D_1-protein degradation at low temperatures, *Biochim. Biophys. Acta - Bioenergetics,* 1019(3) : 269-275.

Aro, E.M., Kettunen, R. and Tyystjarvi, E. (1992) ATP and light regulate D1 protein modification and degradation. Role of D1 in photoinhibition. *FEBS Lett.* 297(1-2): 29-33.

Aro, E.M., Virgin, I. and Andersson, B. (1993a) Photoinhibition of photosystem II. Inactivation, protein damage and turnover., *Biochim. Biophys. Acta* 1143: 113-134.

Arvidsson, P.O. and Sundby, C (1999). A model for the topology of the chloroplast thylakoid membrane. *Aust. J. Plant Physiol.* 26: 687–694.

Asada, K. and Takahashi, M. (1987) Production and scavenging of active oxygen in photosynthesis. In: Kyle D.J., Osmond C.B. and Arntzen, Ch.J. (eds) Topics in Photosynthesis, Photoinhibition, vol 9. 227-288. Elsevier, Amsterdam.

Asada, K. (1992a) Production and scavenging of active oxygen in chloroplasts., *Molecular Biology of Free Radical Scavenging Systems*, ed. Scandalios, J.G., 173-192.

Asada, K. (1992b) Ascorbate-peroxidase: a hydrogen-peroxide scavenging enzyme in plants. *Physiol. Plant.* 85: 235-241.

Asada, K. (1999) The water-water cycle in chloroplasts: Scavenging of active oxygens
and dissipation of excess photons. *Annu. Rev. Plant Physiol. Plant Mol. Biol.,* 50: 601-639.

Barbato, R., Friso, G., Giardi, M.T., Rigoni, F. and Giacometti, G.M. (1991) Breakdown of the Photosystem II reaction center D1 protein under photoinhibitory conditions: Identification and localization of the C-terminal degradation products. *Biochemistry* 30: 10220-10226.

Barbato, R., Friso, G., Rigoni, F., Dalla Vechi, F. and Giacometti, G.M. (1992) Structural changes and lateral distribution of PS II during donor side photoinhibition of thylakoids. *J. Cell. Biol.* 119, 325-335.

Barber, J. (1994) Molecular basis of the vulnerability of photosystem II to damage by light., *Aust. J. Plant Phys.*, 22: 201-208.

Barber, J., Nield, J., Morris E.P., Zheleva, D. and Hankamer, B. (1997) The structure, function and dynamics of photosystem II. *Physiol. Plant.* 100, 817-827.

Barber J. (1998) Photosystem two. *Biochim. Biophys. Acta.* 1365(1-2): 269-277.

Barber, J. and Andersson, B. (1992) Too much of a good thing: light can be bad for photosynthesis., *Trends in Biol. Sci.*, 17: 61-66.

Barber, J. and De Las Rivas, J. (1993) A fuctional model for the role of cytochrome b559 in the protection against donor and acceptor side photoinhibition. *Proc. Natl. Acad. Sci. U.S.A.* 90, 10942-10946.

Barber, J. and Kuhlbrandt, W (1999) Photosystem II. *Curr. Op. Struct. Biol.* 9(4): 469-475.

Barta, Cs., Kálai, T., Vass, I., Hideg, K. and Hideg, É. (2002) Dansyl- and dhodamine based fluorescent sensors for detecting singlet oxygen and superoxide production in plants *in vivo*. *Acta Biol. Szegediensis* 46: 149-150.

Bennett, J. (1983) Regulation of photosynthesis by reversible phosphorylation of the light-harvesting chlorophyll *a/b* protein. *Biochem. J.* 212: 1–13.

Bilski, B., Hideg, K., Kálai, T., Bilska, M.A. and Chignell, C.F. (2003) Interaction of singlet molecular oxygen with double fluorescent and spin sensors. *Free Rad. Biol. Med.* (34)4: 489-495.

Björn LO (1971) Simple methods for the calibration of light measuring equipment. *Physiologia Plantarum* 25: 300-307.

Blubaugh, D.J., Atamian M., Babcock, G.T., Golbeck, J.H. and Cheniae GM. (1991) Photoinhibition of hydroxylamine-extracted photosystem II membranes: identification of the sites of photodamage. *Biochemistry* 30(30): 7586-7597.

Bolwell, G.P. and Wojtaszek, P. (1997) Mechanisms for the generation of reactive oxygen species in plant defenses. *Physiol. Molec. Plant. Pathol.* 51: 347-366.

Bornman, J. (1989) New trends in photobiolgy: target sites of UV-B radiation in photosynthesis of higher plants., *J. Photochem. Photobiol.*, 4: 145-158.

Bornman, J. and Vogelmann, T.C. (1991) The effect of UV-B radiation on leaf optical properties measured with fiber optics. *J. Exp. Bot.* 42, 547-554.

Bowler, C., Slooten, L., Vandenbranden, S., De Rycke, R., Botterman, J., Sybesma, C., Van Montagu, M. and Inzé, D. (1991) Manganese superoxide dismutase can reduce cellular damage mediated by oxygen radicals in transgenic plants. *EMBO J.* 10: 1723-1732.

Bowler, C., Van Montagu, M. and Inzé, D. (1992) Superoxide dismutase and stress tolerance. *Annu. Rev. Plant Physiol. Plant Mol. Biol.* 43: 83-116.

Bowler, C. and Fluhr, R. (2000) The role of calcium and activated oxygen as signals for controlling cross-tolerance, *Trends Plant Sci.* 241-246.

Brandle, J.R., Campbell, W.F., Sisson, W.B. and Caldwell, M.M. (1977) Net photosynthesis, electron transport capacity and ultrastructure of Pisum sativum L. exposed to ultraviolet-B radiation. *Plant Physiol.* 60: 165-168.

Britt, A.B. (1996) DNA damage and repair in plants. *Annu. Rev. Plant Physiol. Plant Mol. Biol.* 47, 75-100.

Brosché, M. and Strid, A. (2000) Ultraviolet-B radiation causes tendril coiling in Pisum sativum. *Plant Cell Physiol.* 41(9): 1077-1079.

Buettner, G.R. (1993) The pecking order of free radicals and antioxidants: lipid peroxidation, alpha-tocopherol, and ascorbate. *Arch. Biochem. Biophys.* 300(2): 535-43.

Cadenas, E. (1989) Biochemistry of oxygen toxicity., *Annu. Rev. Biochem.*, 58: 79-110.

Caldwell, M.M., Ballare, C.L., Björn, L.O., Bornman, J.F., Flint, S.D., Kulandaivelu, G., Teramura, A.H. and Tevini, M. (1998) Effects of increased solar ultraviolet radiation on terrestrial ecosystems. *J. Photochem. Photobiol. B.: Biol.*, 46: 40-52.

Caldwell, M.M., Bornman, J.F., Flint, S.D., Björn, L.O., Teramura, A.H., Kulandaivelu, G. and Tevini, M. (2003) Terrestrial ecosystems, increased solar ultraviolet radiation and interactions with other climatic change factors. *J. Exp. Bot.* 54(384): 879-89.

Cánovas, P.M. and Barber, J. (1993) Detection of a 10 kDa breakdown product containing the C terminus of the D1-protein in photoinhibited wheat leaves suggests an acceptor-side mechanism. *FEBS Lett* 324: 341-344.

Carletti, P., Masi, A., Wonisch, A., Grill, D., Tausz, M. and Ferretti, M. (2003) Changes in antioxidant and pigment pool dimensions in UV-B irradiated maize seedlings. *Environ. Exp. Bot.* 50 (2): 149-157.

Caspi, V., Malkin, S., and Marder, J.B., (2000) Oxygen Uptake Photosensitized by Disorganized Chlorophyll in Model Systems and Thylakoids of Greening Barley. *Photochemistry and Photobiology*. 71(4): 441–446.

Cen, Y.P. and Björn, L.O. (1994) Action spectra from enhancement of ultraweak light emission by ultraviolet radiation (270-340 nm) in leaves of *Brassica napus*, *Journal of Photochem. Photobiol. Biol. B.* 22: 125-129.

Cerovic, Z., Berger, M., Goulas, Y., Tosti, S. and Moya, I. (1993) Simultaneous measurement of changes in red and blue fluorescence in illuminated isolated chloroplasts and leaf pieces: The contribution of NADPH to the blue fluorescence signal. *Photosynth. Res.* 36: 193-204.

Chapelle, E.W., Wood, F.M., McMurtrey, J.E. and Newcourt, W.W. (1984) Laser induced fluorescence of green plants. 1: A technique for remote detection of plant stress and species differentiation. *Applied Optics* 23: 134-138.

Chapelle, E.W., McMurtrey, J.E. and Kim, M.S. (1991) Identification of the pigment-responsible for the blue-fluorescence band in the laser induced fluorescence (LIF) spectra of green plants, and the potential of the band in remotely estimating rates of photosynthesis. *Remote Sens. Environ.* 36: 213-218.

Chappel, J. and Hahlbrock, K. (1984) Transcription of plant defense genes in response to UV-light or fungal elicitor. *Nature* 311: 76-78.

Chen, G.-X., Blubaugh, D.J., Homann, P.H., Golbeck, J.H. and Cheniae, G.M.(1995) Superoxide contributes to the rapid inactivation of specific secondary donors of the photosystem II reaction center during photodamage of manganese-depleted photosystem II membranes. *Biochemistry* 34: 2317-2332.

Cornic, G. (2000) Drought stress inhibits photosynthesis by decreasing stomatal aperture – not by affecting ATP synthesis. *Trends Plant Sci.* 5: 187–188.

Costa, H., Gallego, S.M. and Tomaro, M.L. (2002) Effect of UV-B radiation on antioxidant defense system in sunflower cotyledons. *Plant Sci.* 162: 939-945.

Creed, D. (1984) The photosphysics and photochemistry of the near-UV absorbtion of amino-acids: tyrosine and its simple derivatives. *Photochem. Photobiol.* 39: 563-575.

Cunningham, M.L., Krinsky, N.I., Giovanazzi, S.M. and Peak, M.J. (1985) Superoxide anion is generated from cellular metabolites by solar radiation and its components. *J. Free Rad. Biol. Med.* 1(5-6): 381-385.

Dai, Q.J., Peng, S.B., Chavez, A.Q. and Vergara , B.S. (1994) Intraspecific responses of 188 rice cultivars to enhanced UV-B radiation. *Environ. Exp. Bot.* 34 : 422–433.

Deák, M., Horváth, G.V., Davletova, S., Torok, K., Sass, L., Vass, I., Barna, B., Kiraly, Z. and Dudits, D. (1999) Plants ectopically expressing the iron-binding protein, ferritin, are tolerant to oxidative damage and pathogens. *Nat. Biotechnol.* 17(2): 192-196.

Del Rio, L.A., Lyon, D.S., Olah, I., Glick, B. and Salin, M.L. (1983) Immunocytochemical evidence for a peroxisomal localization of manganese superoxide dismutase in leaf protoplasts from a higher plant. *Planta* 158: 216-224.

Del Rio, L.A., Pastori, G.M., Palma, J.M., Sandalio, L.M., Corpas, F.J., Jiménez, A., López-Huertas, E. and Hernandéz, A.J. (1998) The activated oxygen role of peroxisomes in senescence. *Plant Physiol.* 116: 1195-2000.

De Las Rivas, J., Andersson, B. and Barber, J. (1992) Two sites of primary degradation of the D1 protein induced by acceptor or donor side photoinhibition in PS II core complexes. *FEBS Lett.*, 301: 246-252.

De Las Rivas, J., Shipton, C.A., Ponticos, M. and Barber, J. (1993) Acceptor side mechanism of photoinduced proteolysis of the D1 protein in photosystem II reaction centers. *Biochemistry* 32(27): 6944-6950.

DeLong, J.M. and Steffen, K.L. (1998) Lipid peroxidation and α-tocopherol content in α-tocopherol-supplemented membranes during UV-B exposure. *Environ. Exp. Bot.* 39: 177–185.

DeLucia, E. H., Day, T. A. and Vogelmann, T. C. (1992) Ultraviolet-B and visible light penetration into neddles of two species of subalpine conifers during foliar development. *Plant Cell Environ.* 15: 921-929.

Demmig Adams, B. (1990) Carotenoids and photoprotection in plants: A role for the xanthophyll zeaxanthin. *Biochim. Biophys. Acta* 1020(1): 1-24.

Demmig-Adams, B. and Adams, W.W. (1992), Photoprotection and other responses of plants to high light stress. *Annu. Rev. Plant Physiol. Plant Mol. Biol.* 43 : 599–626.

Demmig-Adams, B. and Adams, W.W. (1996) The role of xantophyll cycle Carotenoids in the protection of photoynthesis. *TIPS* 1: 21-26.

Depka, B., Jahns, P. and Trebst, A. (1998) Beta-Carotene to zeaxanthin conversion in the rapid turnover of the D1 protein of photosystem II. *FEBS Lett.* 424(3): 267-270.

Desikan, R., Mackerness, S.A.H., Hancock, J.T. and Neill, S. (2001) Regulation of the Arabidopsis transcriptome by oxidative stress. *Plant Physiol.* 127: 159-172.

Dixon, D.P., Cummins, I., Cole, D.J. and Edwards, R. (1998) Glutathione mediated detoxification systems in plants. *Curr. Opin. Plant Biol.* 1(3): 258-266.

Durner, J. and Klessig, D.F.(1999) Nitric oxide as a signal in plants. *Curr. Opin. Plant. Biol.* 2(5): 369-374.

Durner, J., Wendehenne, D. and Klessig, D.F. (1998) Defense gene induction in tobacco by nitric oxide, cyclic GMP, and cyclic ADP-ribose. *Proc. Natl. Acad. Sci. U. S. A.* 95(17): 10328-10333.

Durrant, J. R., Giorgi, L. B., Klug, D. R. and Porter, G. (1990) Characterization of triplet states in isolated photosystem II reaction centers: oxygen quenching as a mechanism for photodamage., *Biochim. Biophys. Acta,* 1017: 167-175.

Flint, S.D. and Caldwell, M.M. (1996) Scaling plant ultraviolet spectral responses from laboratory action spectra to field spectral weighting factors. *J. Plant Phys.* 148: 107-114.

Flint, S.D. and Caldwell, M.M. (2003) A biological spectral weighting function for ozone depletion research with higher plants. *Physiol. Plant.* 117: 137-144.

Fork, D.C. and Satoh, K. (1986) The control by state transitions of the distribution of excitation energy in photosynthesis. *Annu. Rev. Plant Physiol. Plant Mol. Biol.* 37: 335-361.

Foyer, C.H., Lelandis, M. and Kunert, K.J. (1994) Photooxidative stress in plants. *Phys. Plant.* 92: 696-717.

Foyer , C.H., Lopez-Delgado, H., Dat, J.F. and Scott, I.M. (1997) Hydrogen peroxide- and glutathione-associated mechanisms of acclimatory stress tolerance and signalling. *Physiol. Plant.* 100: 241-254.

Frederick, J.E. and Lubin, D. (1988) Possible long-term changes in biologically active ultraviolet radiation reaching the ground. *Photochem. Photobiol.* 47(4): 571-578.

Friso, G., Spetea, C., Giacometti, G. M., Vass, I. and Barbato, R. (1994a) Degradation of photosystem II reaction center D1-protein induced by UV-B radiation in isolated thylakoids. Identification and characterization of C- and N-terminal breakdown products., *Biochim. Biophys. Acta* 1184: 78-84.

Friso, G., Barbato, R., Giacometti, G. M. and Barber, B. (1994b) Degradation of D2 protein due to UV-B irradiation of the reaction centre of photosystem II. *FEBS Lett.* 339: 217-221.

Friso, G., Vass, I., Spetea, C., Barber, J. and Barbato, R. (1995) UV-B induced degradation of the D1 protein in isolated reaction centre of photosystem II. *Biochim. Biophys. Acta* 1231: 41-46.

Fryer, M.J., Oxborough, K., Mullineaux, P.M. and Baker, N. (2002) Imaging of photo-oxidative stress responses in leaves. *J. Exp. Bot.* 53(372): 1249-1254.

Gal, A., Zer, H. and Ohad, I. (1997) Redox-controlled thylakoid protein phosphorilation. News and views. *Physiol. Plant.* 100: 869-885.

Gao, W., Zheng, Y., Slusser, J.R. and Heisler, G.M. (2003) Impact of enhanced ultraviolet-B irradiance on cotton growth, development, yield, and qualities under field conditions. *Agricult. Forest Meteorol.* 120 (1-4): 241-248.

Genty, B., Briantais, J.M. and Baker, N.R. (1989) The relationship between the quantum yield of photosynthetic electron-transport and quenching of chlorophyll fluorescence, *Biochim. Biophys. Acta* 990: 87-92.

Gilmore, A.M. and Yamamoto, H.Y. (1993) Linear models relating xanthophylls and lumen acidity to non-photochemical fluorescence quenching. Evidence that antheraxanthin explains zeaxanthin-independent quenching. *Photosynth. Res.* 35: 67–78.

Girotti, A.W. (2001) Photosensitized oxidation of membrane lipids: reaction pathways, cytotoxic effects, and cytoprotective mechanisms. *J. Photochem. Photobiol. Biol. B.* 63(1-3): 103-113.

Gombos, Z., Wada, H., and Murata, N. (1994) The recovery of photosynthesis from low temperature photoinhibition is accelerated by the unsaturation of membrane lipids: a mechanism of chilling tolerance. *Proc. Natl. Acad. U.S.A.* 91: 8787-8791.

Goulas, Y., Moya, I. and Schmuck, G. (1990) Time-resolved spectroscopy of the blue fluorescence. *Photosynth. Res.* 25: 299-307.

Green, S.A., Simpson, D.J., Zhou, G., Ho, P. S. and Blough, N.V. (1990) Intramolecular Quenching of Excited Singlet States by Stable Nitroxyl Radicals *J. Am. Chem. Soc.*, 112: 7337-7346.

Green, R. and Fluhr, R. (1995) UV-B induced PR-1 accumulation is mediated by active oxygen species. *Plant Cell* 7: 203-212.

Greenberg, B.M., Gaba, V., Mattoo, A.K. and Edelman, M. (1987) Identification of a primary in vivo degradation product of the rapidly turning-over 32 kDa protein of photosystem II. *EMBO J.* 6: 2865-2869.

Greenberg, B.M., Gaba, V., Canaani, O., Malkin, S., Mattoo, A.K. and Edelman, M. (1989) Separate photosensitizers mediate degradation of the 32 kDa photosystem II reaction centre protein in the visible and UV-spectral regions. *Proc. Natl. Acad. Sci. U.S.A.* 86: 6617-6620.

Haber, F. and Weiss, J. (1984) The catalytic decomposition of H_2O_2 by iron salts. *Proc. R. Soc. London (Biol)* A147: 332-351.

Hatchard, C.G. and Parker, C.A. (1956) A new sensitive chemical actinometer: II. Potassium ferrioxalate as a standard chemical actinometer. *Philos. Trans. Royal Soc. of London Series A - Mathematical, Physical and Engineering Sciences* 235: 518-536.

Hankovszky, H.O., Kálai, T., Hideg, É., Jekő, J. and Hideg, K. (2001)

Synthesis and Study of Double (EPR Active and Fluorescent) Chemosensors in the Presence of Fe^{3+} Ion. *Synth. Commun.* 31: 975-986.

Halliwell, B. (1999) Antioxidant defense mechanisms: from the beginning to the end (of the beginning). *Free Rad. Res.*, 31: 261-272.

Halliwell, B. and Gutteridge, J. M (1985) Free radicals in biology and medicine., Oxford, Calderon Press, UK.

Harbour, J. R. and Bolton, J. R. (1978) The involvement of the hydroxyl radical in the destructive photooxidation of chlorophylls *in vivo* and *in vitro*., *Photochem. Photobiol.* 28: 231-234.

Hideg, É. and Vass, I (1996) UV-B induced free radical production in plant leaves and isolated thylakoid membranes. , *Plant Sci.*, 115: 251-260.

Hideg, É., Spetea, C. and Vass, I (1994 a) Singlet oxygen and free radical production during acceptor- and donor side induced photoinhibition. Studies with spin trapping EPR spectroscopy. *Biochim. Biophys. Acta* 1186: 143-152.

Hideg, É., Spetea, C. and Vass, I (1994 b) Singlet oxygen production in thylakoid membranes during photoinhibition as detected by EPR spectroscopy. *Photosynth. Res.* 39: 191-199.

Hideg, É., Spetea, C. and Vass, I. (1995) Superoxide radicals are not the main promoters of acceptor side induced photoinhibitory damage in spinach thylakoids. *Photosynth. Res.* 46: 399-407.

Hideg, É. and Vass, I. (1996) UV-B induced free radical production in plant leaves and isolated thylakoid membranes. *Plant Sci.* 115: 251-260.

Hideg, É., Mano, J., Ohno, C.H. and Asada, K. (1997) Increased levels of monodehydroascorbate radical in UV-B irradiated broad bean leaves. *Plant Cell Physiol.* 38: 684-690.

Hideg, É., Kálai, T., Hideg, K. and Vass, I. (1998) Photoinhibition of photosynthesis *in vivo* results in singlet oxygen production detection via nitroxide-induced fluorescence quenching in broad bean leaves. *Biochemistry* 37 (33): 11405-11411.

Hideg, É., Takátsy, A., Sár, C., Vass, I. and Hideg, K. (1999) Utilizing new adamantly spin traps in studying UV-B induced oxidative damage of photosystem II. *J. Photochem. Photobiol. B. Biol.* 48: 174-179.

Hideg, É., Kálai, T., Hideg, K. and Vass, I. (2000 a) Do oxidative stress conditions impairing photosynthesis in the light manifest as photoinhibition? *Phil. Trans. R. Soc. Lond.*, 355: 1511-1516.

Hideg, É., Vass, I, Kálai, T. and Hideg, K. (2000 b) Singlet oxygen detection with sterically hindered amine derivatives in plants under light stress. *Meth. Enzymol.* 319: 76-85.

Hideg, É., Ogawa, K., Kálai, T. and Hideg, K. (2001) Singlet oxygen imaging in *Arabidopsis thaliana* leaves under photoinhibition by excess photosynthetically active radiation. *Phys. Plant.* 112: 10-14.

Hideg, É., Barta, Cs., Kálai, T., Vass, I., Hideg, K. and Asada, K. (2002a) Detection of singlet oxygen and superoxide with fluorescent sensors in leaves under stress by photoinhibition or UV radiation. *Plant Cell Physiol.* 43: 1154-1164.

Hideg, É., Juhász, M., Bornman, J.F. and Asada, K. (2002b) The distribution and possible origin of blue-green fluorescence in control and stressed barley leaves. *Photochem. Photobiol. Sci.* 1: 934-941.

Hirt, H. (1997) Multiple roles of MAP kinases in plant signal transduction. *Trends Plant Sci.* 2 (1): 11-15.

Hodgson, R. A. and Raison, J. (1991) Superoxide production by thylakoids during chilling and its implication in the susceptibility of plants to chilling induced photoinhibition., *Planta*, 183: 222-228.

Horton, P., Ruban, A.V. and Walters, A.G. (1996) Regulation of light harvesting in green plants. *Annu Rev Plant Physiol Plant Mol Biol.* 47: 655-684.

Hundal, T. Virgin, I., Styring, S. and Andersson, B. (1990) Changes in the organization of photosystem II following light-induced D1 protein degradation. *Biochem. Biophys. Acta* 1017: 235-241.

Inoue, K., Sakurai, H. and Hiyama, T. (1986) Photoinactivation of photosystem I in isolated chloroplasts., *Plant Cell Physiol.* 27: 961-968.

Inzé, D. and Van Montagu, M. (1995) Oxidative stress in plants. *Curr. Op. Biotech.* 6: 153-158.

Jansen, M.A.K., Gaba, V., Greenberg, B.M., Mattoo, A.K. and Edelman, M. (1996) Low threshold levels of ultraviolet-B in a background of photosynthetically active radiation trigger rapid degradation of the D2 protein of photosystem II. *Plant J.* 9: 693-699.

Jansen, M.A.K., Gaba, V. and Greenberg, B.M. (1998) Higher plants and UV-B radiation: balancing, damage, reapir and acclimation. *Trends Plant Sci.* 3(4): 131-135.

Jeong, W.J., Park, Y.I., Suh, K., Raven, J.A., Yoo, O.J. and Liu, J.R. (2002) A large population of small chloroplasts in tobacco leaf cells allows more effective chloroplast movement than a few enlarged chloroplasts. *Plant Physiol.* 129(1): 112-121.

Johnson, G.A., Mantha, S.V. and Day, T.A. (2000) A spectrofluorometric survey of UV-induced blue-green fluorescence in foliage of 35 species. *J. Plant Physiol.* 156: 242-252.

Jones LW and Kok B (1966) Photoinhibition of chloroplast reactions. I. Kinetics and action spectra. *Plant Physiology* 41, 1037-1043.

Jordan, B.R., Chow W.S., Strid A. and Anderson, J.M. (1991) Reduction in cab and psb A RNA transcripts in response to supplementary ultraviolet-B radiation. *FEBS Lett.* 284(1):5-8.

Kakani, V.G., Reddy, K.R., Zhao, D. and Sailaja, K. (2003) Field crop responses to ultraviolet-B radiation: a review. *Agric. Forest Meteorol.* 120(1-4): 191-218.

Kálai, T., Hideg, É., Vass, I., Hideg, K. (1998) Double (fluorescent and spin) sensors for detection of reactive oxygen species in the thylakoid membrane. *Free Rad. Biol and Med.*, 24 (4): 649-652.

Karpinski, S., Reynolds, H., Karpinska, B., Wingsle, G., Creissen, G. and Mullineaux, P. (1999) Systemic signalling and acclimation in response to excess excitation energy in *Arabidopsis*. *Science* 284: 654-657.

Kerr, J.B. and McElroy, C.T. (1993) Evidence for large upward trends of ultraviolet-B radiation linked to ozone depletion. *Science* 262: 1032-1034.

Kettunen, R., Tyystjarvi, E. and Aro, E.M. (1996) Degradation pattern of photosystem II reaction center protein D1 in intact leaves. The major photoinhibition-induced cleavage site in D1 polypeptide is located amino terminally of the DE loop. *Plant Physiol.* 111(4): 1183-1190.

Kramer, G.F., Norman, H.A., Krizek, D.T. and Mirecki, R.M. (1991) Influence of UV-B radiation on polyamines, lipid peroxidation and membrane lipids in cucumber. *Phytochemistry* 30: 2101-2108.

Kim, B.C., Tennessen, D.J. and Last R.L. (1998) UV-B-induced photomorphogenesis in *Arabidopsis thaliana*. *Plant J.*, 15(5): 667-674.

Knox, J. P. and Dodge, A. D. (1985 a) The photodynamic action of eosin, a singlet-oxygen generator. Some effects on leaf tissue of *Pisum sativum* L. *Planta* 164: 22-29.

Krasnovsky, A. A. Jr. (1994) Singlet molecular oxygen and primary mechanisms of photooxidative damage of chloroplasts. Studies based on detection of oxygen and pigment phosphorescence. *Proc. Roy. Soc. Edinburgh* 102B: 219-235.

Kühlbrandt, W. (1994) Structure and function of the plant light-harvesting complex, LHC-II. *Curr. Opin. Struct. Biol.* 4: 519–528.

Kühlbrandt, W., Wang, D.N. and Fujiyoshi, Y. (1994) Atomic model of plant light-harvesting complex by electron crystallography. *Nature* 367(6464): 614-621.

Kyle D.J., Ohad, I. and Arntzen, C.J. (1984) Membrane protein damage and repair: Selective loss of quinone-protein function in chloroplast membranes. *Proc. Natl. Acad. Sci. U.S.A.* 94: 328-332.

Landry, L.G., Chapple, C.C. and Last, R.L. (1995) Arabidopsis mutants lacking phenolic sunscreens exhibit enhanced ultraviolet-B injury and oxidative stress. *Plant. Physiol.* 109(4): 1159-1166.

Lang, M., Stober, F. and Lichtenthaler, H.K. (1991) Fluorescence emission spectra of plant leaves and plant constituents. *Radiat. Environ. Biophys.* 30(4): 333-347.

Latouche, G., Cerovic, Z.G., Montagnini, F., Moya, I. (2000) Light-induced changes of NADPH fluorescence in isolated chloroplasts: a spectral and fluorescence lifetime study. *Biochim. Biophys. Acta Bioenerg.* 1460(2-3) : 311-329.

Lawlor, D.W. (2002) Limitation to photosynthesis in water-stressed leaves: stomata vs. metabolism and the role of ATP. *Ann Bot (Lond).* 89 Spec No: 871-885.

Lee, J. and Seliger, H.H. (1964) Quantum yield of the ferrioxalate actinometer. *Journal of Chemical Physics* 40: 519-523.

Li, Y., Yue, M. and Wang, X.L. (1998) Effects of enhanced ultraviolet-B radiation on crop structure, growth and yield components of spring wheat under field conditions. *Field Crops Res.* 57: 253–263.

Li, Y., Yue, M., Wang X.L., and Hu, Z.D. (1999) Competition and sensitivity of wheat and wild oat exposed to enhanced UV-B radiation at different densities under field conditions. *Environ. Exp. Bot.* 41: 47–55.

Li, Y., Zu, Y.Q., Chen, H.Y., Chen, J.J., Yang, J.L. and Hu , Z.D. (2000a) Intraspecific responses in crop growth and yield of 20 wheat cultivars to enhanced ultraviolet-B radiation under field conditions. *Field Crops Res.* 67: 25–33.

Li, Y., Zu, Y.Q., Chen, H.Y., Chen, J.J., Yang, J.L. and Hu , Z.D. (2000b) Intraspecific differences in physiological responses of 20 wheat cultivars to enhanced ultraviolet-B radiation under field conditions. *Environ. Exp. Bot.* 44 (2): 95–103.

Lichtenthaler, H.K. and Schweiger, J. (1998) Cell wall bound ferulic acid , the major substance of blue-green fluorescence emission from plants. *J. Plant Pysiol.* 152:272-282.

Luttge, U. (2002) CO(2)-concentrating: consequences in crassulacean acid metabolism. *J. Exp. Bot.* 53(378): 2131-2142.

Mackerness, S.A.H. (2000) Plant responses to ultraviolet-B (UV-B: 280-320 nm) stress: What are the key regulators? *Plant Growth Reg.* 37: 27-39.

Mackerness, S.A.H., Surplus, S.L., Jordan, B.R. and Thomas, B. (1998) Effects of supplementary ultraviolet-B radiation on photosynthetic transcripts at different stages of leaf development and light levels in pea (*Pisum sativum* L.): role of active oxygen species and antioxidant enzymes. *Photochem.Photobiol.* 68: 88-96.

Mackerness S.A.H., John, C.F., Jordan, B. and Thomas, B. (2001) Early signalling components in ultraviolet-B responses: distinct roles for different reactive oxygen species and nitric oxide. *FEBS Lett.* 489: 237-242.

Macpherson, A.N., Telfer, A., Barber, J. and Truscott, T.G. (1993) Direct detection of singlet oxygen from photosystem II reaction centers., *Biochim. Biophys. Acta*, 1143: 301-309.

Madronich, S., McKenzie, R.L., Bjorn, L.O. and Caldwell, M.M. (1998) Changes in the biologically active ultraviolet radiation reaching the Earth's surface. *Photochem. Photobiol, B.* 46(1-3): 5-19.

Maier-Maercker, M. (1999) Predisposition of trees to drought stress by ozone. *Tree Physiol.* 19(2): 71-78.

Malanga, G. and Puntarulo, S. (1995) Oxidative stress and antioxidant content in Chlorella vulgaris after exposure to ultraviolet-B radiation. *Physiol. Plant.* 94: 672-679.

Masi, A., Ghisi R., Ferretti, M. (2002) Measuring low-molecular-weight thiols by detecting the fluorescence of their SBD-derivatives: application to studies of diurnal and UV-B induced changes in *Zea mays* L. *J. Plant Physiol.* 159: 499–507.

Mattoo, A.K., Hoffman-Falk, H., Marder, J.B. and Edelman, M. (1984) Regulation of protein metabolism: coupling of electron transport *in vivo* degradation of the rapidly metabolised 32kDa protein of chloroplast membranes. *Proc. Natl. Acad. Sci. U.S.A.* 84:1497-1501.

Mazza, C.A., Boccalandro, H.E., Giordano, C.V., Battista, D., Scopel, A.L. and Ballaré, C.L. (2000) Functional significance and induction by solar radiation of ultraviolet-absorbng sunscreens in filed-grown soybean crops. *Plant Physiol.* 122:117-125.

Mehler, A.H. (1951a) Studies on reactions of illuminated chloroplasts. I. Mechanism of the reduction of oxygen and other Hill reagents. *Arch. Biochem.* 33(1):65-77.

Mehler, A.H. (1951b) Studies on reactions of illuminated chloroplasts. II. Stimulation and inhibition of the reaction with molecular oxygen. *Arch. Biochem.* 34(2): 339-351.

Melis, A. (1999) Photosystem-II damage and repair cycle in chloroplasts: what modulates the rate of photodamage in vivo? *Trends Plant Sci.*, 4 (4): 130-135.

McCord, J.M. and Fridovich, I. (1969a) Superoxide dismutase. An enzymic function for erythrocuprein (hemocuprein). *J. Biol. Chem.* 244(22): 6049-6055.

McCord, J.M. and Fridovich, I. (1969b) The utility of superoxide dismutase in studying free radical reactions. I. Radicals generated by the interaction of sulfite, dimethyl sulfoxide, and oxygen. *J. Biol. Chem.* 244(22): 6056-63.

McFarland, M. and Kaye, J. (1992) Chlorofluorocarbons and ozone. *J. Photochem. Photobiol.* 55: 911-929.

McRae, D.G. and Thompson, J.E. (1983) Senescence dependent changes in superoxide anion production by illuminated chloroplasts from bean leaves. *Planta* 158: 185-193.

Mishra, N.P., Mishra, R.K. and Singhal, G.S. (1993) Involvement of active oxygen species in photoinhibition of photosystem II: protection of photosynthetic efficiency and inhibition of lipid peroxidation by superoxide dismutase and catalase. *J. Photochem. Photobiol. B. Biol.* 19: 19-24.

Mittler, R. (2002) Oxidative stress, antioxidants and stress tolerance. Trends Plant Sci. 7(9): 405-410.

Miyao, M. (1994) Involvement of active oxygen species in degradation of the D1 protein under strong illumination in isolated subcomplexes of photosystem II. *Biochemistry* 33: 9722-9730.

Møller, I.M. (2001) Plant mitochondria and oxidative stress: electron transport, NADPH turnover, and metabolism of reactive oxygen species. *Annu. Rev. Plant Physiol. Plant Mol. Biol.* 52: 561–591.

Morales, F., Cerovic, Z. G. and Moya, I. (1994) Characterization of blue-green fluorescence in the mesophyll of sugar beet (*Beta vulgaris* L.) leaves affected by iron deficiency. *Plant Physiol.*, 106: 127-133.

Morales, F., Cerovic, Z.G. and Moya, I. (1996) Time-resolved blue-green fluorescence of sugar beet (*Beta vulgaris* L.) leaves. Spectroscopic evidence for the presence of ferulic acid as the main fluorophore of the epidermis. *Biochem. Biophys. Acta* 1273: 251-262.

Morré, D.J., Brightman, A.O., Wu, L.Y., Barr, R., Leak, B. and Crane, F.L. (1988) Role of plasma membrane redox activities in elongation growth in plants. *Physiol. Plant* 73: 187-193.

Mullineaux, P. and Karpinski, S. (2002) Signal transduction in response to excess light: getting out of the chloroplast. *Curr Op. Plant Biol.* (5)1: 43-48.

Murphy, T.M. (1983) Membranes as targets of ultraviolet radiation. *Physiol. Plant.* 58: 381-388.

Nicole, I., De Laat, J., Dore, M., Duguet, J.P. and Bonnel, C. (1990) Use of U.V. radiation in water treatment: measurement of photonic flux by hydrogen peroxide actinometry. *Water Res.* 24, 157-168.

Noctor, G., Veljovic-Jovanovic, S., Driscoll, S., Novitskaya, L. and Foyer, C.H. (2002) Drought and oxidative load in the leaves of C3 plants: a predominant role for photorespiration? *Ann. Bot.* (Lond). 89 Spec No: 841-50.

Noctor, G. and Foyer, C.H. (1998) Ascorbate and glutathione: keeping active oxygen under control. *Annu Rev Plant Physiol Plant Mol Biol.* 49: 249-279.

Nouges, S., and Baker, N.R. (2000) Effects of drought on photosynthesis in Mediterranean plants grown under enhanced UV-B radiation. *J Exp Bot.* 51(348): 1309-17.

Oberschall, A., Deak, M., Torok, K., Sass, L., Vass, I., Kovacs, I., Feher, A., Dudits, D. and Horvath, G.V. (2000) A novel aldose/aldehyde reductase protects transgenic plants against lipid peroxidation under chemical and drought stresses. *Plant J.* 24(4): 437-46.

Ohad, I., Adir, N., Koike, H., Kyle, D.J. and Inoue, Y. (1990) Mechanism of photoinhibition in vivo. A reversible light-induced conformational change of reaction center II is related to an irreversible modification of the D1 protein. *J. Biol. Chem.* 265(4): 1972-1979.

Ochsner, M.(1997) Photophysical and photobiological processes in the photodynamic therapy of tumours. *J. Photochem. Photobiol. Biol.* 39(1): 1-18.

Overmyer, K., Brosché, M. and Kangasjarvi, J. (2003) Reactive oxygen species and hormonal control of cell death. *Trends Plant Sci.* 8(7): 335-42.

Panagopoulos, I., Bornman, J.F. and Björn, L.O. (1990) Effects of ultraviolet radiation and visible light on growth, fluorescence induction, ultraweak luminescence and peroxidase activity in sugar beet plants., *J.Photochem. Photobiol. B.: Biol.*, 8(1): 73-87.

Pang, Q. and Hays, J.B. (1991) UV-inducible and temperature-sensitive photoreactivation of cyclobutane pyrimidine dimers in *Arabidopsis thaliana. Plant Physiol.* 95, 536-543.

Pardha Saradhi, P., Alia, Arora, S. and Prasad, K.V. (1995) Proline accumulates in plants exposed to UV radiation and protects them against UV induced peroxidation. *Biochem. Biophys. Res. Commun.* 209: 1–5.

Park, Y.I., Chow, W.S. and Anderson, J.M. (1996) Chloroplast Movement in the Shade Plant *Tradescantia albiflora* Helps Protect Photosystem II against Light Stress. *Plant Physiol.* 111(3): 867-875.

Pastori, G., Foyer, C.H. and Mullineaux, P. (2000) Low temperature-induced changes in the distribution of H_2O_2 and antioxidants between the bundle sheath and mesophyll cells of maize leaves. *J. Exp. Bot.* 51(342): 107-113.

Pfannschmidt, T., Nilsson, A. and Allen, J.F. (1999) Photosynthetic control of gene expression. *Nature,* 397: 625-628.

Pfannschmidt T. (2003) Chloroplast redox signals: how photosynthesis controls its own genes. *Trends Plant Sci.* 8(1): 33-41.

Pfündel, E.E., Pan, R.S. and Dilley, R.A. (1992) Inhibition of violaxanthin deepoxidation by ultraviolet-B radiation in isolated chloroplasts and intact leaves. *Plant Physiol.* 98(4): 1372-1380.

Pfündel, E. and Bilger, W. (1994) Regulation and possible function of the violaxanthin cycle. *Photosynth. Res.* 42: 89–109.

Powles, S.B. (1984) Photoinhibition of photosynthesis induced by visible light., *Annu. Rev. Plant Physiol.*, 35: 15-44.

Prasad, T.K., Anderson, M.D., Martin, B.A. and Stewart, C.R. (1994) Evidence for chilling induced oxidative stress in maize seedlings and a regulatory role for hydrogen peroxide. *Plant Cell*, 6: 65-74.

Quaite, F.E., Sutherland, B.M. and Sutherland, J.C. (1992) Action spectrum of DNA damage in alfalfa lowers predicted impact of ozone depletion. *Nature* 358, 576-578.

Rao, M.V. and Ormrod, D.P. (1995) Impact of UV-B and O_3 on the oxygen free radical scavenging system in *Arabidopsis* thaliana genotypes differing in flavonoid biosynthesis. *Potochem. Photobiol.* 62: 719-726.

Redmond, R. W. and Gamlin, J. N. (1999) A compilation of singlet oxygen yields from biologically relevant molecules. *Photochem. Photobiol.* 70: 391–475.

Renger, G., Volker, M., Eckert, H. J., Fromme, P., Hohm-Veit, S. and Graber, P.(1989) On the mechanism of of photosystem II deterioriation by UV-B irradiation., *Photochem. Photobiol.*, 49: 97-105.

Rinalducci, S., Pedersen, J.Z. and Zolla, L. (2004) Formation of radicals from singlet oxygen produced during photoinhibition of isolated light-harvesting proteins of photosystem II., *Biochim. Biophys. Acta* 1608(1): 63-73.

Rozema, J. van de Staaij, Björn, L.O. and Caldwell, M.M. (1997) UV-B as an environmental factor in plant life: stress and regulation. *Trends Ecol. Evol.* 12: 22-28.

Rozema, J., Bjorn, L.O., Bornman, J.F., Gaberscik, A., Hader, D.P., Trost, T., Germ, M., Klisch, M., Groniger, A., Sinha, R.P., Lebert, M., He, Y.Y., Buffoni-Hall, R., de Bakker, N.V., van de Staaij, J., Meijkamp, B.B. (2002) The role of UV-B

radiation in aquatic and terrestrial ecosystems--an experimental and functional analysis of the evolution of UV-absorbing compounds. *J. Photochem. Photobiol. B.* 66(1): 2-12.

Ruban, A.V., Pascal, A., Robert, B. and Horton, P. (2002) Activation of zeaxanthin is an obligatory event in the regulation of photosynthetic light harvesting. *J. Biol. Chem.* 277(10): 7785-7789.

Rundel RD (1983) Action spectra and estimation of biologically effective UV radiation. *Physiologia Plantarum* 58: 360-366.

Rutherford, W. and Faller, P. (2001) The heart of photosynthesis in glorious 3D. *Trends Biochem. Sci.* (26)1: 341-344.

Scandalios, J.G. (2002) The rise of ROS. *Trend Biochem. Sci.* 27(9): 483-486.

Schweikert, C., Liszkay, A. and Schopfer, P. (2002) Polysaccharide degradation by Fenton reaction- or peroxidase-generated hydroxyl radicals in isolated plant cell walls, *Phytochemistry,* 61(1): 31-35.

Shadle, G.L., Wesley, S.V., Korth, K.L., Chen, F., Lamb, C. and Dixon, R.A. (2003) Phenylpropanoid compounds and disease resistance in transgenic tobacco with altered expression of L-phenylalanine ammonia-lyase. *Phytochemistry* 64(1): 153-161.

Sharma, Y. K., Leon, J., Raskin, I. and Davis, K.R. (1996) Ozone-induced responses in *Arabidopsis thaliana* - the role of salicylic acid in the accumulation of defense-related transcripts and resistance. *Proc. Natl. Acad. Sci. U.S.A.* 93: 5099-5104.

Sonoike, K. (1995) Selective photoinhibition of photosystem I in isolated thylakoid membranes from cucumber and spinach. *Plant Cell Physiol.* 36: 825-830.

Sonoike, K. and Terashima, I. (1994) Mechanism of photosystem-I photoinhibition in leaves of *Cucumis sativus* L. *Planta* 194: 287-293.

Spetea, C., Hideg, E. and Vass, I. (1996) The quinone electron acceptors are not the main sensitizers of UV-B induced protein damage in isolated photosystem II reaction center and core complexes. *Plant Sci.* 115: 207-215.

Spetea C., Hundal, T., Lohmann, F. and Andersson, B. (1999) GTP bound to chloroplast thylakoid membranes is required for light-induced, multienzyme degradation of the photosystem II D1 protein. *Proc. Natl. Acad. Sci. U.S.A.*96: 6547-6552.

Spetea, C., Keren, N., Hundal, T., Doan, J.M., Ohad, I. Andersson, B. (2000) GTP enhances the degradation of the photosystem II D1 protein irrespective of its conformational heterogeneity at the Q(B) site. *J. Biol. Chem.* 275(10): 7205-7211.

Stapleton, A.E. (1992) Ultraviolet radiation and plants: burning questions. *Plant Cell* 4: 1353-1358.

Strid, A., Chow, W.S. and Anderson, J.M. (1990) Effects of supplementary UV-B radiation on photosynthesis in *Pisum sativum*. *Biochim. Biophys. Acta*, 1020: 260-268.

Strid, A. (1993) Alteration in expression of defence genes in Pisum sativum after exposure to supplementary ultraviolet-B radiation. *Plant Cell Phys.* 34: 949-953.

Strid, A., Chow, W.S. and Anderson, J.M. (1994) UV-B damage and protection at the molecular level in plants. *Photosynth. Res.* 39: 475–489.

Styring, S., Virgin, I., Ehrenberg, A. and Andersson, B. (1990) Strong light photoinhibition of electron transport in Photosystem II. Impairement of the function of the first quinone acceptor. *Biochim. Biophys. Acta* 1050: 269-278.

Sullivan, J.H. and Teramura, A.H. (1990) Field study of the interaction between solar ultraviolet-B and drought on photosynthesis and growth in soybean. *Plant Physiol.* 92: 141-146.

Sundby, C., McCaffery, S. and Anderson, J.M. (1993) Turnover of the photosystem II D1 protein in higher plants under photoinhibitory and nonphotoinhibitory irradiance. *J. Biol. Chem.* 268(34): 25476-25482.

Tabaeizadeh, Z. (1998) Drought-induced responses in plant cells. *Int Rev Cytol.* 182:193-247.

Takahashi, M. and Asada, K. (1982) Dependence of oxygen affinity for Mehler reaction on photochemical activity of chloroplast thylakoids. *Plant Cell Physiol.* 23: 1457-1462.

Takahashi, M.A. and Asada,K. (1983) Superoxide anion permeability of phospholipids membranes and chloroplast thylakoids. *Arch. Biochem. Biophys.* 226: 558-566.

Takahashi, M. and Asada, K. (1988) Superoxide production in the aprotic interior of chloroplast thylakoids., *Arch. Biochem. Biopys.*, 267 (2): 714-722.

Takeuchi, Y., Fukumoto, R., Kasahra, H., Sakaki, T. and Kitao, M. (1995) Peroxidation of lipids and growth inhibition induced by UV-B irradiation. *Plant Cell Rep.* 14: 566–570.

Takeuchi, Y., Kubo, H., Kasahara, H. and Sakaki, T. (1996) Adaptive alterations in the activities of scavengers of active oxygen in cucumber cotyledons irradiated with UV-B. *J. Plant Physiol.* 147: 589–592.

Tanielian, C., Golder, L. and Wolff, C. (1984) Production and quenching of singlet oxygen by the sensitizer in dye-sensitized photo-oxygenations, *J. Photochem.* 25(2-4):117-125.

Telfer, A. and Barber, J. (1989) Evidence for the photo-induced oxidation primary electron donor P680 in the isolated photosystem two reaction center., *FEBS Letters*, 246, 223-228.

Telfer, A., Bishop, S.M., Phillips, D. and Barber, J. (1994) Isolated photosynthetic reaction center of photosystem II as a sensitizer for the formation of singlet oxygen: detection and quantum yield determination usning a chemical trapping technique. *J. Biol. Chem.* 269: 13244-13253.

Teramura, A.H. and Sullivan, J.H. (1990) Effects of UV-B radiation on soybean yield and seed quality: a six-year field study. *Physiol. Plant.* 80: 5-11.

Teramura, A.H. and Sullivan, J.H. (1994) Effects of UV-B irradiation on photosynthesis and growth of terrestrial plants. *Photosynth. Res.* 39: 463-473.

Tevini, M (1988) The effects of UV radiation on plants. *J. Photochem. Photobiol. B. Biol.* 2(3): 401-407.

Tevini, M. and Teramura, A.H. (1989) UV-B effects on terrestrial plants., *Photochem. Photobiol.* 50 (4): 479-487.

Thordal-Christensen, H., Zhang, Z., Wei, Y. and Collinge, D.B. (1997) Subcellular localization of H_2O_2 in plants. H_2O_2 accumulation in papillae and hypersensitive response during the barley-powdery mildew interaction. *Plant J.* 11: 1187–1194.

Tiedemann, A. V. (1997) Evidence for a primary role of active oxygen species in induction of host cell death during infection of bean leaves with *Botrytis cinerea.Physiol. Molec. Plant Pathol.* 50 (3): 151-166.

Tjus, S. E., Lindberg Moller, B. and Scheller, H. V. (1998) Photosystem I is an early target of photoinhibition in barley illuminated at chilling temperatures., *Plant. Physiol.*, 116: 755-764.

Tjus, S. E., Moller, B. L. and Scheller, H. V. (1999) Photoinhibition of photosystem I damages both reaction center proteins PSI-A and PSI-B and acceptor-side located small photosystem I polypeptides. *Photosynth. Res.* 60: 75-86.

Trebst, A. and Depka, B. (1997) Role of carotene in the rapid turnover and assembly of photosystem II in *Chlamydomonas reinhardtii*, *FEBS Lett.* , 400(3): 359-362.

Trebst, A., Depka, B. and Holländer-Czytko, H. (2002) A specific role for tocopherol and of chemical singlet oxygen quenchers in the maintenance of photosystem II structure and function in *Chlamydomonas reinhardtii*, *FEBS Lett.* , 516(1-3): 156-160.

Turcsányi, E. and Vass, I. (2000) Inhibition of photosynthetic electron

transport by UV-A radiation targets the photosystem II complex. *Photochemistry and Photobiology* 72: 513-520.

Van Bereusegem, F., Vranová, E., Dat, J. and Inzé, D. (2001) The role of active oxygen species in plant signal transduction. *Plant Sci.* 161: 405-414.

Van Camp, W. and Inzé, D. (1998) H_2O_2 and NO: redox signals in disease resistance. *Trends in Plant Sci.*, 3(9): 330-334.

Van Camp, W., Capiau, K., Van Montagu, M., Inzé, D. and Slooten, L. (1996) Enhancement of oxidative stress tolerance in transgenic tobacco plants overproducing Fe-superoxide dismutase in chloroplasts. *Plant Phys.* 112: 1703-1714.

Vass, I. (1996) Adverse effect of UV-B light on the structure and function of the photosynthetic apparatus. In *Handbook of photosynthesis* (ed. M. Pessarakli), pp: 931-949, New York: M. Dekker 931-949.

Vass, I., Styring, S., Hundall, T., Koivuniemi, A., Aro, E.M. and Andersson, B. (1992) Reversible and irreversible intermediates during photoinhibition of photosystem II: stable reduced Q_A species promote chlorophyll triplet formation., *Proc. Natl. Acad. Sci.*, USA, 89: 1408-1412.

Vass, I. and Styring, S.(1992) Spectroscopic characterization of triplet forming states in photosystem II. *Biochemistry* 31(26): 5957-5963.

Vass, I. and Styring, S. (1993) Characterization of chlorophyll triplet promoting states in photosystem II sequentially induced during photoinhibition., *Biochemistry* 32: 3334-3341.

Vass, I., Sass, L., Spetea, C., Bakou, A., Ghanotakis, D. and Petrouleas, V. (1996)
UV-B induced inhibition of photosystem II electron transport studied by EPR and chlorophyll fluorescence. Impairment of donor and acceptor side components. *Biochemistry* 35, 8964-8973.

Vladimirov, Y.A., Roshchupkin, D.I. and Fesenko, E.E. (1970) Photochemical reactions in amino acid residues and inactivation of enzymes during UV-irradiation. A review. *Photochem. Photobiol.* 11(4):227-246.

Vranová, E., Inzé, D. and Van Breusegem, F. (2002) Signal transduction during oxidative stress. *J. Exp. Bot.* 53(372): 1227-1236.

Wada, M., Grolig, F. and Haupt, W. (1993) New trends in photobiology : Light-oriented chloroplast positioning. Contribution to progress in photobiology. *J. Photochem. Photobiol. B: Biol.* (17) 1: 3-25.

Wagner, B.A., Buettner, G.R. and Burns, C.P. (1994) Free radical-mediated lipid peroxidation in cells: oxidizability is a function of cell lipid bis-allylic hydrogen content. *Biochemistry.* 33(15): 4449-53.

Waterworth, W.M., Jiang, Q., West, C.E., Nikaido, M. and Bray, C.M. (2002) Characterization of Arabidopsis photolyase enzymes and analysis of their role in protection from ultraviolet-B radiation. *J. Exp. Bot.* 53(371): 1005-1015.

White, A.L. and Jahnke, L.S. (2002) Contrasting effects of UV-A and UV-B on photosynthesis and photoprotection of beta-carotene in two *Dunaliella spp. Plant Cell Physiol.* 43: 877-884.

Willekens, H., Chamnongpol, S., Davey, M., Schraudner, M., Langebartels, C., Van Montagu, M., Inzé, D. and Van Camp, W. (1997) Catalase is a sink for H_2O_2 and is indispensable for stress defence in C3 plants. *EMBO J.* 16(16): 4806-4816.

Wise, R.R. and Naylor, A.W. (1987) Chilling-enhanced photooxidation. The peroxidative destruction of lipids during chilling injury to photosynthesis and ultrastructure. *Plant Physiol.* 83: 272-277.

Young, A.J. and Frank, H.A. (1996) Energy transfer reactions involving carotenoids: quenching of chlorophyll fluorescence. *J. Photochem. Photobiol.* 36: 3–15.

Zolla, L. and Rinalducci, S. (2002) Involvement of active oxygen species in degradation of light-harvesting proteins under light stresses. *Biochemistry* 41(48):14391-14402.

Zouni, A., Witt, H. T., Kern, J., Fromme, P., Krauss, N., Saenger, W. and Orth, P. (2001) Crystal structure of photosystem II from *Synechococcus elongatus* at 3.8 Å resolution. *Nature* 409: 739–743.

Zhang, J., Hu, X., Henkow, L., Jordan, B.R., Strid, A. (1994) The effects of ultraviolet-B radiation on the CF_0F_1-ATPase. *Biochim. Biophys. Acta* 1185: 295-302.

Vandewalle, P.L., Petersen, N.O. (1987) Oxidation of reduced cytochrome *c* by hydrogen peroxide: implications for superoxide assays. *FEBS Lett.* 210(2): 195-198.

ACKNOWLEDGEMENTS

Since I have joined the Laboratory of Molecular Stress- and Photobiology in the Institute of Plant Biology, Biological Research Center of the Hungarian Academy of Sciences, in 2000, I have received priceless scientific guidance, support, many advices from my supervisor, Dr. Éva Hideg, who answered each of my questions with a lot of patience, to whom I am extremely grateful.

I am also grateful to Dr. Imre Vass for giving me the support to work in the projects presented in the thesis and for his scientific guidance.

We are grateful to Dr. Tamás Kálai and Dr. Kálmán Hideg, from the Medical University of Pécs, Department of Medicinal and Organic Chemistry, for synthetizing the fluorescent reactive oxygen sensors used in this work. We would like as well to thank for the help of Prof. Kozi Asada, Fukuyama University, Japan, who made possible the LSM and fluorescence microscopy studies.

I am also grateful to each member of the Molecular Stress and Photobiology: to László Sass and András Szilárd for helping me out with computer work, to Dr. Péter Kós, Dr. Zsuzsanna Deák for their scientific guidance, to Erzsébet Bárdosi and Gabriella Fleit for their laboratory help, and to my fellow colleagues, Otilia Cheregi, Dr. Cosmin Sicora and Krisztián Cser for their friendly support.

LIST OF PUBLICATIONS

CSENGELE BARTA

I. JOURNAL ARTICLES

Barta, Cs., Kálai, T., Vass, I., Hideg, É. (2002) Dansyl- and rhodamine-based fluorescent sensors for detecting singlet oxygen and superoxide production in plants *in vivo*. *Acta Biologica Szegediensis* 46, 149-150.

Hideg, É., **Barta**, Cs., Kálai, T., Vass, I., Hideg, K., Asada, K. (2002) Detection of singlet oxygen and superoxide with fluorescent sensors in leaves under stress by photoinhibition or UV-radiation. *Plant Cell Physiology* 43, 1154-1164.

Barta, Cs., Kálai, T., Hideg, K., Vass, I., Hideg, É. (2004) Differences in the ROS generating efficacy of various ultraviolet wavelengths in detached spinach leaves. *Functional Plant Biology* 31, 23-28.

II. CONFERENCE PROCEEDINGS

Hideg, É., Asada, K., **Barta, Cs**., Bornman, J., F., Dudits, D., Hideg, K., Horváth, G. V., Kálai, T., Oberschall, A., Ogawa, K., Sár, C., Szilágyi, A., Vass, I. (2000) Detecting ROS in plants under UV-B stress (Plant and Ultraviolet-B Radiation Congress, Japan).

Barta, Cs., Kálai, T., Sár, C., Hideg, K., Vass, I., Hideg, É. (2001) Reaktív oxigén növényekben: újabb mérési lehetőségek (IVth Hungarian Photosynthesis Meeting, Szeged, HAS-BRC).

Hideg, É., Kálai, T., **Barta, Cs**., Ogawa, K., Vass, I., Hideg, K., Asada, K. (2001) Detecting stress induced reactive oxygen production in plants (9thCongress of the European Society for Photobiology", Lillehammer, Norway).

Barta, Cs., Kálai, T., Vass, I., Hideg, K., Hideg É. (2002) Action spectrum of ROS production under different wavelength UV stress (IInd Chemistry and Biochemistry of Antioxidants Course, Wageningen, The Netherlands).

Barta, Cs., Kálai, T., Vass, I., Hideg, K., Hideg É. (2002) Az UV sugárzás reaktív oxigénkeltő hatásának vizsgálata spenót levelekben (IIIrd Hungarian Plant Physiology Conference, Biological Research Center, Szeged).

Barta, Cs., Ogawa, K., Asada, K., Hideg, É. (2003) The role of superoxide-dismutase in detoxifying reactive oxygen species in tobacco leaves exposed to UV-radiation (10th Congress of the European Society for Photobiology, Vienna, Austria).

Barta, Cs., Vass, I., Hideg, É (2003) A szuperoxid diszmutáz szerepe a 290, illetve 360 nm-es UV besugárzásnak kitett dohánylevelekben keletkező reaktív oxigén formák semlegesítésében (Vth Hungarian Photosynthesis Conference and Advanced Photosynthesis School, Noszvaj, Hungary)

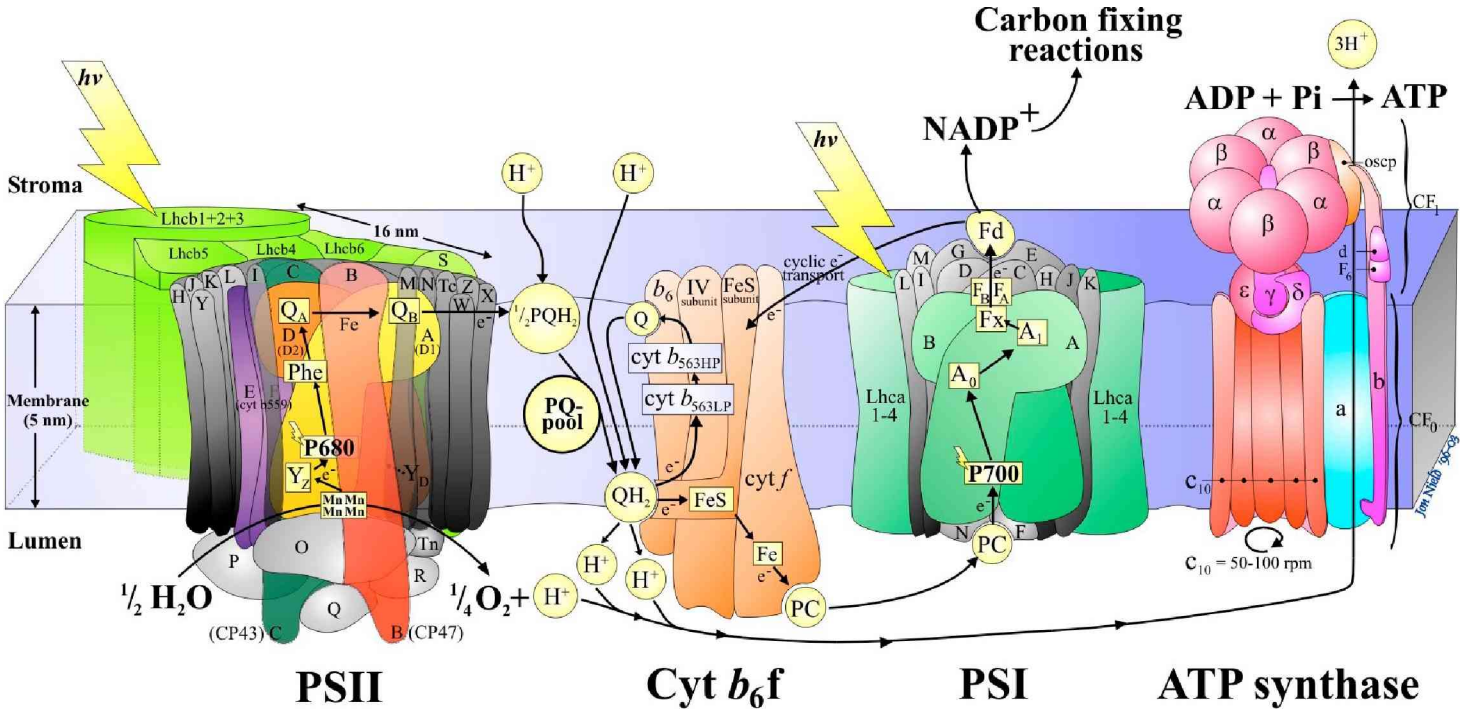

Fig.1.5. The organization of the photosynthetic electron transport chain components in the thylakoid membranes (Nield, 2003)

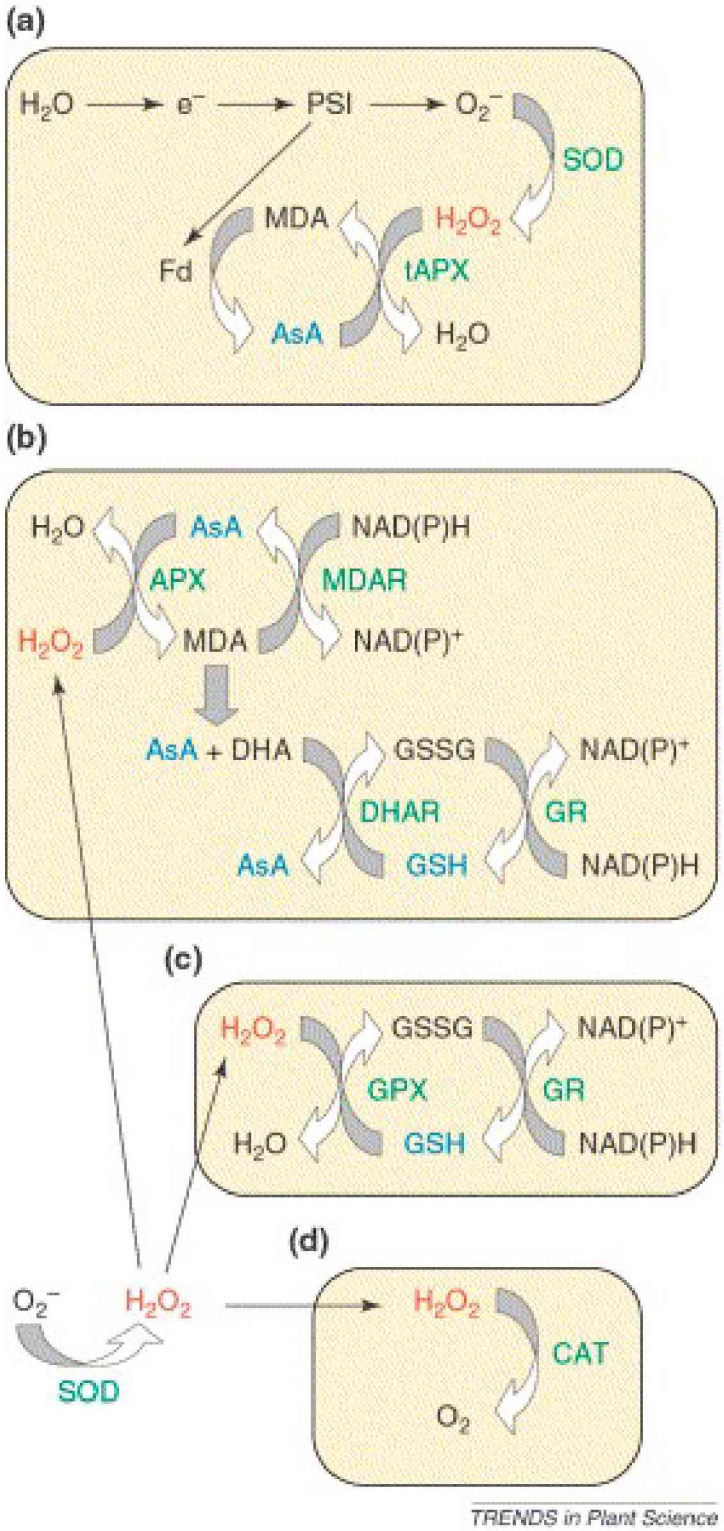

Fig. 1.6.: Pathways for reactive oxygen intermediate (ROS) scavenging in plants. The water–water cycle a.). The ascorbate–glutathione cycle b.). The glutathione peroxidase (GPX) cycle c.). Catalase (CAT) d.) (Mittler, 2002).

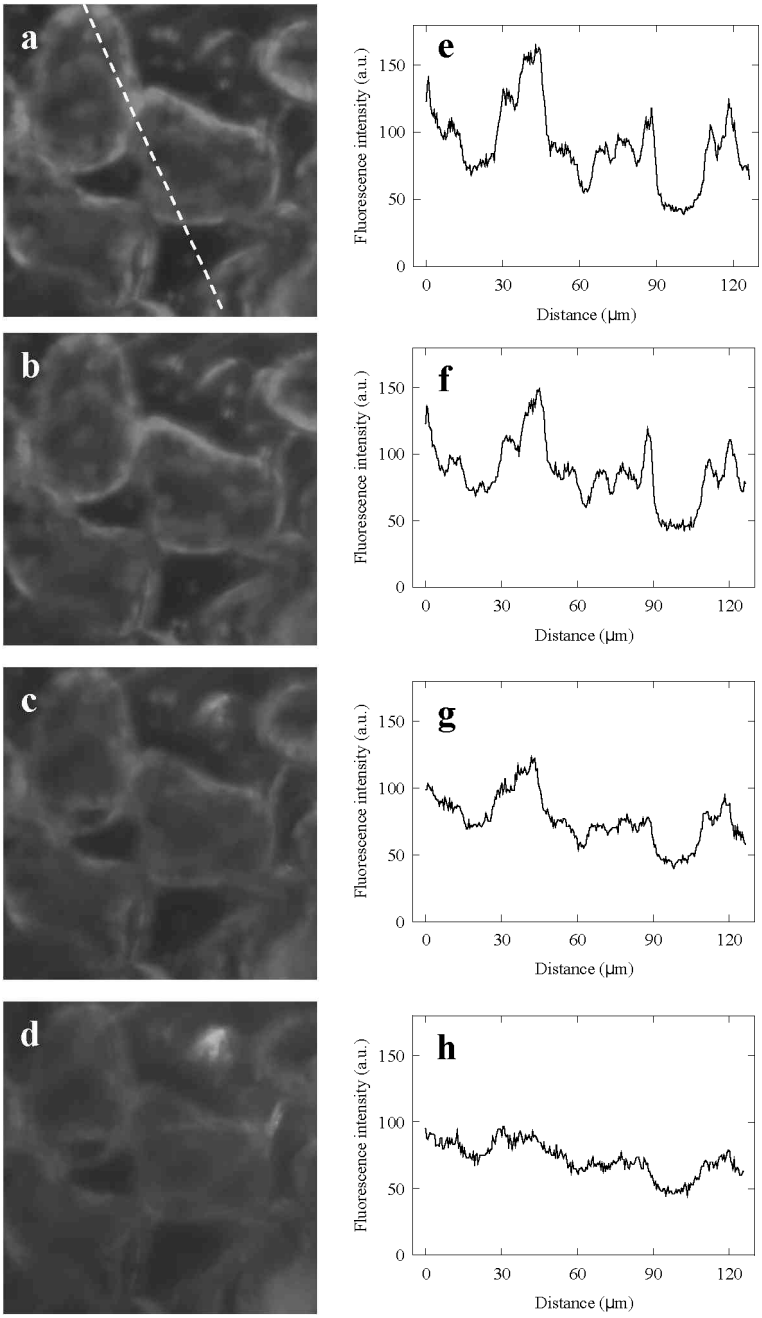

Fig. 4.9.: LSM images of 351 nm excited green (515 < λ < 550 nm) fluorescence from a DanePy infiltrated spinach leaf (a-d), fluorescence intensity along the diagonal line showed in (e-h) and histograms of fluorescence images. After infiltration, the leaf was exposed to 1800 μmol m^{-2} s^{-1} PAR for 0 min (a,e) 15 min (b,f) 30 min (c,g) 45 min (d,h). LSM image size 115 x 115 μm.

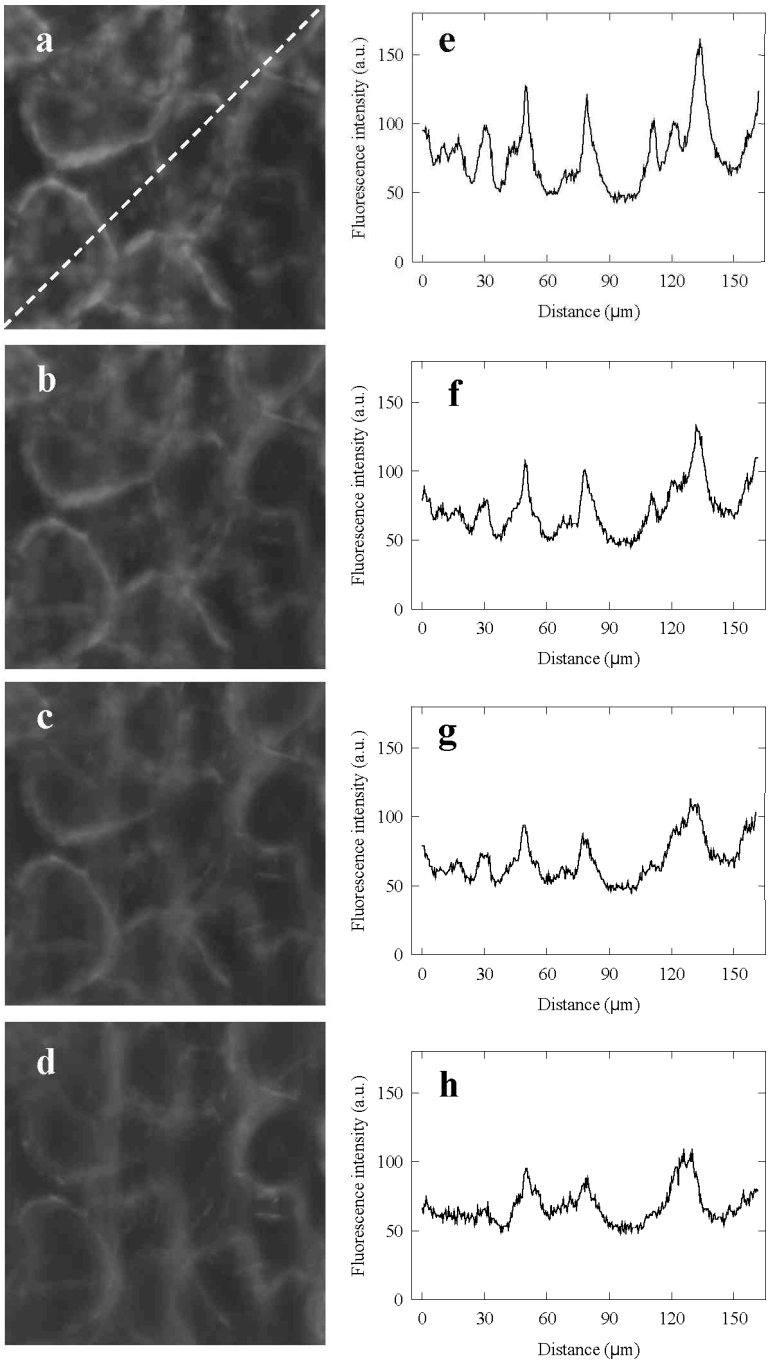

Fig. 4.10.: LSM images of 351 nm excited green (515 < λ < 550 nm) fluorescence from a HO-1889NH infiltrated spinach leaf (a-d), fluorescence intensity along the diagonal line showed in (a) (e-h) and histograms of fluorescence images. After infiltration, the leaf was exposed to photoinhibition for 0 min (a,e) 15 min (b,f) 30 min (c,g) 45 min (d,h). LSM image size 115 x 115 μm.

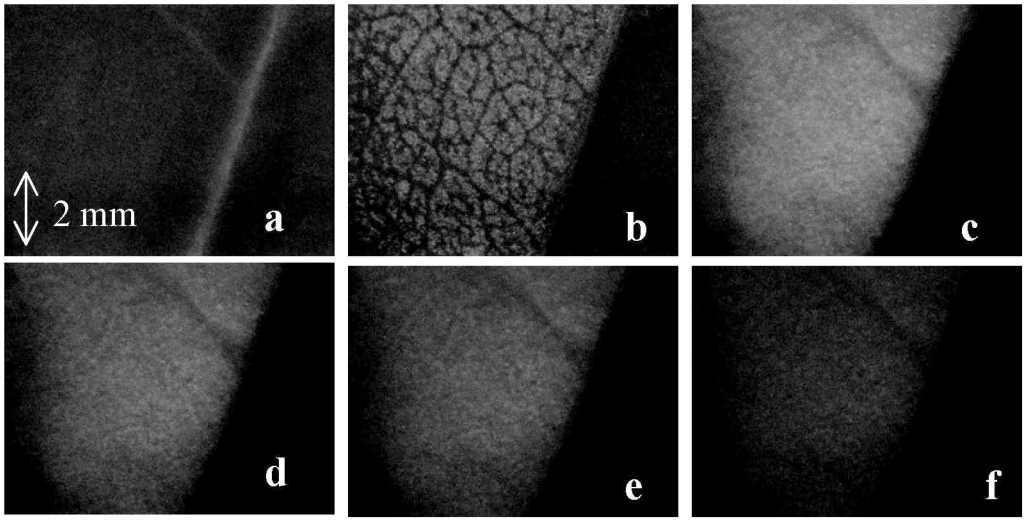

Fig. 4.11.: UV (295-375 nm) excited 410-640 nm images of DanePy infiltrated spinach leaves. Leaf pictures were taken in reflected (a.) and transmitted (b.) visible illumination. 410-640 nm fluorescence images of same leaf segment as (a.) and (b.) after 0 minutes (c.) , 15 minutes (d.), 45 minutes (e.) and 75 minutes (f.) irradiation by 1800 µmol m^{-2} s^{-1} PAR.

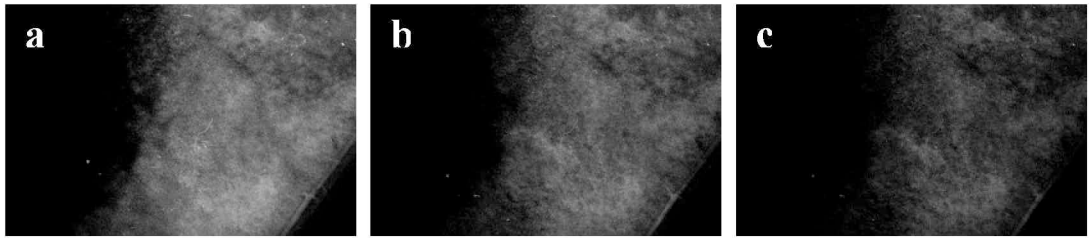

Fig. 4.12.: UV (295-375 nm) excited 410-640 nm images of HO-1889NH infiltrated spinach leaves. The fluorescence image of the leaf was taken after 0 minutes (a.) , 45 minutes (b.) and 75 minutes (c.) of irradiation by 1800 µmol m^{-2} s^{-1} PAR.

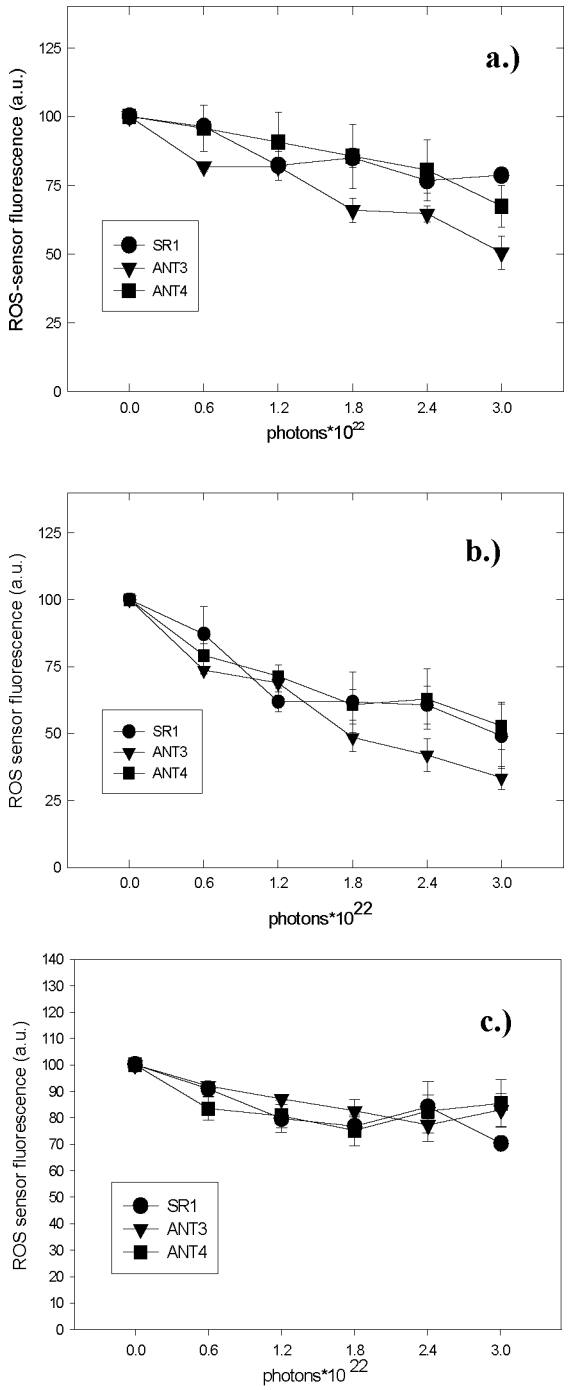

Fig.4.17.: Fluorescence quenching of DanePy (a.) and HO-1889NH (b.) in SR1 (circles), ANT3 (triangles) and ANT4 (squares) Nicotiana tabaccum plants exposed to 2x10 ^{22} 290±8 nm UV-B irradiation. Calculated $O_2^{-\bullet}$- induced changes of ROS sensor fluorescence, given as HO-1889NH fluorescence minus DanePy fluorescence at each time point (c.).

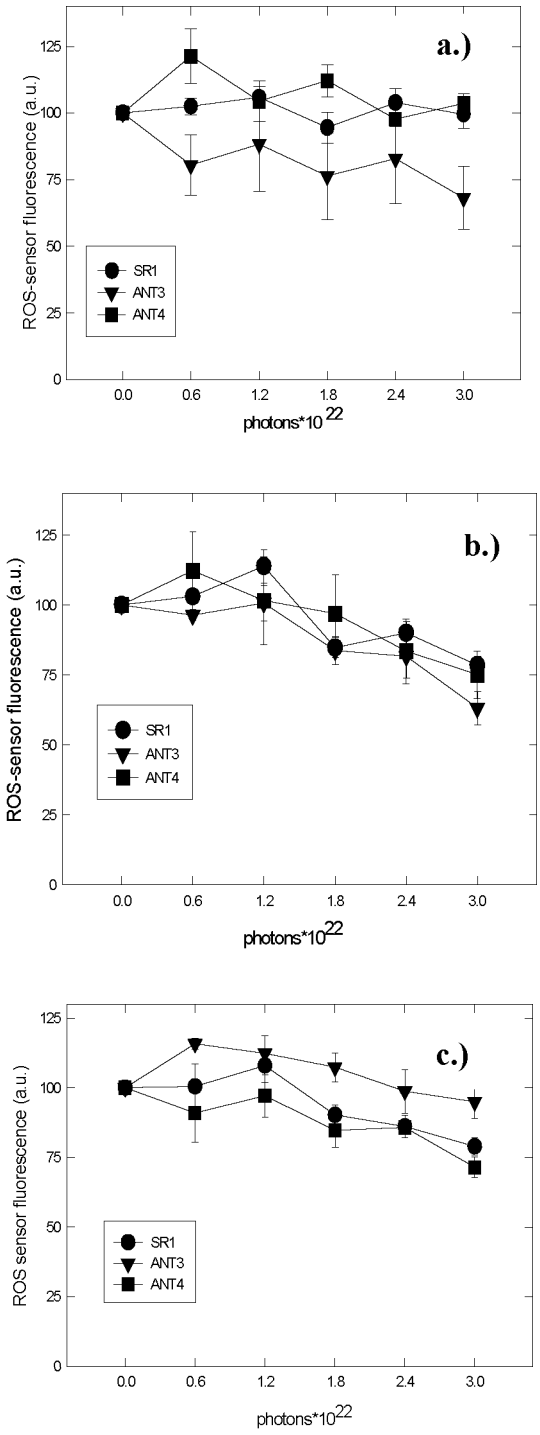

Fig. 4.19.: Fluorescence quenching of DanePy (a.) and HO-1889NH (b.) in SR1 (circles), ANT3 (triangles) and ANT4 (squares) Nicotiana tabaccum plants exposed to 2x10 ^{22} 360±8 nm UV-A irradiation. Calculated $O_2^{-\bullet}$ induced changes of ROS sensor fluorescence, given as HO-1889NH fluorescence minus DanePy fluorescence at each time point (c.)

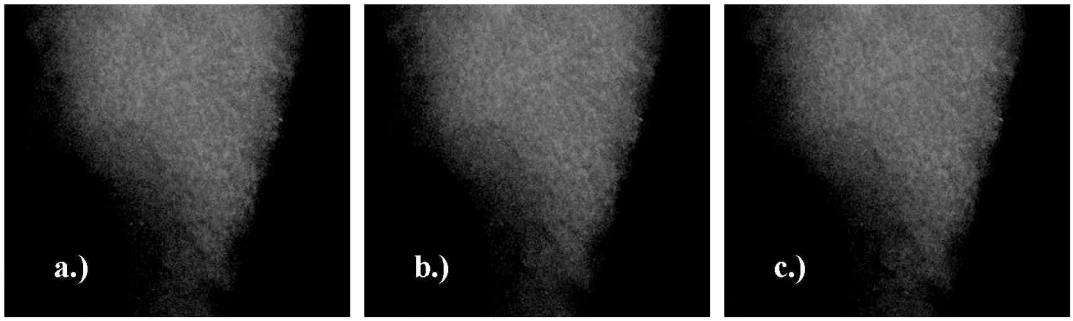

Fig. 4.22.: Fluorescence images of 280-360 nm UV-irradiated (excitation: 295-375 nm) spinach leaves infiltrated with DanePy, recorded by using a 410-640 nm filter. The 410-640 nm fluorescence images of same leaf segment are recorded at 0 minutes (a.), 30 minutes (b.), 60 minutes (c.) of illumination.

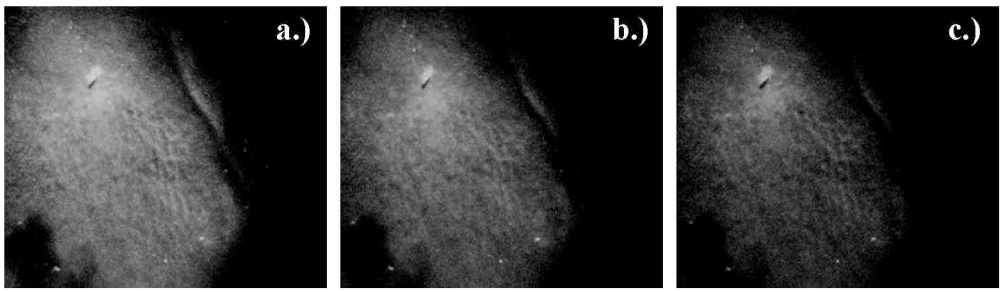

Fig. 4.23.: Fluorescence images of 280-360 nm UV-irradiated (excitation: 295-375 nm) spinach leaves infiltrated with HO-1889NH, recorded by using a 410-640 nm filter. The 410-640 nm fluorescence images of same leaf segment are recorded at 0 minutes (a.), 30 minutes (b.), 60 minutes (c.) of illumination.

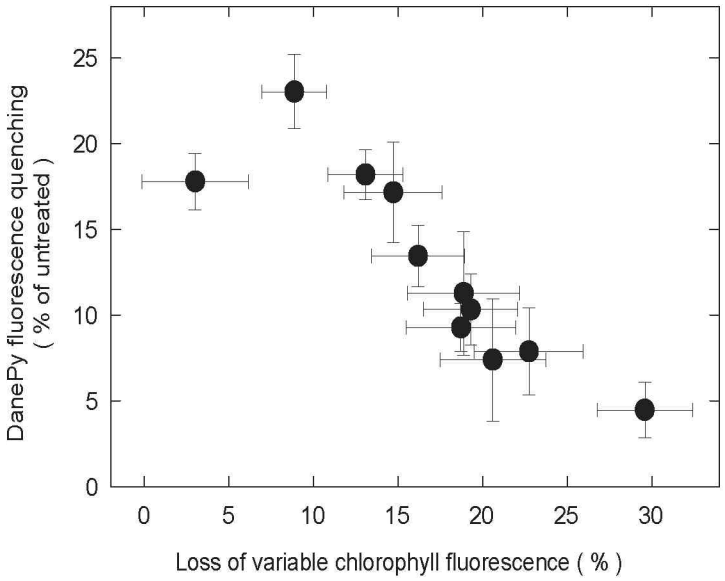

Fig. 4.27.: Singlet oxygen production estimated from the DanePy fluorescence quenching in spinach leaves irradiated with equal doses of $2x10^{22}$ photons did not show positive correlation with the loss of photosynthetic electron transport activity. Different data points represent different wavelengths.

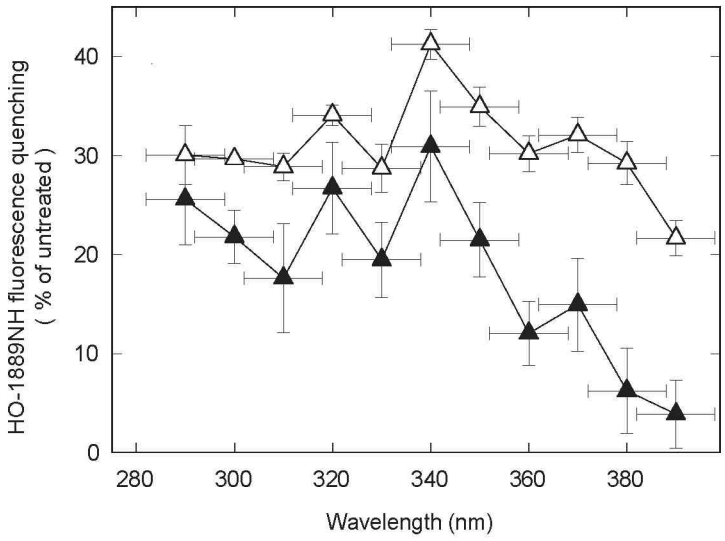

Fig.4.28.: Fluorescence quenching of HO-1889NH in UV-irradiated spinach leaves (empty triangles) . Superoxide production in UV-irradiated spinach leaves: the fluorescence quenching of the $^1O_2$ and $O_2^{-\bullet}$ reactive sensor was corrected for $^1O_2$-initiated quenching, measured as DanePy fluorescence loss (full triangles).